January 2012

Fluxon Dynamics In Two-Gap Superconductor-Based Long Josephson Junction

Bal Ram Ghimire

FLUXON DYNAMICS IN TWO-GAP SUPERCONDUCTOR-BASED LONG JOSEPHSON JUNCTION

by

Bal Ram Ghimire
Bachelor of Science, Hemawatinandan Bahuguna Garhwal University, Dehradun
Master of Science, Hemawatinandan Bahuguna Garhwal University, Dehradun
Masters of Science, Southern Illinois University, Edwardsville

A Dissertation

Submitted to the Graduate Faculty

of the

University of North Dakota

in partial fulfillment of the requirements

for the degree of

Doctor of Philosophy

Grand Forks, North Dakota
August
2012

This dissertation, submitted by Bal Ram Ghimire in partial fulfillment of the requirements for the degree of Doctor of Philosophy from the University of North Dakota, has been read by the Faculty Advisory Committee under whom the work has been done and is hereby approved.

Dr. Ju H. Kim_____
Chairperson

Dr. William A. Schwalm_____

Dr. Graeme Dewar_____

Dr. Kanishka Marasinghe_____

Dr. Mark Hoffmann_____

This dissertation meets the standards for appearance, conforms to the style and format requirements of the Graduate School of the University of North Dakota, and is hereby approved.

Wayne Swisher
Dean of the Graduate School
_____7/12/2012_____
Date

PERMISSION

Title FLUXON DYNAMICS IN TWO-GAP SUPERCONDUCTOR-BASED LONG JOSEPHSON JUNCTION

Department Physics and Astrophysics

Degree Doctor of Philosophy

In presenting this dissertation in partial fulfillment of the requirements for a graduate degree from the University of North Dakota, I agree that the library of this University shall make it freely available for inspection. I further agree that permission for extensive copying for scholarly purposes may be granted by the professor who supervised my dissertation work or, in his absence, by the chairperson of the department or the dean of the Graduate School. It is understood that any copying or publication or other use of this dissertation or part thereof for financial gain shall not be allowed without my written permission. It is also understood that due recognition shall be given to me and to the University of North Dakota in any scholarly use which may be made of any material in my dissertation.

Signature: Bal Ram Ghimire

Date 7/12/2012

TABLE OF CONTENTS

LIST OF FIGURES

Figure Page

ACKNOWLEDGMENTS

It is my pleasure to express my deepest gratitude to those who guided, inspired, and helped me to achieve my goals at the University of North Dakota. I would like to express appreciation to my dissertation advisor Dr. Ju H. Kim for his support, guidance, patience, and being an excellent advisor. Without his guidance throughout my graduate studies it would not have been possible to achieve my goal. I would like to thank Dr. William A. Schwalm who helped me whenever I needed his help. Also, I would like to thank Drs. Graeme Dewar, Kanishka Marasinghe, and Mark R. Hoffmann for their valuable advice and support, and for serving in my dissertation committee. My immense thanks also go to other professors, secretary, and graduate students in the Department of Physics and Astrophysics at the UND for their creative suggestions.

I would like to thank Tribhuvan University, Nepal, for granting me seven years of study-leave for my higher education in the United States. I would like to thank my family, my mother, my parents-in-law, my brothers, and all my friends for their continued love and support. Finally, my especial thanks go to my lovely wife Kusum, my daughters, Nitisha and Nimant, and my son Nitin for their love, sacrifices, encouragements, and being so wonderful towards me throughout my studies.

ABSTRACT

A superconducting tunnel junction with two-gap superconductors, such as MgB_2 and iron-based superconductors, can lead to more interesting phase dynamics than those with one-gap superconductors. The phase dynamics in a long Josephson junction (LJJ) may be described by using the sine-Gordon equation. The difference in the phase dynamics between the LJJ with two-gap superconductors and that with the one-gap superconductors arises due to the presence of multiple tunneling channels between the superconductor (S) layers and the inter-band Josephson effect within the same S layer. The inter-band Josephson effect leads to both spatial and temporal modulation of the critical current between the two adjacent *S* layers. In this work, the effects of critical current modulation on the trajectories of the single Josephson vortex (i.e., fluxon) and the current-voltage characteristics of the two-gap superconductor-based LJJ are estimated. Also, the possibility of a broken time-reversal symmetry state ground state of a single LJJ due to the presence of additional tunneling channels is investigated by using a microscopic model for two-gap superconductors. The consequence of this broken time reversal ground state is discussed. Finally, the equation of motion for fluxon for coupled LJJs interacting via both the magnetic induction effect and charging effect is investigated. As the inter-band Josephson effect is found to affect the dynamics of a single fluxon in a single LJJ, this effect is explicitly taken into account for a two-coupled LJJ stack. This

equation of motion is expected to be an excellent starting point for exploring interesting LJJ properties such as collective dynamics of fluxons as well as fractional fluxons.

CHAPTER I

INTRODUCTION

1.1 Josephson Effect

Tunneling of electron pairs between two superconductors across an insulator is essential for electronics application of superconductors. In 1962, Josephson predicted a phenomenon of Cooper pair tunneling in a superconductor junction. This junction consists of two superconductor (S) layers that are separated by an insulating material. The tunneling phenomenon is called the Josephson effect, which was confirmed by Anderson and Rowell in 1963. In the absence of a bias voltage between the two S layers, the tunneling of a Cooper pair through the insulator in the junction leads to Josephson current. The Josephson current density at zero bias voltage is given by

$$J = J_c \sin\phi\,, \tag{1.1}$$

where J_c is the critical current density which depends on the physical properties of the junction, and $\phi = \theta_1 - \theta_2$ is the phase difference between the order parameter of the two superconductor layers. Here θ_l denotes the phase of the order parameter for l-th superconductor layer. Note that the superconductor order parameter is represented by a complex variable ψ_l (i.e., $\psi_l = |\psi_l| \exp(\theta_l)$, where $|\psi_l|$ is the amplitude). The phenomenon described by the current-phase relation of Eq. (1.1) is called the DC Josephson effect. In other words, this effect represents a nonlinear current flow across the junction in the absence of bias voltage.

When a bias voltage is applied across the junction, a normal current begins to flow. The applied bias voltage is related to the temporal dependence of the phase difference. Applying a constant DC bias voltage V across the junction, the temporal dependence of the phase difference ϕ may expressed as

$$V = \frac{\Phi_0}{2\pi}\frac{d\phi}{dt}, \tag{1.2}$$

where $\Phi_0 = h/2e$ is the magnetic flux quantum. This relation between the voltage and phase difference indicates that the Josephson current oscillates with the frequency $\omega = 2\pi V/\hbar$. The phenomenon described by the voltage-phase relation of Eq. (1.2) is called the AC Josephson effect.

In device applications, the Josephson junctions may be separated into two types, depending on their length. The junction is either short or long depending on the size of the system relative to the Josephson magnetic length λ_J. This length $\lambda_J = \sqrt{\Phi_0/2\pi\mu_0 J_c d'}$ characterizes the scale in which an external magnetic field can yield a spatial variation in the phase difference. Here, μ_0 is the magnetic permeability of free space and d' is an effective thickness of the superconducting electrodes. Note that Josephson magnetic length λ_J is different than the London penetration depth λ_L. The London penetration depth is the length scale over which an external magnetic field can penetrate into the superconducting layer. If the length of the junction L_x is much shorter than the Josephson length (i.e., $L_x \ll \lambda_J$), then only the temporal dependence of the phase difference between the superconducting order parameters is important. This type of junction is called short Josephson junction (SJJ). Among many device applications of the SJJ, the superconducting quantum interference device (SQUID) is one of the well-known examples. The SQUID is used to measure very weak magnetic field of order of

hundredth of pico-tesla (i.e., 10^{-14} T) in a living organism. On the other hand, when the length L_x is much longer than the Josephson length (i.e., $L_x \gg \lambda_J$), then the spatial dependence of the phase difference is important in determining the junction property in a magnetic field. This type of junction is called long Josephson junction (LJJ). Among many device applications of LJJs, the Josephson vortex quantum bit may serve as a good candidate for realizing quantum computers [52] due to its long decoherence time. LJJs may be used in integrated digital circuits for fast digital information processing due to low heat generation. Also, Josephson flux-flow transistors and ultra-fast switches are other applications for LJJs.

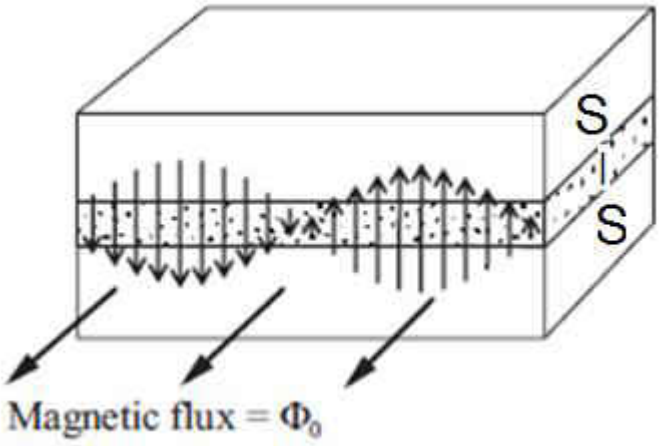

Figure 1. The effect of magnetic field on the tunneling currents in a uniform LJJ is schematically illustrated. Arrows indicate the strength and direction of Josephson currents.

When an external magnetic field is applied in a LJJ, a super-current flows on the surface of the superconductor layers to screen out the field. On the other hand, the

Josephson current flows across the junction through the insulator. The applied magnetic field affects this tunneling current because the phase difference between the two superconducting layers varies with the position. The effect of magnetic field on the tunneling currents in a LJJ is illustrated in Fig. 1. The figure illustrates the spatial variation of the Josephson current in an external magnetic field. The Josephson current and the super-current are combined to form a current loop as shown below in Fig. 2. This current loop, which is called Josephson vortex or fluxon, contains one unit of magnetic flux quantum (i.e., Φ_o).

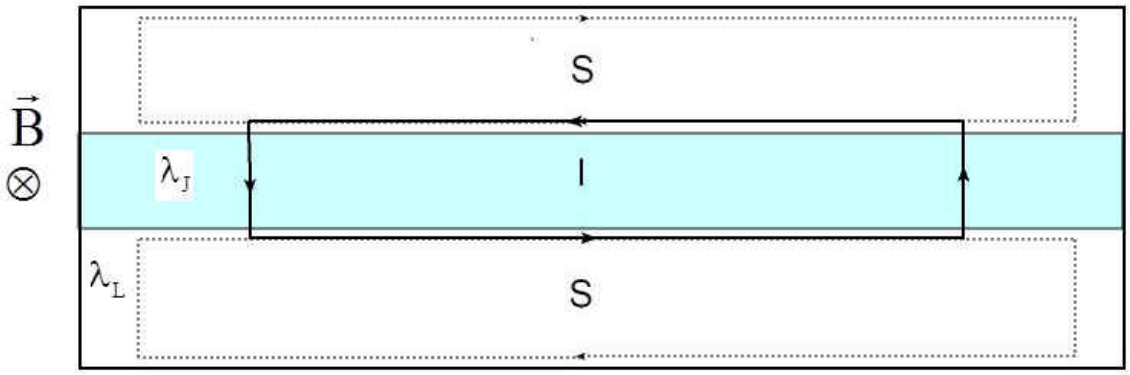

Figure 2. A schematic diagram of a long Josephson junction showing a circulating current loop due to super-current in the superconductor (S) layers and Josephson current in the insulator layer, forming a Josephson vortex is illustrated. The cross inside the circle indicates that the magnetic field is pointing into the page. $\boldsymbol{\lambda_L}$ and $\boldsymbol{\lambda_J}$ are London penetration depth and Josephson length, respectively.

For fabrication of a LJJ, various superconductors such as niobium [56], aluminum, MgB_2 and iron-pnictides may be used. As the junction property depends on the superconducting state, the nature of superconductivity in these materials can strongly influence the phase dynamics of a LJJ. This suggests that a LJJ with one-gap superconductors will have a different junction property that with two-gap

superconductors. In next section, the differences between the one-gap and two-gap superconductors as well as LJJ with these two types of superconductors are discussed. Also, the microscopic theory of the superconductivity for both one-gap and two-gap superconductors will be discussed.

1.2 BCS Theory: One-Gap and Two-Gap Superconductors

A single energy gap is present in one-gap superconductors. Hence, one gap superconductors have only one electronic band participating in superconductivity. Here, one-gap refers to the fact that there is only one type of superconducting condensate in the system, resulting in only one energy gap in the quasi-particle excitation spectrum. In general, for a superconductor that has one energy gap, the critical temperature (i.e., superconducting transition temperature) is lower than that for a multi-gap superconductor. The phase dynamics of a LJJ with one-gap superconductors, such as aluminum and lead, had been extensively studied by many authors [2, 40, 45, and 60]. For the LJJ with the one gap superconductors, there exists one possible tunneling channel between the two S layers. Therefore, a LJJ exhibits the conventional Josephson effect. Physics involving the fluxon dynamics in the LJJ has been studied extensively for the conventional one-gap superconductors. However the phase dynamics of LJJ with multi-gap superconductors has been much less studied [4, 5, 6].

As a way to understand the remarkable phenomenon of the sudden disappearance of electrical resistivity of a material at low temperature, the pairing theory for electrons was proposed. The temperature at which the electrical resistivity drops to zero is called the

critical temperature. At this temperature, the material changes its ground state from the normal to superconducting phase as the temperature is decreased. The critical temperature of a superconductor depends on the nature of the pairing interaction. The critical temperature of mercury, a well-known one-gap superconductor, is 4.1 K. Recently discovered multi-gap superconductors such as MgB_2 and iron-pnictides have a much higher critical temperature than that of the conventional S-wave one-gap superconductor.

Theoretical [50, 51, 58, 59, 64, 65, 66, 67] and experimental studies [49] suggest that a strongly anisotropic electron-phonon interaction for high density (E_{2g}) phonon. These specific modes couple strongly to the electrons in the σ-bands, rather than those in the π-bands, and play an important role in the superconducting state of MgB_2. From these studies indicate the evidence of two stable energy gaps. Note that the two-gap superconductivity allows the critical temperature to remain large. This useful property may be exploited in the device applications involving LJJs. Both MgB_2 and iron-pnictides have multiple gap energies, reflecting the presence of multiple condensates. Here the two-gap superconductor refers to the fact that the two electronic bands are participating in superconductivity. In Fig. 3, the electronic bands that participate in superconductivity are schematically illustrated as those crossing the Fermi energy ε_F. When one band crosses the Fermi energy as shown in Fig. 3a, only one condensate is form in the superconducting state. However, when two bands cross the Fermi energy as shown in Fig. 3b, two condensates are formed. Each condensate is represented by an order parameter. Hence MgB_2 and iron-pnictides have two-pseudo order parameters.

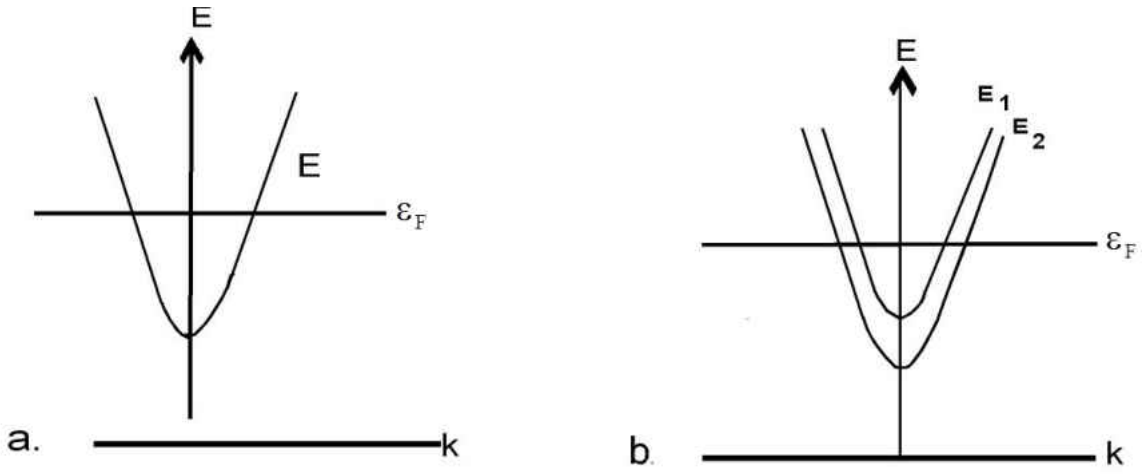

Figure 3. Energy spectrum of a single electron as a function of wave vector for (a) one-gap and (b) two-gap superconductor are schematically illustrated.

A microscopic description of the superconducting state for both one-gap and two-gap superconductors is possible by extending the theory of superconductivity, which is known as BCS theory, developed by Bardeen, Cooper, and Schrieffer in 1957 [28]. This BCS theory was used to model the property of type-I superconductors successfully. According to the BCS theory, electrons that are close to the Fermi-level form into pairs known as Cooper pair. The pairing interaction between the electrons is mediated by the crystal lattice vibration (i.e., phonon). Due to the interaction between electrons and phonons, an effective attractive interaction between electrons appears. Although electrons are fermions and obey the Pauli's exclusion principle, the Cooper pairs behave like bosons are therefore they can condense into the same lowest energy state.

For an one-gap superconductor, the BCS Hamiltonian for a type-I superconductor in the momentum-space representation is given by

$$\widehat{H}_{BCS} = \sum_k \varepsilon_k \, c_{k\sigma}^{\dagger} c_{k\sigma} - \sum_{kk'} V_{kk'} \, c_{k\uparrow}^{\dagger} c_{-k\downarrow}^{\dagger} c_{-k'\downarrow} \, c_{k'\uparrow} \tag{1.3}$$

where $V_{kk'}$ is the pairing matrix element. Here, $\varepsilon_k = (\hbar^2 k^2/2m) - \varepsilon_F$ is the kinetic energy. The second term in Eq. (1.3) is the pairing interaction Hamiltonian, which indicates that two electrons with an up-spin in the *–k'* state and a down-spin in the *k'* state are destroyed, while two electrons with a down-spin in the *k* state and an up-spin in the *–k* states are created. Note that $c_{k\sigma}^{\dagger}$ and $c_{k\sigma}$ denote, respectively, an operator which creates and destroys an electron with the momentum *k* and spin σ. These fermion operators obey the anti-commutation relation

$$\left\{c_{k\sigma}, c_{k'\sigma'}^{\dagger}\right\} = c_{k\sigma}c_{k'\sigma'}^{\dagger} + c_{k'\sigma'}^{\dagger}c_{k\sigma} = \delta_{kk'}\delta_{\sigma\sigma'}, \tag{1.4}$$

and

$$\{c_{k\sigma}, c_{k'\sigma'}\} = \left\{c_{k\sigma}^{\dagger}, c_{k'\sigma'}^{\dagger}\right\} = 0. \tag{1.5}$$

The particle number operator $n_{k\sigma}$ is given by $n_{k\sigma} = c_{k\sigma}^{\dagger} c_{k\sigma}$. Within the BCS theory, one can obtain the ground state energy and quasi-particle energy spectrum of the system. The mean-field theory of the BCS model can be solved by making a rotational transformation to diagonalize the Hamiltonian. This rotation of the Hamiltonian is called Bogoliubov transformation.

The BCS theory can be extended to multi-band systems. Applying the Bogoliubov transformations, Suhl *et al.* obtained the critical temperature for multi-band systems. In a two-gap superconductor, there are two types of superconducting condensates in the system, yielding two pseudo-order parameters. Hence, the BCS model for a one-gap superconductor must be extended to account for these two condensates. The BCS Hamiltonian for the two-gap superconductor is given by

$$\widehat{H}_{TB,l} = \sum_i \varepsilon^i \, c_{\sigma,l}^{i\dagger} c_{\sigma,l}^{i} + \widehat{H}_l^{pair}, \tag{1.6}$$

where $i = s, d$ denotes that electronic bands that participate in pairing interaction. Here the pair interaction contribution to the Hamiltonian is given by

$$\hat{H}_l^{pair} = -V_{ss} c_{\uparrow,l}^{s\dagger} c_{\downarrow,l}^{s\dagger} c_{\downarrow,l}^{s} c_{\uparrow,l}^{s} - V_{dd} c_{\uparrow,l}^{d\dagger} c_{\downarrow,l}^{d\dagger} c_{\downarrow,l}^{d} c_{\uparrow,l}^{d} - V_{sd}\left(c_{\uparrow,l}^{s\dagger} c_{\downarrow,l}^{s\dagger} c_{\downarrow,l}^{d} c_{\uparrow,l}^{d} + h.c.\right). \qquad (1.7)$$

Here, for definiteness, the superscripts s and d are used to represent the two electronic bands. The last term of Eq. (1.7) accounts for the pair interaction between electrons in the s and d bands. Here the $c_{\uparrow,l}^{s\dagger} c_{\downarrow,l}^{s\dagger} c_{\downarrow,l}^{s} c_{\uparrow,l}^{s}$ term indicates that a Cooper pair in the s-band of the l-th S layer is destroyed while another Cooper-pair is created in the same band. Similarly, the $c_{\uparrow,l}^{d\dagger} c_{\downarrow,l}^{d\dagger} c_{\downarrow,l}^{d} c_{\uparrow,l}^{d}$ term represents creation of a Cooper pair by destroying another Cooper pair in the same d-band. Also, the $c_{\uparrow,l}^{s\dagger} c_{\downarrow,l}^{s\dagger} c_{\downarrow,l}^{d} c_{\uparrow,l}^{d}$ term represents tunneling of a Cooper from the d-band to s-band and depends on the phase of the two condensates.

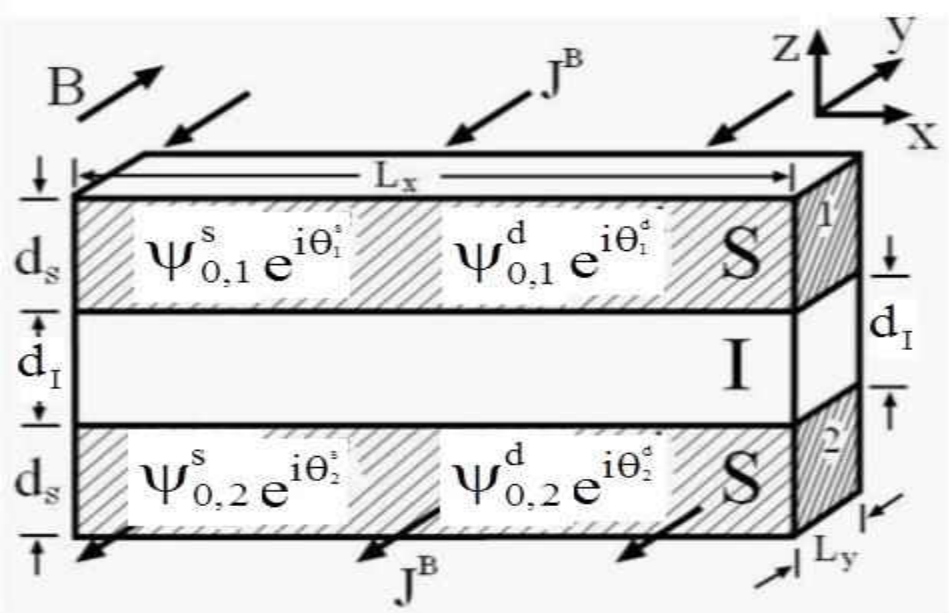

Figure 4: A schematic diagram for a LJJ with two-gap superconductors is illustrated.

The inter-band phase difference in the two-gap superconductors can lead to a different tunneling property than that for one-gap superconductors. This difference is

attributed to the two tunneling channels for electrons in two-gap superconductor junctions due to the presence of two condensates. This internal freedom reflects the number of electronic bands participating in superconductivity. Therefore, the phase dynamics of the order parameters for the two-gap superconductor tunnel junction, as illustrated in Fig. 4, differs from that of the one-gap superconductor junction. In Fig. 4, a LJJ with a two-gap superconductor, represented by two pseudo-order parameters $\psi_{0,l}^{s}\exp(i\theta^{s})$ and $\psi_{0,l}^{d}\exp(i\theta^{d})$, is shown schematically. Here, L_x and L_y denote the dimensions of the junction in the x- and y- direction, respectively. Note that J^B is the bias current density and B is the externally applied magnetic field. The thickness of both the S and I layer are denoted by d_S and d_I, respectively. There are two tunneling channels between the two superconducting layers. One channel is between the two *s*-bands of two adjacent layers and other is the channel between the *s*-band of one layer and *d*-band of the other layer. When an electron tunnels leaving one band, a hole is created in that band. The presence of two tunneling channels in the LJJ shows that there are two types of relative phase dynamics. These phase dynamics are due to the interplay between the inter-band Josephson effect and the conventional Josephson effect. The inter-band Josephson effect describes tunneling between two electronic bands in the same S layer. This effect determines the dynamics of the phase difference between the two condensates. On the other hand, the conventional Josephson effect describes tunneling between two adjacent S layers. This effect determines the dynamics of the phase difference across two adjacent S layers. The effects due to two tunneling channels in a LJJ, as shown in Fig. 4, may appear in measurable physical quantities such as changes in

the macroscopic quantum tunneling rate and the presence of extra step structure [17], in addition to the conventional Shapiro steps, in the current voltage (I-V) characteristics.

The phase dynamics of a LJJ may depend on the symmetry of the superconducting order parameter. As suggested by Ota and coworkers, the gap symmetry can affect [12] the Josephson current across the grain boundaries in poly-crystalline samples as well as the current-voltage (I-V) characteristics of the multi-gap intrinsic LJJ stacks. In the two-gap superconductor based LJJ, multiple channels are expected for superconducting tunneling current between the two superconducting electrodes. Two-gap superconductor has two types of pairing symmetry. The ground state of the system is the phase-locked state. If the two S-wave pseudo-order parameters have the same phase in σ- and π-band, then there will be 0-phase locked between holes and electrons. This is the S_{++} pairing symmetry. Similarly, if the two bands are in opposite phase, then there will be π-phase locked between the electrons and holes. This is the S_{+-} pairing symmetry.

The fluctuations about the phase-locked state of the two condensates can arise. When these fluctuations are small, the inter-band Josephson effect can yield collective excitation [5]. In a multi-gap superconductor, there are two small phase oscillation modes: the in-phase and out-of-phase mode. The out-of phase mode is called the Josephson-Leggett (JL) mode, and the in-phase mode is called the Josephson-plasma mode. Blumberg and coworkers observed the JL mode in MgB_2, using Raman scattering [4]. Theoretical studies of a hetero-Josephson junction suggest that the phase dynamics of a LJJ are affected by the JL mode since the total energy of the two-gap superconductors depends on the relative phase of the two condensates as well as the relative density of electrons.

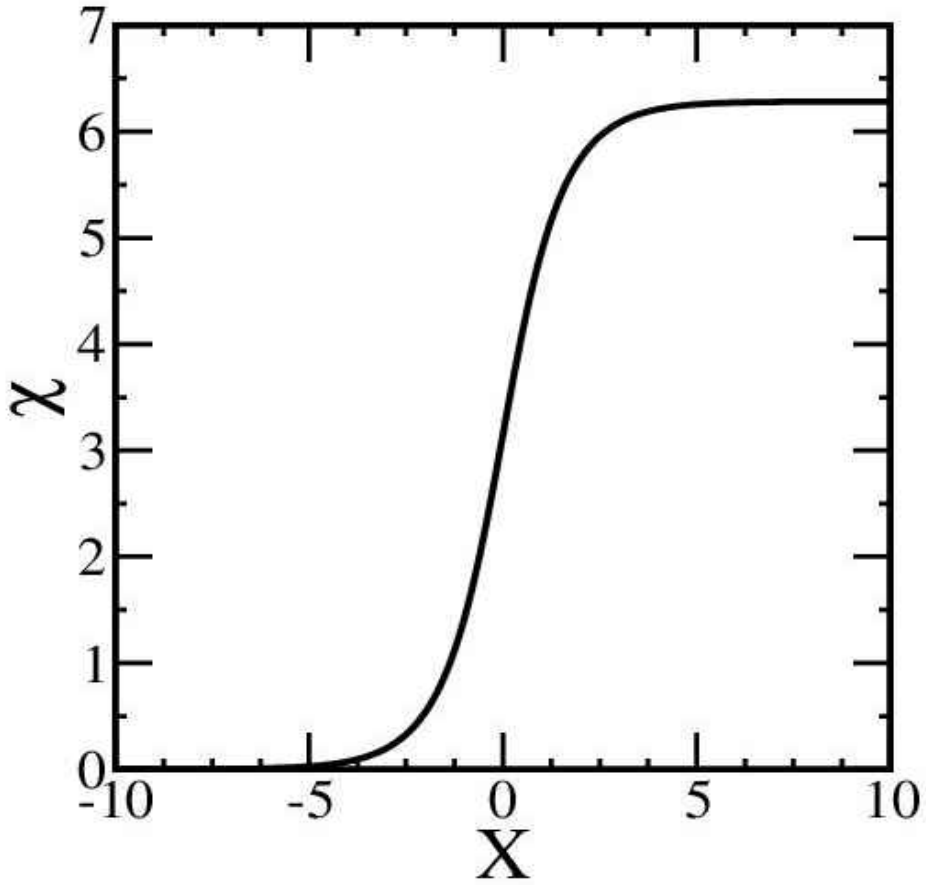

Figure 5. Relative phase difference χ of two pseudo-order parameters is plotted as a function of position x to illustrate the single-kink solution.

Fluctuations about the phase-locked state may not necessarily remain small, but they may become large. Tanaka and coworkers claim that when the amplitude of relative phase fluctuation grows to the non-linear region and becomes stabilized, excitation of an *i*-soliton can change the amplitude of the critical current density [21]. Results of the magnetic response of a superconducting ring experiment with two pseudo-order parameters by H. Bluhm and co-workers indicate that a stable soliton-shaped phase difference χ between the two condensates is attainable [18]. This result supports the suggestion that the phase fluctuations can grow and produce a 2π-phase texture [19]. The

i-soliton is the topological excitation of the phase fluctuation in which the inter-band phase difference rotates by 2π, as shown in Fig. 5. The *i*-soliton does not carry a magnetic flux. The excitation of *i*-soliton represents the phase fluctuations due to the inter-band Josephson effect which is the hallmark of multi-gap superconductors.

Kupulevaksky and coworkers explored soliton states in two-gap superconductors in mesoscopic thin-walled cylinders in external magnetic fields by using the Ginzburg-Landau approach [22]. Tanaka and coworkers [21] suggested that a phase domain surrounded by *i*-soliton wall, can arise in two dimensions since an *i*-soliton may be considered as a one-dimensional quantum phase dislocation. Also, an *i*-soliton wall may carry a fractional flux quantum when one end of the soliton wall is terminated by the fractional vortex while the other end is attached to a sample edge [21]. A vortex-molecule may be formed when two fractional vortices, with a unit fluxoid quantum as the total magnetic flux, are connected by an *i*-soliton bond [23]. These fractional vortices have been observed in a multi-layered superconductor by using both magnetic force and scanning Hall probe microscopy [31].

The *i*-solitons are different than the fluxons (i.e., Josephson vortices). A Josephson vortex arises due to the tunneling of Cooper pair between two separate superconductors, but the *i*-soliton arises due to the interaction between particles within the same superconductor. Also, the fluxons have one unit of magnetic flux quantum, but the *i*-solitons do not carry any magnetic flux. Hence, they do not interact with either magnetic field or super-currents. However, an *i*-soliton may be formed and driven by a non-equilibrium charge density or by sufficiently strong superconducting currents. From the study of phase texture in a weakly coupled multilayer structure and two-gap

superconductors, Gurevich and Vinokur suggested that spontaneous appearance of a soliton-like phase texture represents the breakdown of phase-locked state. This breakdown can arise when the applied current density along the superconductor layers exceeds the critical value [24].

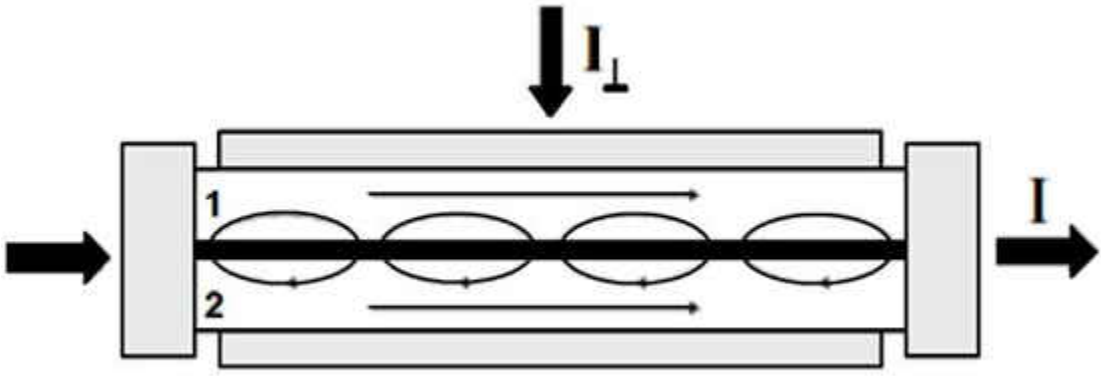

Figure 6. Formation of phase texture in current carrying bi-layer [24] is shown schematically. The bold line indicates the interlayer Josephson contact and the gray rectangles represent the current leads.

The effects of phase fluctuations may appear as either additional resonances in the AC Josephson effect or a static 2π-kink in the phase difference. If the 2π-phase texture exists in each S layer, then this *i*-soliton may change the phase dynamics of the LJJ by inducing a critical current density modulation [68]. In Fig. 6, the formation of phase textures in current-carrying bi-layer is illustrated. Here, the bold line indicates the interlayer Josephson contact and the gray rectangles represent the current leads. Previous studies [6, 23, 24, 25, 48, 69] show that a moving fluxon can radiate electromagnetic (EM) waves when its speed varies due to the bias current larger than the critical

(threshold) value. The interference between the emitted EM waves can rise to clearly discernible steps in the I-V characteristics. This suggests that, if the critical current modulation is generated by large fluctuations of the phase difference, this may affect the properties of the junction due to change in the phase dynamics.

1.3 Broken Time Reversal Symmetry State

The dynamics of the relative phase of the two condensates may produce an interesting phenomenon in the ground state of the system. One of these interesting properties is a broken time reversal symmetry state. In the absence of external magnetic field, there are no net currents in the ground state of a LJJ. However, in the LJJ with one-gap and two-gap superconductor layer, the ground state satisfies the condition of no net current density via maintaining the inter-band phase difference of either 0 or π. This state is called the time-reversal symmetry invariant (TRSI) state. On the other hand, if the phase difference between the two condensates differs from either 0 or π, then system is said to have phase frustration. When the phase frustration is maintained, the ground state may have non-zero current density in the absence of an external magnetic field while satisfying the condition of zero net current flow. This ground state is called the broken time-reversal symmetry (BTRS) state. Theoretical studies of superconductor-insulator-superconductor (hetero-Josephson) junctions between one- and two-gap superconductors suggest that the [15] the time-reversal symmetry is violated in the ground state.

The relative phases of the condensates in the ground state reflect the time-reversal symmetry of the junction. To study the TRSI and BTRS state, one needs to focus on the

phase frustration. The time-reversal symmetry breaking within two-gap superconductors was studied by Tanaka *et al*. [32] and Lin *et. al*. [33]. They realized that when the inter-band interaction is very weak compared with the intra-band interaction, it can break time-reversal symmetry as a result of competition between inter-band Josephson and biquadratic interaction. The inter-band Josephson interaction tends to lock the relative phase to either 0 or π, while the biquadratic interaction tends to lock the relative phase to $\pm\pi/2$. Tanaka and coworkers claim that when the inter-band coupling J is greater than zero (i.e. $J > 0$), the Josephson interaction in the S_{++}-symmetry state will lock the relative phase χ to 0. However, when $J < 0$, the Josephson interaction in the S_{+-}-symmetry state will lock the relative phase to π. If the phase difference between two condensates differs from the phase-locked value of either 0 or π, then there is phase frustration which breaks the time-reversal symmetry in the ground state.

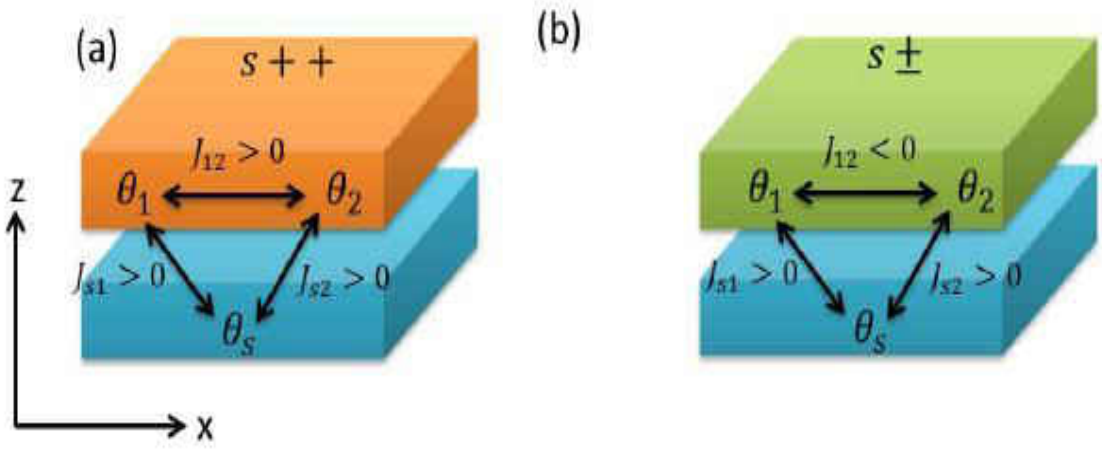

Figure 7: Josephson junction between two-gap superconductors with (a) S_{++} and (b) S_{+-} pairing symmetry and s-wave one-gap superconductor [33].

Phase frustration may also occur in a Josephson junction. This situation is similar to a two-gap superconductor with both inter-band Josephson and biquadratic interaction. A

junction between a two-gap superconductor with either the S_{++} or S_{+-}-symmetry and a conventional S-wave superconductor may yield a different behavior due to either absence or presence of phase frustration, respectively. In Fig. 7a, the Josephson junctions between two-gap superconductor with the S_{++} pairing symmetry (i.e., $J > 0$) and one-gap S-wave superconductor is illustrated. In this case the effective interaction between condensates is attractive, and they have the same phase (i.e., $\theta_1 = \theta_2 = \theta_s$). This means that there is no phase frustration, and the time-reversal symmetry is preserved. Similarly, a junction between a two-gap superconductor with the S_{+-}-symmetry ($J < 0$) and a one-gap S-wave superconductor is illustrated in Fig. 7b. The effective interaction between condensates is repulsive, and their phases are not the same in the ground state.

The phase frustration and the BTRS state can also be described in terms of boundary conditions in the junction interface. Boundary conditions in the junction interface are described in terms of current density of the individual condensate. When the non-zero individual currents satisfy the condition of zero net current flow in the ground state, the system is strongly frustrated, resulting in broken time-reversal symmetry state. In Chapter III, the time reversal symmetry invariant and broken time-reversal symmetry state in junction with two-gap superconductors will be investigated.

1.4 Coupled Long Josephson Junctions

Another interesting aspect of a LJJ is the phase dynamics of coupled junctions. When a multiple number of coupled junctions are stacked vertically, the single LJJ property which was discussed above may be enhanced. For one-gap superconductors, there have

been numerous studies of phase dynamics in a stack of long Josephson junctions [34, 36, 37, 38, 57]. Machida *et al.* proposed [34] a theoretical model for describing the superconducting phase and charge dynamics in intrinsic LJJ stacks. Starting with a BCS Hamiltonian and using functional integral formalism and accounting for the low energy fluctuations in the very thin superconductor layers, Machida *et al.* obtained the effective action for the system. Using the Euler-Lagrange equation for relevant variables, they derived the equations of motion for the relative phases. In a stack of LJJs, conventional Josephson tunneling as well as magnetic induction interaction between the junctions determines the dynamics of the phase difference. Here, the magnetic induction coupling arises as the induced magnetic field of the super-current in one S layer affects the magnetic field of the adjacent S layers. The magnetic induction coupling between the junctions induces the collective dynamics of the fluxons in the presence of the bias current. If the thickness of the superconductor layers is comparable to the charge screening length, then the charging effect is not negligible. In this case, the capacitive coupling between junctions may also have to be accounted for. Machida *et al*.[34] and Sakai *et al*. [35-36] obtained the set of coupled equations of motion for the phases by using two different approaches. These two approaches had been shown to yield an identical result when the charging effect is neglected.

The outline of the remainder of this dissertation work is as follows. In Chapter II, fluxon dynamics in a LJJ with two-gap superconductors is discussed. In Chapter III, the time reversal symmetry invariance and broken time-reversal symmetry state in the ground state of a single LJJ with two superconductors is reported. In Chapter IV, the

magnetic induction coupling effect is used to derive the equation of motion for a fluxon in coupled LJJs with two-gap superconductors. The result of this work is discussed in Chapter V. Finally, the conclusions of the dissertation work are presented in Chapter VI.

CHAPTER II

FLUXON DYNAMICS OF LJJS WITH TWO-GAP SUPERCONDUCTORS

In this chapter, the equation of motion for the phase difference is derived by starting from the microscopic model for two-gap superconductors. Namely, the phase dynamics in the long Josephson junction (LJJ) is described by using BCS theory. For LJJ, with two-gap superconductors, variation in the relative phase of condensates in the two electronic bands plays an important role in characterizing the junction property. To study the effect of inter-band Josephson effect in the fluxon dynamics, the equation of motion for the inter-band phase difference is derived. Also, the effect of large fluctuations in the relative phase on the phase dynamics is discussed.

2.1 Theoretical Model for Phase Dynamics

In this section, a microscopic model is used to describe the LJJ. Namely, the superconductor layers are described by the BCS Hamiltonian while the dissipation and boundary effects of the junction are neglected for simplicity. In Chapter V, these effects, which account for realistic LJJs, are included in numerical calculations. The model Hamiltonian $\widehat{H}$ for describing superconductivity in each superconductor (S) layer is expressed as a sum of two contributions: $\widehat{H} = \widehat{H}_{TB,l} + \widehat{H}_T$. The Hamiltonian $\widehat{H}_{TB,l}$ denotes the contribution due to two-gap superconductivity while the Hamiltonian $\widehat{H}_T$

accounts for electron tunneling between the two adjacent S layers. One may write the Hamiltonian $\widehat{H}_{TB,l}$ for the two-gap superconductor as

$$\widehat{H}_{TB,l} = \int dr\left(\sum_i \varepsilon^i \, c_{\sigma,l}^{i\dagger} c_{\sigma,l}^{i} + \widehat{H}_l^{pair}\right), \tag{2.1}$$

where ε^i is the energy of electrons in the i-band (i = s, d) about the Fermi energy. For definiteness, it is assumed that s and d are the two electronic bands that participate in superconductivity. The Hamiltonian $\widehat{H}_l^{pair}$ accounts for the pairing interaction between electrons in the l-th S layer and may be written as

$$\widehat{H}_l^{pair} = -V_{ss} c_{\uparrow,l}^{s\dagger} c_{\downarrow,l}^{s\dagger} c_{\downarrow,l}^{s} c_{\uparrow,l}^{s} - V_{dd} c_{\uparrow,l}^{d\dagger} c_{\downarrow,l}^{d\dagger} c_{\downarrow,l}^{d} c_{\uparrow,l}^{d} - V_{sd}\left(c_{\uparrow,l}^{s\dagger} c_{\downarrow,l}^{s\dagger} c_{\downarrow,l}^{d} c_{\uparrow,l}^{d} + h.c.\right), \tag{2.2}$$

where V_{ij} is the pairing interaction matrix element for the electrons in i and j-bands. Also, $c_{\sigma,l}^{i\dagger}$ and $c_{\sigma,l}^{i}$ denote the creation and annihilation operators for an electron with spin σ in i-band. The Hamiltonian $\widehat{H}_T$ describes the electron tunneling between the two adjacent S layers and is expressed in terms of tunneling matrix element T_{ij} for an electron from j to i-band as

$$\widehat{H}_T = \sum_{\sigma,i\neq j}\left(T_{ij} c_{\sigma,1}^{i\dagger} c_{\sigma,2}^{j} + h.c.\right). \tag{2.3}$$

In the discussion below, theses Hamiltonians $\widehat{H}_{TB,l}$ and $\widehat{H}_T$ are used to account for interesting phase dynamics in LJJ with two-gap superconductors.

One interesting hallmark of two-gap superconductivity is an inter-band Josephson effect between electrons in the two different electronic bands within the same S layer. The inter-band pairing interaction describes the Josephson effect due to tunneling of the condensates between the two bands. The presence of inter-band Josephson effect in a multi-gap superconductor had been suggested by Leggett. By following Leggett [5], one

can see that the eigenvalues of the pairing operator $\hat{\psi}_l^i$ may be introduced to express the free energy contribution from the two-band Hamiltonian $\hat{H}_{TB,l}$ as

$$\hat{H}_{TB,l} = f_l^s(|\psi_l^s|^2) + f_l^d\left(|\psi_l^d|^2\right) - V_{ss}|\psi_l^s|^2 - V_{dd}\left|\psi_l^d\right|^2 - J, \tag{2.4}$$

where $f_l^i\left(|\psi_l^i|^2\right)$ corresponds to the kinetic energy of electrons in the *i*-band. The complex pseudo-order parameter ψ_l^i for a two-gap superconductor is given by

$$\psi_l^i = \left|\psi_l^i\right| e^{i\theta_l^i}. \tag{2.5}$$

In Eq. (2.4), the J term accounts for the contribution from inter-band Josephson-coupling. This contribution arises as a result of the pairing interaction between the electrons in *s* and *d* electronic bands which are participating in superconductivity. This term depends explicitly on the relative phase of the two pseudo-order parameters. The inter-band Josephson-coupling term is given by

$$\begin{aligned} J_l &= V_{sd}\left(\psi_l^{s*}\psi_l^d + \psi_l^{d*}\psi_l^s\right) \\ &= 2V_{sd}|\psi_l^s|\left|\psi_l^d\right|\cos\chi_l, \end{aligned} \tag{2.6}$$

where $\chi_l = \theta_l^d - \theta_l^s$ is the phase difference between the pseudo-order parameters representing two superconducting condensates. It is straightforward to see that when there is no inter-band pairing interaction between electrons (i.e., $V_{sd} = 0$), the order parameters which minimize the free energy of Eq. (2.4) can be considered as being independent. However, the non-zero inter-band interaction between electrons in the two-bands of the same S layer will be considered in this work.

The conditions for minimizing the free energy yield the coupled gap equations of the form

$$\Delta_l^i = \sum_j V_{ij}\,\psi_l^j\ . \tag{2.7}$$

It is straightforward to see that the relative phase χ for the non-trivial solutions of this coupled gap equations are either $\chi = 0$ or π. These solutions $\chi_l = 0$ and π represent the phase-locked states and correspond to the S_{++} (for $V_{sd} > 0$) and S_{+-} (for $V_{sd} < 0$) pairing symmetry state, respectively.

Due to the presence of various other interactions in the system, small as well as large phase fluctuations about the phase-locked state can occur in the two-gap superconductors. These fluctuations can yield small phase oscillations when the amplitude is small and can lead to 2π-phase textures which may appear as kinks in χ_l when the amplitude is large. These phase textures can modify the phase dynamics of LJJ by causing resonances in the AC Josephson effect when two electronic bands are not in equilibrium. The effects of the phase textures can be examined by using the functional integral formulation. The partition function Z for the LJJ in the presence of electromagnetic field is given by

$$Z = Tr\, e^{-\beta H}\,, \tag{2.8}$$

where $\beta = 1/T$ and T is the absolute temperature. For simplicity, the fundamental constants are set to unity: $\hbar = c = k_B = 1$. The Hamiltonian $\widehat{H}$ of Eq. (2.1) is used to derive the Ginzburg-Landau free energy for the two-gap superconductor by writing the partition function Z in terms of Grassmann variables $\bar{c}^i_{k,\sigma}$ and $c^i_{k,\sigma}$ as

$$Z = \int D[\bar{c}^s, c^s] D[\bar{c}^d, c^d] e^{-S[\bar{c}^s, c^s, \bar{c}^d, c^d]}, \tag{2.9}$$

where the action S is given by

$$S = \int_0^\beta d\tau \left[\sum_{i,k,\sigma} \left(\bar{c}^i_{k,\sigma} \partial_\tau\, c^i_{k,\sigma}\right) + H\right], \tag{2.10}$$

where $\partial_\tau = \partial/\partial\tau$. The momentum-space representation of the BCS Hamiltonian for the two-gap superconductor in terms of Grassmann variables is given by

$$H = \sum_{k,\sigma} \left(\varepsilon_k^s \, \bar{c}_{k,\sigma}^s \, \partial_\tau c_{k,\sigma}^s + \varepsilon_k^d \bar{c}_{k,\sigma}^d \partial_\tau \, c_{k,\sigma}^d\right)$$

$$- \sum_{kk'} V_{kk'}^{ss} \, \bar{c}_{k,\uparrow}^s \bar{c}_{-k,\downarrow}^s \, c_{-k',\downarrow}^s \, c_{k',\uparrow}^s \; - \; \sum_{kk'} V_{kk'}^{dd} \, \bar{c}_{k,\uparrow}^d \bar{c}_{-k,\downarrow}^d \, c_{-k',\downarrow}^d \, c_{k',\uparrow}^d$$

$$- \sum_{kk'} V_{kk'}^{sd} \left(\bar{c}_{k,\uparrow}^s \bar{c}_{-k,\downarrow}^s \, c_{-k',\downarrow}^d \, c_{k',\uparrow}^d + h.c.\right), \tag{2.11}$$

where $V_{kk'}^{ij}$ is the pairing interaction matrix element for the *i*- and *j*-band electrons. For describing the pairing interaction between electrons, it may be convenient to introduce the Nambu representation:

$$\bar{C}_k^i = \left(\bar{c}_{k,\uparrow}^i \;\; c_{-k,\downarrow}^i\right), \text{ and } \quad C_k^i = \begin{pmatrix} c_{k,\uparrow}^i \\ \bar{c}_{-k,\downarrow}^i \end{pmatrix}.$$

In this representation, the pair fields $\bar{A}_k^i$ and A_k^i are expressed as

$$\bar{A}_k^i = \bar{C}_k^i \tau_+ C_k^i, \tag{2.12}$$

$$A_k^i = \bar{C}_k^i \tau_- C_k^i, \tag{2.13}$$

by using Pauli matrices. Here $\tau_\pm = (\tau_1 \pm i\tau_2)/2$ and three Pauli matrices are given by

$$\tau_1 = \begin{pmatrix} 0 & 1 \\ 1 & 0 \end{pmatrix},$$

$$\tau_2 = \begin{pmatrix} 0 & -i \\ i & 0 \end{pmatrix},$$

$$\tau_3 = \begin{pmatrix} 1 & 0 \\ 0 & -1 \end{pmatrix}.$$

Substituting $\bar{C}_k^i$ and C_k^i into Eqs. (2.12) and (2.13), one can obtain the pair fields $\bar{A}_k^i$ and A_k^i as

$$\bar{A}_k^i = \bar{c}_{k\uparrow} \bar{c}_{-k\downarrow}, \tag{2.14}$$

$$A_k^i = c_{-k\downarrow} c_{k\uparrow}. \tag{2.15}$$

In the Nambu representation, one can rewrite the partition function *Z* as

$$Z = \int D[\bar{C}^s, C^s] D[\bar{C}^d, C^d] e^{-S[\bar{C}^s, C^s, \bar{C}^d, C^d]}, \tag{2.16}$$

where the action S is given by

$$S = \int_0^\beta d\tau \ \ \sum_k \left[\bar{C}_k^s (\partial_\tau I + \varepsilon_k^s \tau_3) C_k^s + \bar{C}_k^d \left(\partial_\tau I + \varepsilon_k^d \tau_3\right) C_k^d\right]$$

$$- \int_0^\beta d\tau \sum_{kk'} \left[V_{kk'}^{ss} \bar{A}_k^s A_{k'}^s + V_{kk'}^{dd} \bar{A}_k^d A_{k'}^d + V_{kk'}^{sd} (\bar{A}_k^s A_{k'}^d + \bar{A}_k^d A_{k'}^s)\right]. \tag{2.17}$$

Here, the interaction contributions in the action S represent the two-body Coulomb interaction. As a way to reduce the two-body interaction terms, one needs to introduce the Hubbard-Stratonovich transformation. Before making this transformation, it is convenient to write the action S as

$$S = \int_0^\beta d\tau \ \sum_k \left[\bar{C}_k^s (\partial_\tau I + \varepsilon_k^s \tau_3) C_k^s + \bar{C}_k^d \left(\partial_\tau I + \varepsilon_k^d \tau_3\right) C_k^d\right]$$
$$- \int_0^\beta d\tau \ \sum_{kk'} (\bar{A}_k^s \quad \bar{A}_k^d) V_{kk'} \begin{pmatrix} A_k^s \\ A_k^d \end{pmatrix} \tag{2.18}$$

where $V = V_{kk'}$ is the pairing interaction matrix

$$V = \begin{pmatrix} V^{ss} & V^{sd} \\ V^{sd} & V^{dd} \end{pmatrix}. \tag{2.19}$$

The Hubbard-Stratonovich transformation maps the two-body interaction terms into non-interacting terms by introducing an auxiliary field (i.e., the Hubbard-Stratonovich field) representing electron pairing. For complex auxiliary fields $\phi = \phi_1 + i\phi_2$ and $\bar{\phi} = \phi_1 - i\phi_2$, it is straightforward to see that

$$\int d\phi_1 d\phi_2 \ e^{-\frac{(\phi_1^2 + \phi_2^2)}{V}} = \pi V \ ,$$

indicating that unity may be express in terms of these complex fields as

$$\int \frac{d\bar{\phi} \, d\phi}{2\pi i V} e^{-\frac{\bar{\phi}\phi}{V}} = 1 \ . \tag{2.20}$$

This relation, along with the transformations

$$\bar{A}_k = (\bar{A}_k^s \quad \bar{A}_k^d), \text{ and } \quad A_k = \begin{pmatrix} A_k^s \\ A_k^d \end{pmatrix},$$

may be used to rewrite the partition function Z and the action S as

$$Z = \int D[\bar{C}, C] D[\bar{\phi}, \phi] e^{-S[\bar{C}, C, \bar{\phi}, \phi]} \tag{2.21}$$

and

$$S = \int_0^\beta d\tau \{\sum_k [\bar{C}_k^s (\partial_\tau I + \varepsilon_k^s \tau_3) C_k^s + \bar{C}_k^d (\partial_\tau I + \varepsilon_k^d \tau_3) C_k^d] - \sum_{kk'} [\bar{\phi}_k V^{-1} \phi_{k'} + \bar{A}_k V^{-1} A_{k'}]\}, \tag{2.22}$$

respectively. By shifting the auxiliary fields ϕ and $\bar{\phi}$ (i.e., $\bar{\phi}_k \to \bar{\phi}_k + \bar{A}_{k'} V$ and $\phi_k \to \phi_k + V A_{k'}$), one can rewrite the action S as

$$S = \int_0^\beta d\tau \left[\sum_{i,k} \bar{C}_k^i (\partial_\tau I + \varepsilon_k^i \tau_3) C_k^i + \sum_{k,k'} (\bar{\phi}_k V^{-1} \phi_{k'} + \bar{A}_k \phi_k + \bar{\phi}_k A_{k'})\right]. \tag{2.23}$$

Here, ϕ and $\bar{\phi}$ represent the two-component auxiliary fields

$$\bar{\phi}_k = (\bar{\phi}_k^s \quad \bar{\phi}_k^d) \text{ and } \quad \phi_k = \begin{pmatrix} \phi_k^s \\ \phi_k^d \end{pmatrix}.$$

The inverse of the interaction matrix, V^{-1}, may be written as

$$V^{-1} = \frac{1}{V^{ss} V^{dd} - (V^{sd})^2} \begin{pmatrix} V^{dd} & -V^{sd} \\ -V^{sd} & V^{ss} \end{pmatrix}. \tag{2.24}$$

Hence, one can express the $\bar{\phi}_k V^{-1} \phi_{k'}$ term in the action of Eq. (2.23) as

$$\bar{\phi}_k V^{-1} \phi_{k'} = \frac{V^{dd}}{det(V)} \bar{\phi}_k^s \phi_{k'}^s + \frac{V^{ss}}{det(V)} \bar{\phi}_k^d \phi_{k'}^d - \frac{V^{sd}}{det(V)} (\bar{\phi}_k^s \phi_{k'}^d + \bar{\phi}_k^d \phi_{k'}^s)$$

$$= \frac{\bar{\phi}_k^s \phi_{k'}^s}{g_{ss}} + \frac{\bar{\phi}_k^d \phi_{k'}^d}{g_{dd}} - \frac{g_{sd}}{g_{ss} g_{dd}} (\bar{\phi}_k^s \phi_{k'}^d + \bar{\phi}_k^d \phi_{k'}^s), \tag{2.25}$$

where $det(V) = 1/[V^{ss} V^{dd} - (V^{sd})^2]$ is the determinant of the matrix V, $g_{ss} = det(V)/V^{dd}$, $g_{dd} = det(V)/V^{ss}$, and $g_{sd} = det(V)\, V^{sd}/V^{dd}\, V^{ss}$. By substituting Eq. (2.25) into Eq. (2.23), one may evaluate the partition function of Eq. (2.16). The fermion freedom in the functional integral may be integrated out by performing Grassmann

integration. When the fermion degrees are integrated out, the effective action S_{eff} may be written as

$$S_{eff} = \int_0^\beta d\tau \sum_{k,k'} \left[\sum_i \frac{\bar{\phi}_k^i \phi_{k'}^i}{g_i} - \frac{g_{sd}}{g_{ss} g_{dd}} \left(\bar{\phi}_k^s \phi_{k'}^d + \bar{\phi}_k^d \phi_{k'}^s \right) \right] - \sum_i T_r ln G_i^{-1}. \quad (2.26)$$

Similarly the effective action for the LJJ with two-gap superconductors can be expressed as

$$S_{eff} = S_{gap} + S_{field} - Tr\hat{G}^{-1},$$

where the actions S_{gap} and S_{field} are the contribution from the pairing energy represented by the pseudo-order parameters and electromagnetic field, respectively. The fermion contribution of the $Tr\hat{G}^{-1}$ term is obtained by carrying out the functional integral over the Grassmann variables $\bar{C}$ and C. Here the inverse Green function $\hat{G}^{-1}$ is a 8×8 matrix which consists of a 4×4 matrix for each two-gap superconductor layer. One can extract the contribution to the action S involving the superconducting phase degree of freedom by doing the unitary transformation on the Green function and by taking only second order tunneling contributions [47, 48]. The phase contribution S_{phase} to the effective action S_{eff} can be obtained by using the imaginary-time functional integral approach [34]. As the phase contribution S_{phase} may be written as

$$S_{phase} = \int d\tau \int d\vec{r}\, L_{phase},$$

one can obtain the Lagrange density L_{phase} of the system from Eq. (2.26). A detailed discussion on the expansion of the $\sum_i T_r ln G_i^{-1}$ term of Eq. (2.26) may be found in appendix A. The phase contribution L_{phase} to the effective Lagrange density is needed to obtain the equation of motion for the fluxon. The Lagrange density L_{phase} (see appendix A) for describing the phase dynamics can be expressed as

$$L_{phase} = \frac{d_s}{8\pi e^{*2}} \sum_{i,l} \left[\frac{1}{\mu_i^2} \left(\frac{\partial \theta_l^i}{\partial \tau} + e^* A_l^0 \right)^2 + \frac{1}{\lambda_i^2} \left(\frac{\partial \theta_l^i}{\partial x} - e^* A_l^x \right)^2 \right]$$

$$+ \sum_{i,j} \frac{J^{ij}}{e^*} \cos\phi^{ij} + \sum_l \frac{J_{in}}{e^*} \cos\chi_l + L_{EM}, \quad (2.27)$$

where $e^*=2e$ is the charge of Cooper pair and d_s is thickness of the l-th superconductor layer. Here, $\mu_i = \sqrt{\lambda_{TF}^2/4\pi\epsilon_i}$ denotes the charge screening length, and $\lambda_i = \sqrt{m_i^0/4\pi n_i e^{*2}}$ denotes the magnetic penetration depth in the S layer. Here, $\lambda_{TF} = \sqrt{\pi a_0/4k_F}$ is the Thomas-Fermi screening length, ϵ_i is dielectric constant of the S layer, a_0 is Bohr's radius, and k_F is the Fermi vector. Also, J^{ij} is the critical current density between the electronic bands (i-th and j-th) of the adjacent S layers and J_{in} is the inter-band Josephson critical current density between the two bands of the same S layers. The phase difference of the order parameter in a magnetic field is denoted by $\phi^{ij} = \theta_1^i - \theta_2^j - e^* A_{1,2}^z$, where $A_{1,2}^z = \int_1^2 A^z(z)\, dz$. The inter-band critical current density between the two bands within the same S layer is given by

$$J_{in} = 2e^* \frac{V^{sd}\psi^s\psi^d}{V^{ss}V^{dd} - (V^{sd})^2}.$$

The critical current density between the i-th and j-th electronic bands in the two S layers is given by [34, 40, 47]

$$J^{ij} = -\frac{2e^*}{d_s\beta} \int d\tau \sum_n e^{-i\omega_n\tau} \sum_{kk'} T_{ij}^2 \frac{\Delta_k^i \Delta_{k'}^i}{\mathrm{E}_k^i \mathrm{E}_{k'}^i} \left\{ \frac{\mathrm{E}_k^i - \mathrm{E}_{k'}^i}{(\mathrm{E}_k^i + \mathrm{E}_{k'}^i)^2 + \omega_n^2} \left[f(\mathrm{E}_k^i) - f(\mathrm{E}_{k'}^i) \right] \right.$$

$$\left. + \frac{\mathrm{E}_k^i + \mathrm{E}_{k'}^i}{(\mathrm{E}_k^i + \mathrm{E}_{k'}^i)^2 + \omega_n^2} \left[1 - f(\mathrm{E}_k^i) - f(\mathrm{E}_{k'}^i) \right] \right\}, \quad (2.28)$$

where $\omega_n = 2n\pi/\beta$ is the Matsubara frequency. Here, $n = 0, \pm 1, \pm 2, ...$, and $\mathrm{E}_k^i = \left(\varepsilon_k^2 + \Delta_k^{i^2}\right)^{1/2}$ is the quasiparticle energy in the superconducting state, and $f(E)$ is the

Fermi function. The electromagnetic field contribution L_{EM} to the Lagrange density L_{phase} is

$$L_{EM} = \frac{d_I}{8\pi}\left[\epsilon\left(E^z_{l+1,l}\right)^2 + \left(B^y_{l+1,l}\right)^2\right], \tag{2.29}$$

where ϵ is the dielectric constant and d_I is the thickness of the insulator layer. Also, $E^z_{l+1,l}$ and $B^y_{l+1,l}$ denote electric and magnetic field in the insulator between the two adjacent S layers.

The equation of motion for the phase difference may be obtained by minimizing the action. As in classical mechanics, this minimization procedure leads to the Euler-Lagrange equation. The Euler-Lagrange equations for the variables $\theta^s_1, \theta^s_2, \theta^d_1, \theta^d_2, A^z_{1,2}$, $A^x_1, A^x_{2,} A^0_{1,}$ and A^0_2 take the following form:

$$\frac{\partial}{\partial t}\frac{\partial L}{\partial \dot{\theta}^i_l} - \frac{\partial}{\partial x}\frac{\partial L}{\partial \theta'^i_l} - \frac{\partial L}{\partial \theta^i_l} = 0\ , \tag{2.30}$$

where $\dot{\theta}^i_l$ and θ'^i_l denote the derivative of the phase θ^i_l with respect to time and position, respectively. Note that θ^i_l represents the phase of the pseudo-order parameter for the condensates in the *i*- band in *l*-th S layer. As the equations of motion may be described in terms of the phase differences ϕ^{ss}, ϕ^{dd} and χ_i, it is be useful to define the following phase differences of *l*-th two-gap S layer:

$$\chi_l = \theta^s_l - \theta^d_l,$$

$$\phi^{ss} = \theta^s_1 - \theta^s_2 - e^* A^z_{1,2},$$

$$\phi^{dd} = \theta^d_1 - \theta^d_2 - e^* A^z_{1,2}.$$

and

$$\phi^{sd} = \theta^s_1 - \theta^d_2 - e^* A^z_{1,2}.$$

Euler-Lagrange equations for different variables can be combined to obtain the coupled equation involving three phase variables. After some substitutions, one can show that this coupled equation has three contributions. One is contribution of phase difference between the two adjacent S layers ϕ^{ss} and other two are the contributions due to the relative phases χ_1 and χ_2 within the S layer. Therefore, the coupled equation can be represented as the sum of three parts as

$$P_1 + P_2 + P_3 = 0, \tag{2.31}$$

where

$$P_1 = a\epsilon \frac{\partial^2 \phi^{ss}}{\partial t^2} + b\epsilon \frac{\partial^2 \phi^{ss}}{\partial x^2} + \frac{2J^{ss}}{e^*} \sin \phi^{ss} + \frac{J^{sd}}{e^*} \sin(\phi^{ss} + \chi_2) + \frac{J^{ds}}{e^*} \sin(\phi^{ss} - \chi_1), \tag{2.32}$$

Note that Eq. (2.32) accounts for the contribution of phase difference between the two adjacent S layers ϕ^{ss}. From this equation it is clear that the contribution of ϕ^{ss} in the equation of motion is affected by inter-band Josephson effect. Other two contributions are

$$P_2 = a \frac{d_s d_I}{2\mu_d^2} \frac{\partial^2 \chi_1}{\partial t^2} - b \frac{d_s d_I}{2\lambda_d^2} \frac{\partial^2 \chi_1}{\partial x^2} + \frac{J_{in}}{e^*} \sin \chi_1, \tag{2.33}$$

and

$$P_3 = a \frac{d_s d_I}{2\mu_d^2} \frac{\partial^2 \chi_2}{\partial t^2} - b \frac{d_s d_I}{2\lambda_d^2} \frac{\partial^2 \chi_2}{\partial x^2} + \frac{J_{in}}{e^*} \sin \chi_2. \tag{2.34}$$

Note that P_2 and P_3 denote the phase difference equation for the pseudo-order parameters in the first and second S layer, respectively. Here, the constants a and b are given by

$$a = \frac{d_s \mu_d^2}{2\pi d_s d_I e^{*2}(\mu_s^2 + \mu_d^2) + 4\pi\epsilon \mu_s^2 \mu_d^2} \quad \text{and} \quad b = \frac{d_s \lambda_d^2}{2\pi d_s d_I e^{*2}(\lambda_s^2 + \lambda_d^2) + 4\pi \lambda_s^2 \lambda_d^2}, \tag{2.35}$$

The critical current density J^{ss} (J^{dd}) denotes the tunneling between two *s* (*d*)-bands of two adjacent S layers. The inter-band current density J_{in} accounts for the interaction between electrons in the two electronic bands of the same S layer. Note that due to creation and destruction of pair of particles in each electronic band, this process appears as if there is current density J_{in}, but this is not a physical current density.

In writing the equation of motion, it would be convenient to work with the dimensionless coordinates. Hence, for convenience, one can introduce new temporal and spatial coordinates as

$$\bar{t} = t\left[\frac{2\pi d_s d_I e^{*2}(\mu_s^2+\mu_d^2)+4\pi\epsilon\mu_s^2\mu_d^2}{d_s\mu_d^2}\right]^{\frac{1}{2}}, \tag{2.36a}$$

and

$$\bar{x} = x\left[\frac{2\pi d_s d_I e^{*2}(\lambda_s^2+\lambda_d^2)+4\pi\lambda_s^2\lambda_d^2}{d_s\lambda_d^2}\right]^{\frac{1}{2}}. \tag{2.36b}$$

Two other dimensionless coordinates used in the discussion below for convenience can be defined as follows:

$$x' = \left(\frac{2J^{ss}}{e^*}\right)^{1/2}\bar{x}, \quad \text{and} \quad t' = \left(\frac{2J^{ss}}{e^*}\right)^{1/2}\bar{t},$$

and

$$x'' = \left(\frac{2J_{in}\lambda_d^2}{e^* d_I d_s}\right)^{1/2}\bar{x}, \quad \text{and} \quad t'' = \left(\frac{2J_{in}\mu_d^2\epsilon}{e^* d_I d_s}\right)^{1/2}\bar{t}.$$

For simplicity, one may make an assumption that the relative phase in each superconductor is the same (i.e., $\chi_1 = \chi_2 = \chi$). This assumption implies that the phase differences $\phi^{ss}$and ϕ^{dd} between the superconductor layers are the same (i.e., $\phi^{ss} = \phi^{dd}$). With this assumption, one can simplify Eq. (2.31) by making simple substitutions

and one can obtain a coupled equation of motion for the phases in the dimensionless coordinates as

$$\frac{\partial^2\phi^{ss}}{\partial x'^2}-\frac{\partial^2\phi^{ss}}{\partial t'^2}-\left[1+\frac{J^{sd}}{J^{ss}}\cos\chi\right]\sin\phi^{ss}$$

$$+\frac{\partial^2\chi}{\partial x''^2}-\frac{\partial^2\chi}{\partial t''^2}-\sin\chi=0\,. \qquad (2.37)$$

The equation of motion of (2.37) shows that if one can obtain the sine-Gordon equation for relative phase χ phase dynamics in the LJJ becomes simpler. This is one of the important result of the present work.

2.2 Inter-band Josephson Effect

In this section, the equation of motion for the relative phase χ of the two condensates is shown to be described by the sine-Gordon equation. Note that this interesting point is due to the fact that the inter-band Josephson effect is present in the two-gap superconductors. As the sine-Gordon equation has a kink-solution, the single kink solution for the relative phase represents an *i*-soliton.

As a way to derive the sine-Gordon equation for the relative phase of two condensates, one may start with the two-band BCS Hamiltonian in the momentum-space [5] representation as

$$\widehat{H}_{TB}=\widehat{H}_0-E_0-V^{sd}\sum_{kk'}\left(c^{s\dagger}_{k\uparrow}c^{s\dagger}_{-k\downarrow}c^{d}_{-k'\downarrow}c^{d}_{k'\uparrow}+c^{d\dagger}_{k\uparrow}c^{d\dagger}_{-k\downarrow}c^{s}_{-k'\downarrow}c^{s}_{k'\uparrow}\right)$$

$$+\gamma K^2+E_{ng}, \qquad (2.38)$$

where $\widehat{H}_0$ denotes the BCS Hamiltonian for both *s* and *d* band electrons

$$H_0=\sum_k \varepsilon^s_k c^{s\dagger}_{k\uparrow}c^{s}_{k\uparrow}-V^{ss}\sum_{kk'}c^{s\dagger}_{k\uparrow}c^{s\dagger}_{-k\downarrow}c^{s}_{-k'\downarrow}c^{s}_{k'\uparrow}$$

$$+\sum_k \varepsilon_k^d c_{k\uparrow}^{d\dagger} c_{k\uparrow}^d - V^{dd} \sum_{kk'} c_{k\uparrow}^{d\dagger} c_{-k\downarrow}^{d\dagger} c_{-k'\downarrow}^d c_{k'\uparrow}^d \tag{2.39}$$

The γK^2 term in Eq. (2.38) denotes the contribution from the charge imbalance between the two condensates. This contribution depends on both the number of electrons in two condensates *N* and the equilibrium number N^o. This contribution can be written as

$$\gamma \hat{K}^2 = \gamma\left[\left(\hat{N}_s - N_s^0\right) - \left(\hat{N}_d - N_d^0\right)\right]^2, \tag{2.40}$$

where $\hat{K}$ is the relative density fluctuation operator of the system

$$\hat{K} = \left(\hat{N}_s - N_s^0\right) - (\hat{N}_d - N_d^0).$$

The number operator for the electrons in the *s* and *d*-bands are denoted by $\hat{N}_s$ and $\hat{N}_d$, respectively. Here, N_s^0 and N_s^0 denotes the number of electrons in *s* and *d*-band at equilibrium, respectively. The number of electrons in the *s* and *d*-band is determined by assuming that there is no tunneling between the electronic bands. Note that $\gamma = [(1/\rho_s) + (1/\rho_d)]/8$, where ρ_s and ρ_d are the densities of state for the *s* and *d*-band electrons at the Fermi energy, respectively. By noting that the total number of electrons of the system remains conserved (i.e., $N_s + N_d = N$) and by using the Ginzburg-Landau free energy obtained from the BCS Hamiltonian, one may write the Hamiltonian of the system in terms of the pseudo-order parameter $\psi_a$as [6]

$$H = \sum_i \left[f_i |\psi^i|^2 - J^{ii} |\psi^i|^2 - \frac{1}{2m_i} |(\frac{d}{dx} - ie^* A)\psi^i|^2 \right]$$

$$-2V^{sd}|\psi^s||\psi^d|\cos(\theta^s - \theta^d) + E_{ng} + \gamma K^2 \,, \tag{2.41}$$

where θ^i is the phase of the pseudo-order parameter, and f_i is a constant which depends on the *i*-band parameters. Here, the vector potential ***A*** is set to zero (i.e., ***A***=0) by assuming the absence of an external magnetic field. The relative density fluctuation ($\hat{K}$)

of the system is obtained by using the following two relations: i) the number-phase uncertainty relation

$$\left[\hat{K}, (\hat{\theta}^s - \hat{\theta}^d)\right] = -4i\ , \tag{2.42}$$

and ii) the Heisenberg equation of motion for the phase difference

$$\frac{d}{dt}\left(\hat{\theta}^s - \hat{\theta}^d\right) = -\frac{i}{\hbar}\left[\left(\hat{\theta}^s - \hat{\theta}^d\right),\ \hat{H}\right]. \tag{2.43}$$

Here, the phase difference $\hat{\theta}^s - \hat{\theta}^d$ commutes with other terms of the Hamiltonian except $\gamma\hat{K}^2$. This indicates that

$$\frac{d}{dt}\left(\hat{\theta}^s - \hat{\theta}^d\right) = -\frac{i}{\hbar}\left[\left(\hat{\theta}^s - \hat{\theta}^d\right), \gamma\hat{K}\right], \tag{2.44}$$

and

$$\hat{K} = \frac{1}{8\gamma}\frac{d}{dt}\left(\hat{\theta}^s - \hat{\theta}^d\right).$$

Hence, by substituting the expression for *K* and by using Eq. (2.41), one may obtain the Gibb's free energy for the superconducting state of the two-gap superconductor as

$$E = \sum_i \left[f_i\left|\psi^i\right|^2 - J\left|\psi^i\right|^2 - \frac{1}{2m_i}\left|\left(\frac{d}{dx}\psi^i\right)\right|^2\right]$$

$$-2V^{sd}|\psi^s||\psi^d|\cos\chi + \frac{1}{64\gamma}\left(\frac{d\chi}{dt}\right)^2 \tag{2.45}$$

where $\chi = \theta^d - \theta^s$. The Gibb's free energy of Eq. (2.45) may be minimized by setting $\partial E/\partial\chi = 0$ and by noting that

$$\psi^i = |\psi^i|e^{i\theta^i},$$

and

$$\left|\frac{d\psi^i}{dx}\right|^2 = \left|\psi^i\right|^2\left(\frac{d\theta^i}{dx}\right)^2.$$

Also, by using the condition

$$J_e = \sum_i \frac{e}{m_i}\left|\psi^i\right|^2\ \frac{d\theta^i}{dx} = 0 \tag{2.46}$$

that the super-current vanishes in the bulk superconductor, it is straightforward to relate θ^i's as

$$\theta^d = \begin{cases} -\frac{|\psi^s|^2}{|\psi^d|^2}\frac{m_d}{m_s}\theta^s\,, & \text{for } V^{sd} < 0 \\ -\frac{|\psi^s|^2}{|\psi^d|^2}\frac{m_d}{m_s}\theta^s + \pi\,, & \text{for } V^{sd} > 0 \end{cases} \tag{2.47}$$

Noting that the relative phase of the two condensates is $\chi = \theta^s - \theta^d + \delta_0\pi$, it is helpful to denote that δ_0=0 for $J_{in} > 0$ (i.e., S_{++}-symmetry) and that $\delta_0 = 1$ for $J_{in} < 0$ (i.e., S_{+-} -symmetry). After some simplification, one may obtain the sine-Gordon equation

$$\frac{|\psi^s||\psi^d|}{2V^{sd}(m_s|\psi^d|^2+m_d|\psi^s|^2)}\frac{\partial^2\chi}{\partial x^2} - \frac{1}{64\gamma V^{sd}|\psi^s||\psi^d|}\frac{\partial^2\chi}{\partial t^2} - \sin\chi = 0\,, \tag{2.48}$$

for describing the dynamics of the relative phase χ. As discussed above, it is convenient to write the equation of motion in dimensionless coordinates. Hence, one may introduce the following dimensionless coordinates:

$$x'' = \left[\frac{2V^{sd}(m_s|\psi^d|^2 m_d|\psi^s|^2)}{|\psi^s||\psi^d|}\right]^{1/2} x\,, \tag{2.49}$$

$$t'' = t(64\gamma V^{sd}|\psi^s||\psi^d|)^{1/2}. \tag{2.50}$$

The equation of motion for the relative phase χ written in terms of these dimensionless condensates yields the usual sine-Gordon equation

$$\frac{\partial^2\chi}{\partial x''^2} - \frac{\partial^2\chi}{\partial t''^2} - \sin\chi = 0. \tag{2.51}$$

A general single-soliton solution of Eq. (2.51) may be written as

$$\chi(x'', t'') = 4\arctan\left[\exp\left(\pm\frac{x''-v_0t''}{\sqrt{1-v_0^2}}\right)\right], \tag{2.52}$$

where v_0 is the speed of the soliton. This kink solution, which is known as the *i*-soliton, is identical to the functional form of the unperturbed fluxon. However, the property of an

i-soliton is different than that of the fluxon. Unlike *i*-solitons, each fluxon carries a unit of magnetic flux quantum and can be driven by the Lorentz force of the bias current. Note that the *i*-soliton cannot be driven by the bias current. The *i*-soliton solution describes the perturbation effect in the two-gap superconductor system where it may yield large amplitude fluctuations in the relative phase χ of the condensates.

The equation of motion of q. (2.51) for the relative phase χ indicates that Eq. (2.37) which describes the phase dynamics of the LJJ may be simplified. By substituting Eqs. (2.51) and (2.52) into Eq. (2.37), one may see that

$$\frac{\partial^2 \phi^{ss}}{\partial x'^2} - \frac{\partial^2 \phi^{ss}}{\partial t'^2} - \left[1 + \frac{J^{sd}}{J^{ss}} \cos\chi\right] \sin\phi^{ss} = 0, \tag{2.53}$$

indicating that the inter-band Josephson effect induces modulation in the critical current density. The critical current density modulation has two main effects. First, the shape of the fluxon may change, but for small modulation this effect is negligible. Second, the speed of the fluxon becomes modified because the critical current density modulation behaves as a scattering potential for fluxons. To make progress, one may substitute Eq. (2.52) into Eq. (2.37) by writing $\chi = 4\theta$, $\theta = \arctan[\exp(\pm\zeta)]$ and $\zeta = (x'' - v_0 t'')/\sqrt{1 - v_0^2}$ to obtain equation of motion in the dimensionless coordinates as

$$\frac{\partial^2 \phi^{ss}}{\partial x'^2} - \frac{\partial^2 \phi^{ss}}{\partial t'^2} - \left[1 + \frac{J^{sd}}{J^{ss}}\left(1 - \frac{2}{\cos h^2(\alpha' x' + \beta' t')}\right)\right] \sin\phi^{ss} = 0. \tag{2.55}$$

where $\alpha' = \gamma(\alpha_1 - \beta_1 \mathrm{v})$, $\beta' = \gamma(\alpha_1 v - \beta_1)$ and v is the speed of the unperturbed fluxon. Here, the constants α_1 and β_1 depend on the speed v_0 of the *i*-soliton as $\alpha_1 = (J_{in}\lambda_d^2/J^{ss} d_s, d_I)^{1/2}/\sqrt{1 - v_0^2}$ and $\beta_1 = v_0 (J_{in}\mu_d^2 \epsilon/J^{ss} d_s d_I)^{1/2}/\sqrt{1 - v_0^2}$. Noting that $\cos\chi = 1 - (2/\cosh^2\zeta)$, one can see that Eq. (2.55) indicates that the *i*-soliton

excitation in the two-band superconductor can lead to both spatial and temporal modulation of the critical current density across the LJJ. A variation in the critical current density with respect to both position and time can influence the fluxon dynamics.

A soliton in a LJJ behaves as a relativistic particle when its speed approaches the Swihart velocity. The sine-Gordon equation is invariant under a Lorentz transformation. Hence, one may perform the Lorentz transformation, $t' = \gamma(t'' - vx'')$ and $x' = \gamma(x'' - vt'')$, and obtain $\alpha_1 x'' - \beta_1 t'' = \alpha' x' + \beta t'$ where $\alpha' = \gamma(\alpha_1 - \beta_1 v)$ and $\beta' = \gamma(\alpha_1 v - \beta_1)$. Here, $\gamma = (1 - v^2)^{-1/2}$ and v is the speed of the unperturbed fluxon. Noted that the fluxon in both the *s* and *d* bands are similar (i.e., $\phi^{dd} = \phi^{ss}$). By making the Lorentz transformation and by considering the phase dynamics in a moving reference frame, one can rewrite the sine-Gordon equation of Eq. (2.53) as

$$\frac{\partial^2 \phi^{ss}}{\partial x'^2} - \frac{\partial^2 \phi^{ss}}{\partial t'^2} - \left[1 + \frac{J^{sd}}{J^{ss}}\left(1 - \frac{2}{\cos h^2(\alpha' x' + \beta' t')}\right)\right] \sin \phi^{ss} = 0. \qquad (2.56)$$

Although Eq. (2.56) is a good starting point for describing the LJJ property, one needs to add few more phenomenological terms to account for the effects of dissipation and bias current in realistic systems.

To estimate the phase dynamics for a realistic LJJ, one may include additional terms which describe bias current J^B and dissipation terms $\Gamma_1(\partial\phi/\partial t')$ and $\Gamma_2\,(\partial^3\phi/\partial t'\partial^2 x')$ to account for the dissipative interaction between the fluxon and the environment. The bias current in the LJJ acts as a driving force for the fluxon, and the dissipative effects tend to damp the fluxon motion in the LJJ. Accounting for both effects of dissipation and bias current, one may obtain a sine-Gordon equation of

$$\frac{\partial^2 \phi}{\partial x'^2} - \frac{\partial^2 \phi}{\partial t'^2} - \sin \phi = F(\phi, x', t'). \qquad (2.57)$$

Assuming that $\beta' = 0$, perturbation terms in $F(\phi, x', t')$ are given by

$$F(\phi, x', t') = \frac{J^B}{J_c}[1 - 2\,\mathrm{sech}^2(\alpha x')]\sin\phi - \frac{J^B}{J_c} + \Gamma_1 \frac{\partial \phi}{\partial t'} + \Gamma_2 \frac{\partial^3 \phi}{\partial t' \partial^2 x'}. \tag{2.58}$$

Hence, one may account for these realistic junction effects by writing the equation of the motion for a fluxon in a LJJ as

$$\frac{\partial^2 \phi^{ss}}{\partial x'^2} - \frac{\partial^2 \phi^{ss}}{\partial t'^2} - \left[1 + \frac{J^{sd}}{J^{ss}}\left(1 - \frac{2}{\cos h^2 \alpha' x'}\right)\right]\sin\phi^{ss}$$

$$-\Gamma_1 \frac{\partial \phi^{ss}}{\partial t'} - \Gamma_2 \frac{\partial^3 \phi^{ss}}{\partial x'^2 \partial t'} + \frac{J^B}{J_c} = 0, \tag{2.59}$$

where J^{sd} is the inter-band Josephson current, and Γ_1 and Γ_2 are small parameters associated with the dissipative terms. Assuming that the perturbation effects are small, one may consider the solution to the perturbed sine-Gordon equation of Eq. (2.59) as the sum of unperturbed fluxon motion in the LJJ and the perturbation effects on the junction experienced by the fluxon. Thus one can write the unperturbed part of the sine-Gordon equation of Eq. (2.58) as

$$\frac{\partial^2 \phi^{ss}}{\partial x'^2} - \frac{\partial^2 \phi^{ss}}{\partial t'^2} - \sin\phi^{ss} = 0, \tag{2.60}$$

assuming that each perturbation term in *F* is small. The single-fluxon solution to the sine-Gordon equation of (2.60) is given by

$$\phi^{ss} = 4\tan^{-1}\left[\exp\left(\pm\frac{x' - x_0' - \int_0^t v(t')dt'}{\sqrt{1 - v(t')^2}}\right)\right]. \tag{2.61}$$

Here, the fluxon speed $v(t')$ accounts for the time dependence of fluxon motion induced by the critical current modulation. The solution of the unperturbed sine-Gordon equation represents a solitary wave (i.e., kink) propagating with the speed $v(t')$ and is similar to the curve shown in Fig. 5. Here, the solitary wave is representing the changes in the phase ϕ^{ss} either from 0 to 2π (soliton) or from 2π to 0 (anti-soliton) and is traveling with

the speed $v(t')$. The solitary wave can propagate for a long time without changing its shape. The $\pm$ sign in Eq. (2.61) indicates the propagation direction of fluxon. The + sign indicates that the fluxon moves to the right and the – sign denotes that the fluxon moves to the left. The fluxon moving to the left is generally called an anti-fluxon.

To examine the trajectories of the fluxon in a LJJ, one may follow McLaughlin and Scott [25]. According to McLaughlin and Scott, for a single fluxon under the perturbation, the equation of motion for the modulated waveform can be expressed as a pair of first order differential equations. These two equations describe the velocity and position of the fluxon. By carrying out numerical integration of the sine-Gordon equation of Eq. (2.53), one may write the second order differential equation of Eq. (2.53) as two first order differential equation describing velocity v and the position x_0' of the fluxon [25], respectively, as

$$\frac{dv}{dt'} = \mp\frac{1-v^2}{4}\int_{-\infty}^{\infty} dx' F(\phi_0, x', t') \operatorname{sec} h\zeta, \tag{2.62}$$

$$\frac{dx_0'}{dt'} = -\frac{v}{4}\sqrt{1-v^2}\int_{-\infty}^{\infty} dx' F(\phi_0, x', t') \operatorname{sec} h\zeta, \tag{2.63}$$

where

$$\zeta = \zeta(x', t') = \pm\frac{x' - \int_0^{t'} v(t')dt' - x_0'}{\sqrt{1-v^2(t')}}. \tag{2.64}$$

Equations (2.62) and (2.63) describe the fluxon trajectories in the (v, x_0') phase plane. The fluxon trajectories in the presence of perturbation terms *F* may be determined by computing the fluxon speed and the position as a function of time t'. The perturbation terms modulate the unperturbed wave form of Eq. (2.61) and yield the time dependence of fluxon speed. Equations (2.62) and (2.63) describing the fluxon dynamics can be rewritten as

$$\frac{dv}{dt'} = \pm \frac{\pi J^B}{4J_c}(1-v^2)^{\frac{3}{2}} - \Gamma_1 v(1-v^2) - \frac{\Gamma_2}{3}v + (1-v^2)^{\frac{3}{2}}\frac{J^{sd}}{J^{ss}}\int_0^\infty dy\, \gamma_+ \frac{\sinh y}{\cosh^3 y}, \quad (2.65)$$

and

$$\frac{dX}{dt'} = v + (v-v^3)\frac{J^{sd}}{2J^{ss}}\left(1 - 2\int_0^\infty dy\gamma_+ \frac{\sinh y}{\cosh^3 y}\right), \quad (2.66)$$

where

$$\gamma_\pm = \operatorname{sech}^2\alpha\left(\sqrt{1-v^2}y + X\right) \pm \operatorname{sech}^2\alpha\left(\sqrt{1-v^2}y + X\right)$$

and

$$X = \int_0^t dt'\, v(t') + x_0'(t).$$

Velocity of the fluxon far away from the region of the critical current modulation is determined from

$$\frac{dv}{dt'} = \pm\frac{\pi}{4}\frac{J^B}{J_c}(1-v^2)^{\frac{3}{2}} - \Gamma_1 v(1-v^2) - \frac{1}{3}\Gamma_2 v. \quad (2.67)$$

The power-balance velocity v_∞ of a single fluxon which is far away from the critical current modulation is determined by setting $dv/dt = 0$. The fluxon speed may be obtained by solving the cubic equation of

$$\left[\frac{\pi^2}{16}(J^B)^2 + \Gamma_1^2\right]z^3 + \left(\frac{2\Gamma_1\Gamma_2}{3} - \Gamma_1^2\right)z^2 + \left(\frac{\Gamma_2^2}{9} - \frac{2\Gamma_1\Gamma_2}{3}\right)z - \frac{\Gamma_2^2}{9} = 0 \quad (2.68)$$

which may be written as

$$\sum_{i=0}^{3} a_i z^i = 0, \quad (2.69)$$

where $z = (1-v_\infty)^{1/2}$, $a_0 = -\Gamma_2^2/9$, $a_1 = -(\Gamma_2^2/9) - (2\Gamma_1\Gamma_2/3)$, $a_2 = (2\Gamma_1\Gamma_2/3) - \Gamma_1^2$, and $a_3 = \pi^2 j_B^2/16 + \Gamma_1^2$. Here, the solution is bounded by the condition that $0 \le v_\infty \le 1$, since the power-balance velocity is given in units of the Swihart velocity.

Solving Eq. (2.67) numerically, one may find the velocity v as a function of position. By substituting this result into the perturbed sine-Gordon equation, one may compute the

trajectories of the fluxon. The fluxon trajectories indicate that the fluctuations of the relative phase lead to formation of an *i*-soliton in the LJJ which affects the fluxon dynamics. One of the effects of *i*-soliton on the fluxon dynamics is the emission of EM wave by a decelerating fluxon.

2.3 Effects of i-soliton on Phase Dynamics

In this section, the effects of large fluctuations in the relative phase of the *s* and *d* condensates on the fluxon dynamics are examined. According to Tanaka [21], when the amplitude of phase fluctuation grows to the non-linear region and becomes stabilized, a 2p-phase texture representing an *i*-soliton may be excited. Excitation of an *i*-soliton can change the amplitude of the critical current density. Equation (2.37) describes the effects of *i*-soliton excitation on the phase dynamics of the LJJ. From Eq. (2.51) one can obtain that

$$\frac{\partial^2 \phi^{ss}}{\partial x'^2} - \frac{\partial^2 \phi^{ss}}{\partial t'^2} - \frac{J_c}{J_c^0} \sin \phi^{ss} = 0, \tag{2.70}$$

where $J_c/J_c^0 = 1 + (J^{sd}/J^{ss})[1 - 2\,\mathrm{sech}^2(\alpha_0 \bar{x} - \beta_0 \bar{t})]$ is the normalized critical current, $\alpha_0 = [J^{sd}\lambda_d^2/(1 - v_0^2)J^{ss}d_s d_I]^{1/2}$, $\beta_0 = v_0[J^{sd}\mu_d^2\epsilon/(1 - v_0^2)J^{ss}d_s d_I]^{1/2}$, and J_c^0 is the critical current density in the absence of the inter-band Josephson effect (i.e., $J^{sd} = 0$). This equation (2.70) indicates that an *i*-soliton, representing a moving 2π-phase texture, yields both spatial and temporal dependent modulation of the critical current. For simplicity, only the spatial modulation of the critical current density is considered here.

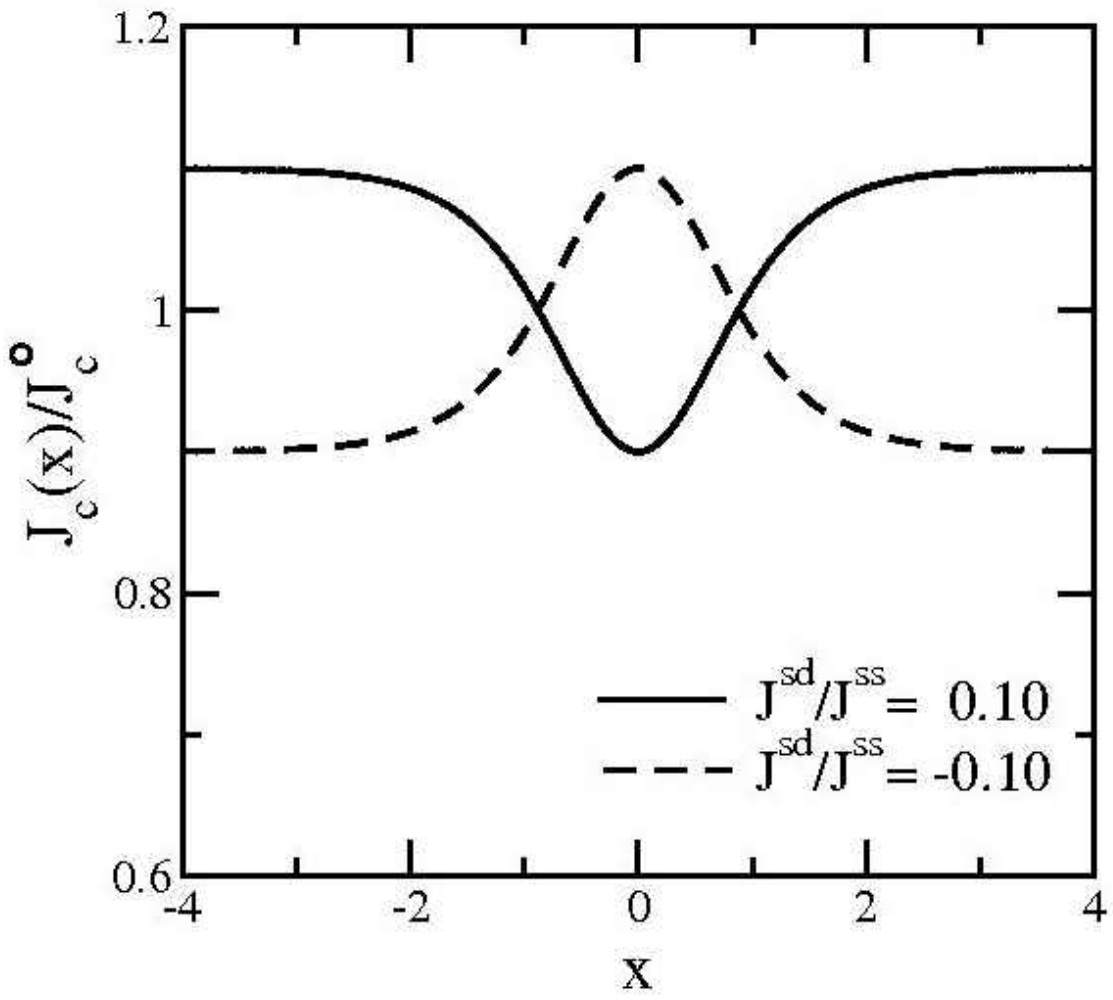

Figure 8. Amplitude modulation of the Josephson current due to an *i*-soliton representing 2π-phase texture with its center at $x = 0$ for $J^{sd}/J^{ss} = 0.10$, (solid curve) and $J^{sd}/J^{ss} -0.10$ (dashed curve).

To examine the spatial variation of the critical current J_c/J_c^0, the plot of J_c/J_c^0 as a function of dimensionless position x for $J^{sd}/J_c^0 = 0.10$ (solid curve) and $J^{sd}/J_c^0 = -0.10$ (dashed curve) are shown in Fig. 8. The curves illustrate the effects of a single *i*-soliton excitation in the S_{++} and S_{+-}-symmetry superconductor, respectively. These curves show that the shape of the critical current modulation depends on the symmetry of the order parameter. However, for $J^{sd}/J^{ss} \ll 1$, the symmetry of the order parameter does not affect the fluxon motion significantly.

The critical current modulation induced by the inter-band Josephson effect influences the fluxon motion in two main ways. First, the shape of the fluxon may become deformed. Second, the speed of the fluxon becomes modified since the critical current modulation behaves as an effective potential. However, only small fluxon potential modulation is taken into account here since the deformation on the shape of fluxon is negligible. In the region of critical current modulation, the fluxon speed may become significantly changed from its unperturbed value. These changes may cause the emission of the electromagnetic waves by a moving fluxon when it decelerates.

To examine the effects of critical current modulation on the emission of EM waves, the perturbation method is used. The calculation is carried out in an inertial reference frame which is moving with the speed of the unperturbed fluxon. This approach is similar to the rest frame of the fluxon [45, 46] considered by Fogal and coworkers. In this approach, one performs the Lorentz transformation

$$\bar{t}' = \frac{\bar{t} - v\,\bar{x}}{\sqrt{1-v^2}} \quad \text{and} \quad \bar{x}' = \frac{\bar{x} - v\,\bar{t}}{\sqrt{1-v^2}}, \tag{2.71}$$

where v is the speed of the unperturbed fluxon. Using this transformation, one can write the sine-Gordon equation of Eq. (2.70) as

$$\frac{\partial^2 \phi^{ss}}{\partial \bar{x}'^2} - \frac{\partial^2 \phi^{ss}}{\partial \bar{t}'^2} - \frac{\bar{J}_c}{J_c^0} \sin \phi^{ss} = 0, \tag{2.72}$$

where $J_c/J_c^0 = 1 + (J^{sd}/J^{ss})[1 - 2\,\mathrm{sech}^2(\alpha_0'\bar{x}' + \beta_0'\bar{t}')]$, $\alpha_0' = (\alpha_0 - \beta_0 v)/\sqrt{1-v^2}$, and $\beta_0' = (\alpha_0 v - \beta_0)/\sqrt{1-v^2}$. When the inter-band Josephson effect is weak (i.e., $J^{sd}/J^{ss} \ll 1$), the solution of Eq. (2.72) may be written as

$$\phi^{ss}(x,t) \approx \phi_0^{ss}(x) + \frac{J^{sd}}{J^{ss}} \phi_1^{ss}(x,t). \tag{2.73}$$

Note that a new notation $(\bar{x}', \bar{t}') \rightarrow (x, t)$ is used in Eq. (2.73). The $\phi_0^{ss}(x)$ term is the unperturbed part and the $J^{sd}\phi_1^{ss}(x,t)/J^{ss}$ term is the leading order correction term of the solution for the unperturbed sine-Gordon equation. Substituting Eq. (2.73) in the sine-Gordon equation of (2.72), one can express it as

$$\frac{\partial^2\phi_0^{ss}}{\partial x^2} - \frac{\partial^2\phi_0^{ss}}{\partial t^2} - \sin\phi_0^{ss}\cos\left[\frac{J^{sd}}{J^{ss}}\phi_1^{ss}(x,t)\right] +$$

$$\frac{J^{sd}}{J^{ss}}\left(\frac{\partial^2\phi_1^{ss}}{\partial x^2} - \frac{\partial^2\phi_1^{ss}}{\partial t^2}\right) - \sin\left[\frac{J^{sd}}{J^{ss}}\phi_1^{ss}(x,t)\right]\cos\phi_0^{ss} = 0. \qquad (2.74)$$

Note that when $J^{sd}/J^{ss} \ll 1$ one can approximate

$$\sin\left[\frac{J^{sd}}{J^{ss}}\phi_1^{ss}(x,t)\right] \cong \frac{J^{sd}}{J^{ss}}\phi_1^{ss}(x,t)$$

and

$$\cos\left[\frac{J^{sd}}{J^{ss}}\phi_1^{ss}(x,t)\right] \cong 1 - \frac{1}{2!}\left[\frac{J^{sd}}{J^{ss}}\phi_1^{ss}(x,t)\right]^2 + \cdots$$

With this approximation, Eq. (2.74) is separated into the unperturbed and correction terms. The unperturbed part of the sine-Gordon equation is given by

$$\frac{\partial^2\phi_0^{ss}}{\partial x^2} - \frac{\partial^2\phi_0^{ss}}{\partial t^2} - \sin\phi_0^{ss} = 0\,. \qquad (2.75)$$

A solution to this unperturbed sine-Gordon equation is

$$\phi_0^{ss}(x) = 4\tan^{-1}[\exp(x)].$$

The spatial and temporal dependence of correction term of ϕ_1^{ss} due to the critical current modulation may be separated as

$$\phi_1^{ss}(x,t) = f(x)e^{-i\omega t}. \qquad (2.76)$$

The separation of variables for the perturbation contribution ϕ_1^{ss} in the rest frame of the fluxon (i.e. $v = 0$) leads to an eigenvalue equation for $f(x)$ as

$$\left[-\frac{d^2}{dx^2} + (1 - 2\,\mathrm{sech}^2\,x)\right]f(x) = \omega^2 f(x). \qquad (2.77)$$

The eigenvalue problem of Eq. (2.77) yields one bound state with $\omega = \omega_b = 0$ and a continuum of scattering states with $\omega^2 = \omega_\kappa^2 = 1 + \kappa^2$. The corresponding normalized eigenfunctions are

$$f(x) = f_b(x) = 2\,\mathrm{sech}\,x \tag{2.78}$$

for $\omega = \omega_b$, and

$$f(x) = f(\kappa, x) = \frac{\kappa + i\tan x}{\sqrt{2\pi\omega_\kappa}}\, e^{i\kappa x} \tag{2.79}$$

for $\omega = \omega_\kappa$. Here the subscripts b and κ denote the bound state and continuum of the scattering state κ, respectively. The bound state $f_b(x)$ is associated with the Goldstone translation mode of the fluxon, while the continuum eigenfunctions $f(\kappa, x)$ represent the radiation modes. Eigen functions of Eqs. (2.78) and (2.79) indicate that the first-order correction $\phi_1^{ss}(x,t)$ due to the critical current modulation may be separated into two parts as

$$\phi_1^{ss}(x,t) = \phi_{trans}^{ss}(x,t) + \phi_{rad}^{ss}(x,t). \tag{2.80}$$

Here, ϕ_{trans}^{ss} and ϕ_{rad}^{ss} represent the bound and continuum eigenstate contribution, respectively. The bound state contribution ϕ_{trans}^{ss} may be written as

$$\phi_{trans}^{ss}(x,t) = \frac{1}{8}\phi_b^{ss}(t) f_b(x). \tag{2.81}$$

The amplitude $\phi_b^{ss}(t)$ of the bound state is determined straightforwardly from the equation of

$$\frac{d^2\phi_b^{ss}(t)}{dt^2} = 4\int_{-\infty}^{\infty} dx(1 - \mathrm{sech}^2\,\xi_0)\frac{\mathrm{sech}\;x}{\mathrm{sech}^2\,x}\;, \tag{2.82}$$

where $\xi_0 = \alpha_0' x + \beta_0' t$. The solution to Eq. (2.81) may be obtained as

$$\phi_b^{ss}(t) = -\frac{8\alpha_0'}{\beta_0'^2}\left(1 - \int_{-\infty}^{\infty} dx\,\frac{\mathrm{sec}\,h^2 x}{e^{2\beta_0' t} e^{2\alpha_0' x} + 1}\right). \tag{2.83}$$

Note that $\phi_b^{ss}(t)$ may be used to evaluate the translation mode contribution $\phi_{trans}^{ss}(x,t)$. This contribution has no effect on the motion of the fluxon center. The continuum eigenstate contribution, representing the radiation modes, is given by

$$\phi_{rad}^{ss}(x,t) = \int_{-\infty}^{\infty} d\kappa \phi(\kappa,t) f(\kappa,x). \tag{2.84}$$

The amplitude $\phi(\kappa,t)$ is determined from

$$\frac{d^2\phi(\kappa,t)}{dt^2} + (1+\kappa^2)\phi(\kappa,t) = Q(\kappa,t), \tag{2.85}$$

where

$$Q(\kappa,t) = 2\int_{-\infty}^{\infty} dx f^*(\kappa,t)(1 - 2\sec h^2\xi_0)\frac{\sin hx}{\cos h^2 x}. \tag{2.86}$$

The contribution to the radiation mode of ϕ_1^{ss} may be estimated by solving Eq. (2.85). For a single modulation of the critical current density a solution to Eq. (2.85) can be obtained more easily by using the relation,

$$\operatorname{sech}^2\xi_0 = \int_{-\infty}^{\infty} \frac{dk}{2\pi} \frac{\pi k}{\sinh\frac{\pi k}{2}} e^{ik\xi_o}, \tag{2.87}$$

which is the Fourier representation of the critical current variation. Using this substitution, one can rewrite $Q(\kappa,t)$ by integrating the right-hand side of Eq. (2.86) over x and one can obtain

$$Q(\kappa,t) = \frac{-i\pi}{\sqrt{2\pi(1+\kappa^2)}}\left\{(1+\kappa^2)\operatorname{sech}\frac{k\pi}{2} - \int_{-\infty}^{\infty} dk \frac{\sec h\frac{\pi k\eta_\kappa}{2}}{2\sin h\frac{\pi k}{2}}[1+\kappa^2-(k\alpha)^2]ke^{ik\beta_o' t}\right\}, \tag{2.88}$$

where $\eta_\kappa = \alpha_o' - (\kappa/k)$. The solution $\phi(\kappa,t)$ may be written as

$$\phi(\kappa,t) = \int_{-\infty}^{\infty} \frac{d\omega}{2\pi} \frac{Q(\kappa,\omega)}{(1+\kappa^2)-\omega^2} e^{i\omega t}, \tag{2.89}$$

where $Q(\kappa,\omega) = \int dt' Q(\kappa,t')\exp(-i\omega t')$. One can evaluate the integration over t' and ω, and write the solution $\phi(\kappa,t)$ as

$$\phi(\kappa,t)=\frac{-i\pi}{\sqrt{2\pi(1+\kappa^2)}}\left[\operatorname{sech}\frac{k\pi}{2}-\int_{-\infty}^{\infty}dk\,\frac{\sec h\frac{\pi k\eta_\kappa}{2}}{\sin h\frac{\pi k}{2}}\frac{1+\kappa^2-(k\alpha_o')^2}{1+\kappa^2-(k\beta_o')^2}ke^{ik\beta_o't}\right]. \qquad (2.90)$$

However, as indicated in Eq. (2.84), one needs to integrate over the continuum variable κ to compute $\phi_{rad}^{ss}(x,t)$. This integral may be evaluated by using the contour integration method.

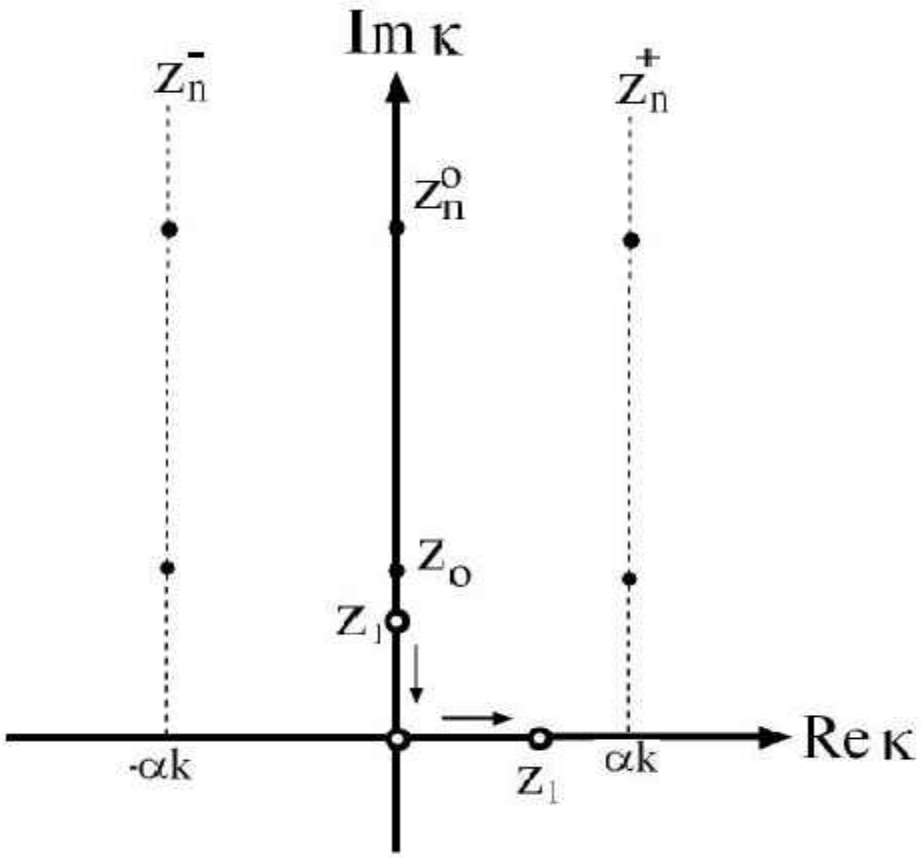

Figure 9. The pole structure for the radiation contribution of Eq. (2.84) to $\phi_1(k,t)$ for a fixed k is shown schematically. The solid circles represent the poles yielding the exponentially localized contribution. The open circles are in the location of z_1 as the fluxon velocity v changes from $v<v_{th}$ to $v>v_{th}$ the shift direction for the pole z_1 is indicated by the arrows.

The radiation contribution $\phi_{rad}^{ss}(x,t)$ of Eq. (2.84) indicates that all the poles are simple, and the residue of each pole may be evaluated separately. The position of the poles that are shown in Fig. 9 are given as follows:

$$z_o = +i,$$

$$z_1 = +i\sqrt{1-(k\beta_o')^2}$$

$$z_n^o = +i(2n+1),$$

and

$$z_n^{\pm} = \pm k\alpha_o' + i(2n+1),$$

where $n = 0,1,2,\ldots$ The residues of the poles structure yield two types of contribution: (i) an exponentially localized contribution around the fluxon center and (ii) a linear traveling wave contribution. Hence, the radiation mode ϕ_{rad}^{ss} may be decomposed into the exponentially localized $\phi_{rad}^{ss\,exp}$ and traveling wave $\phi_{rad}^{ss\,wave}$ contributions: $\phi_{rad}^{ss} = \phi_{rad}^{ss\,exp} + \phi_{rad}^{ss\,wave}$. Note that the exponentially localized contribution $\phi_{rad}^{ss\,exp}$ does not produce a true radiative correction. Only the traveling wave $\phi_{rad}^{ss\,wave}$ gives rise to a true radiative contribution.

The poles that give rise to the traveling wave contribution to the radiation correction are examined below. As indicated by Fourier components of the critical current modulation described by the $(1-2\,\mathrm{sech}^2\,\xi_o)$ factor in Eq. (2.86), the condition for the traveling wave radiative contribution depends on k. For fixed $k < (1/\beta_o')$, the pole at z_1 lies on the imaginary axis. However, as the fluxon speed v increases, the pole z_1 moves down the imaginary axis. At the critical value $v = v_{th}$, the pole z_1 lies in the complex plane and it becomes real for $v > v_{th}$. The changes in the radiation contribution in Eq. (2.86) from this pole may be easily identified by the contour integration since it is

not exponentially localized around the fluxon center but oscillates with x. The oscillatory contribution only arises when $v > v_{th}$. This leads to a radiative contribution of

$$\phi_{rad}^{ss\ wave}(x,t) = -\int_{-\infty}^{\infty} \frac{dk}{2\eta} \frac{\pi k \Xi}{\sin h \frac{\pi k}{2}} (\eta + i \tanh x) \left[\frac{e^{ik(\beta_o' t + \eta x)}}{\cos h \frac{\pi k \eta_-}{2}} + \frac{e^{-ik(\beta_o' t - \eta x)}}{\cos h \frac{\pi k \eta_+}{2}} \right], \qquad (2.91)$$

where $\Xi = 1 - (\alpha_o'^2/\beta_o'^2)$, $\eta = \sqrt{(k\beta_o')^2 - 1}$, and $\eta_\pm = \alpha_o' \mp (\eta/k)$. Equation (2.91) indicates that, for a fixed k, this radiation correction is the superposition of two linear traveling waves with different amplitudes. The two waves travel in opposite directions. The threshold velocity v_{th} for the fluxon is given by

$$v_{th} = v_o \left(\frac{\mu_d^2 \epsilon}{\lambda_d^2} \right)^{1/2}. \qquad (2.92)$$

The dependence of v_{th}on the i-solition velocity $v_o$indicates that, for the case of static spatial variation of the phase (i.e., $v_o = 0$), EM radiation may be emitted by the fluxon whenever it passes through a region where the critical current is affected by the inter-band Josephson effect. Hence, when an array of static i-solitions is excited to yield a spatially periodic modulation of the critical current density, the threshold velocity v_{th} becomes finite. This radiative threshold is similar to that found in earlier studies [26, 28, 29].

The effects of i-solitions on the LJJ was discussed in Chapter II. This revels that the two-gap superconductor has an interesting property. Another interesting property of a LJJ with two-gap superconductors is the appearance of the broken time reversal symmetry state as the ground state of the LJJ. A possibility of phase frustration and the presence of broken time-reversal symmetry ground state of the LJJ is examined in Chapter III.

CHAPTER III

BROKEN TIME REVERSAL-SYMMETRY STATE IN A LJJ

In this chapter, the relationship between phase frustration and the broken time-reversal symmetry state in a LJJ with two-gap superconductors is discussed. To understand the time-reversal symmetry invariant (TRSI) and broken time-reversal symmetry state (BTRS) in the LJJ based on two-gap superconductors, one can first review the TRSI and BTRS state in the tunnel junction between the two-gap and one-gap superconductors [9-15]. Finally, the ground state of the LJJ with two-gap superconductors is examined by using the free energy obtained from the BCS model. By minimizing this free energy, the conditions for the phase frustration for two different S-wave symmetries are obtained. Based on the ground state conditions for the current densities, the TSRI state and BTSR state for Josephson junction with two-gap superconductors are discussed.

3.1 Review of Possibility of Phase Frustration

In this section, the possibility of phase frustration in a two-gap superconductor is reviewed by computing the free energy of the system. Earlier studies [9, 10, 11, 12, 13, 14, 15] indicate that phase frustration and the appearance of broken time reversal symmetry state in a tunnel junction between two-gap and one-gap superconductors are closed related.

The ground state of the junction may be examined by computing the free energy. The free energy for the two-gap superconductor in the absence of an external magnetic field [15] is given by

$$F = \alpha_s|\psi_l^s|^2 + \widetilde{K}_s(\nabla\theta^s)^2 + \beta_s|\psi_l^s|^4 + \alpha_d|\psi_l^d|^2 + \widetilde{K}_d(\nabla\theta^d)^2 + \beta_d|\psi_l^d|^4 - 2J|\psi_l^s||\psi_l^d|\cos(\theta^d - \theta^s), \quad (3.1)$$

where the pseudo-order parameters ψ_l^s and ψ_l^d are non-zero and $\alpha_{s(d)} < 0$. Note that two pseudo-order parameters are coupled by the inter-band Josephson coupling J, representing interactions between electrons in the *s*- and *d*-bands. From Eq. (3.1), for $J > 0$, it is clear that the free energy becomes a minimum for $\theta^s = \theta^d$. However, for $J < 0$, the free energy becomes a minimum for $\theta^s = \theta^d = \pi$. Thus, there is no phase frustration in two-gap superconductors for either $J > 0$ or $J < 0$.

The situation is different in the tunnel junction involving a two-gap superconductor and a one-gap superconductor. Ng and Nagaosa [15] suggested that the free energy density for a Josephson junction [15] is given by

$$\begin{aligned} F \cong\ & \Theta(x)\left[-2\tilde{J}\cos(\theta^s - \theta^d) + \widetilde{K}_s(\nabla\theta^s)^2 + \widetilde{K}_d(\nabla\theta^d)^2\right] \\ & + 2\delta(x)[\tilde{T}_s\cos(\theta^s - \theta) + \tilde{T}_d\cos(\theta^s - \theta)] \\ & + \Theta(-x)\widetilde{K}(\nabla\theta)^2 + \tilde{F}\ , \end{aligned} \quad (3.2)$$

where $\tilde{J} = J_{in}|\psi^s||\psi^d|$, $\tilde{T}_s = T_s|\psi||\psi^s|$, $\tilde{T}_d = T_d|\psi||\psi^d|$, $\widetilde{K}_i = K_i|\psi^i|^2$, $\tilde{F}$ is the part of free energy that is independent of phase angle, and the index $i = s, d$ denotes electronic bands in the two-gap superconductor. Here, T_i represents the coupling between the one-gap superconductor and the electronic bands of the two-gap superconductor. To study a deviation from the phase-locked state, one needs to minimize the free energy with respect

to the phase variables. By minimizing the free energy with respect to the phase of the one-gap superconductor, one can obtain

$$\widetilde{K}\nabla^2\theta = -\delta(x)\left(\tilde{T}_s \sin\theta^s - \tilde{T}_d \sin\theta^d\right). \tag{3.3}$$

Here, the phase variable θ is set to zero (i.e., $\theta = 0$) as a convenient reference point to measure the phases θ^i. Note that Eq. (3.3) becomes

$$\widetilde{K}\nabla^2\theta = 0$$

away from the junction interface (i.e., $x \neq 0$). The solution of this equation may be written as

$$\theta = \beta_s x.$$

Similarly, for the phases of the two pseudo-order parameters, one may obtain the following equations of motion:

$$\nabla^2\theta^s - \frac{\tilde{J}}{\tilde{K}_s}\sin(\theta^s - \theta^d) = 0, \tag{3.4}$$

and

$$\nabla^2\theta^d - \frac{\tilde{J}}{\tilde{K}_d}\sin(\theta^s - \theta^d) = 0. \tag{3.5}$$

By subtracting Eq. (3.5) from Eq. (3.4), one can easily obtain the equation of motion for the relative phase $\chi = \theta^d - \theta^s$ as

$$\frac{d^2\chi}{dx^2} = \frac{1}{\lambda^2}\sin\chi, \tag{3.6}$$

where $\lambda^{-2} = \left|\tilde{J}\right|(\widetilde{K}_s + \widetilde{K}_d)/\widetilde{K}_s\widetilde{K}_d$. A single soliton solution to the steady state sine-Gordon equation of (3.6) is given by

$$\chi(x) = 4\tan^{-1}\left(ae^{-\frac{x}{\lambda}}\right), \tag{3.7}$$

where a is *a* constant which is determined by the boundary conditions. Therefore, one may decomposed the solution of Eq. (3.7) and write θ^s and θ^d as

$$\theta^s(x) = \beta_0 x + \theta^0 + \frac{4\tilde{K}_d}{\tilde{K}_s+\tilde{K}_d}\tan^{-1}\left(ae^{-\frac{x}{\lambda}}\right), \tag{3.8}$$

and

$$\theta^d(x) = \beta_0 x + \theta^0 + \pi - \frac{4\tilde{K}_d}{\tilde{K}_s+\tilde{K}_d}\tan^{-1}\left(ae^{-\frac{x}{\lambda}}\right), \tag{3.9}$$

respectively. The current density in a weak electromagnetic field is given by

$$\vec{J} \cong \frac{1}{\Lambda}\frac{\Phi_0}{2\pi}\nabla\theta\,, \tag{3.10}$$

where Φ_0 is a magnetic flux quantum, $\Lambda = \mathrm{m}/\mathrm{n}_s e^2$, n_s is the number density of the particle. The current density may also be obtained by using the relation

$$\vec{J} = 2e\frac{dF}{d\theta}, \tag{3.11}$$

The current density computed from the above two relations satisfies the boundary conditions at the junction interface. Similarly, one may compute $dF/d\theta^i$ for $\theta = 0$ at the junction interface (i.e., *x=0*) and obtain the current densities for the *s* and *d* bands. By substituting Eq. (3.8) and Eq. (3.9) into the expression for $dF/d\theta^i$, one can obtain

$$\frac{\partial F}{\partial \theta^s} = 2\tilde{T}_s \sin\theta^s = 2\tilde{T}_s \sin\left(\theta^0 + \frac{4\tilde{K}_d}{\tilde{K}_s+\tilde{K}_d}\tan^{-1}a\right), \tag{3.12}$$

$$\frac{\partial F}{\partial \theta^d} = 2\tilde{T}_d \sin\theta^d = 2\tilde{T}_d \sin\left(\theta^0 + \pi - \frac{4\tilde{K}_s}{\tilde{K}_s+\tilde{K}_d}\tan^{-1}a\right). \tag{3.13}$$

By matching the boundary condition to reflect the requirement that the current density is conserved at the junction interface, one can get

$$\tilde{K}\beta_s = -4e[\tilde{T}_s \sin(\theta^0 + b_d \tan^{-1} a) - \tilde{T}_d \sin(\theta^0 - b_s \tan^{-1} a)], \tag{3.14}$$

where $b_d = 4\tilde{K}_d/(\tilde{K}_s + \tilde{K}_d))$ and $b_s = 4\tilde{K}_s/(\tilde{K}_s + \tilde{K}_d)$.

In the ground state, the Josephson junction does not introduce any additional bulk energy to the system. This condition implies that there is no net current flow in the

ground state of the system. Therefore, one can set $\beta_s = 0$. Now Eq. (3.14) indicates that one can obtain

$$\tilde{T}_s \sin\theta^0 - \tilde{T}_d \sin\theta^0 = 0$$

when a=0. This implies that $\theta^0 = 0$ or π. On the other hand, when $a \neq 0$, but a is small, one may write Eq. (3.12) as

$$0 = \tilde{T}_s[\sin\theta^0 \cos(ab_d) + \cos\theta^0 \sin(ab_d)]$$
$$-\tilde{T}_d[\sin\theta^0 \cos(ab_s) - \cos\theta^0 \sin(ab_s)]. \quad (3.15)$$

Equation (3.15) indicates that θ^0 must be different than either 0 or π. If the phase difference between the two condensates becomes something other than 0 or π, then system is said to have phase frustration. The ground state of the junction with phase frustration has non-zero current flow, which breaks the time-reversal symmetry. For LJJ with two-gap and one-gap superconductor, the net current in the Josephson junction is zero (i.e., $J_s + J_d = 0$) in the ground state. The time-reversal symmetry invariant state is represented by the trivial solutions of Eqs. (3.14) and (3.15). These solutions are $\theta^0 = 0$ or π and $a = 0$, indicating that $J_s = J_d = 0$. Also, there are non-trivial solutions($\pm\theta^0$, $\pm a$) $\neq 0$, representing the broken time-reversal states. These solutions are degenerate. The $\theta^0 \lessgtr 0$ solutions correspond to two degenerate time-reversal pairs [15]. In the BTRS state, the current loop circulates through the junction in momentum-space, and not in real space.

3.2 Broken Time-Reversal Symmetry State in the Two-gap LJJ

The broken time-reversal symmetry (BTRS) states in the Josephson junction with two-gap superconductors are examined by using the free energy derived from the BCS

Hamiltonian. By minimizing the free energy with respect to phase variables, one can determine the conditions for phase frustration, yielding the broken time-reversal symmetry state. As in the section 2.1 of Chapter II, the BCS Hamiltonian extended for two-gap superconductors is rewritten as $\widehat{H} = \widehat{H}_{TB,l} + \widehat{H}_T$. The Hamiltonians $\widehat{H}_{TB,l}$ and $\widehat{H}_T$ account for the contribution due to two-gap superconductivity and electron tunneling between the two adjacent superconductor (S) layers. The two-gap Hamiltonian $\widehat{H}_{TB,l}$ may be written in terms of Grassmann variables as

$$\widehat{H}_{TB,l} = \int dr\left(\sum_{i=s,d} \varepsilon^i \, \bar{c}^i_{\sigma,l} c^i_{\sigma,l} + \widehat{H}^{pair}_l\right), \tag{3.16}$$

where ε^i is the energy of electrons in the *i*-band (*i* = *s, d*) about the Fermi energy. The pairing interaction between electrons in the *l*-th S layer is given by

$$\widehat{H}^{pair}_l = -V_{ss}\bar{c}^s_{\uparrow,l}\bar{c}^s_{\downarrow,l}c^s_{\downarrow,l}c^s_{\uparrow,l} - -V_{dd}\bar{c}^d_{\uparrow,l}\bar{c}^d_{\downarrow,l}c^d_{\downarrow,l}c^d_{\uparrow,l} - V_{sd}\left(\bar{c}^s_{\uparrow,l}\bar{c}^s_{\downarrow,l}c^d_{\downarrow,l}c^d_{\uparrow,l} + h.c.\right) \tag{3.17}$$

where V_{ij} is the pairing interaction strength between electrons in the *i* and *j* bands and $\bar{c}^i_{\sigma,l}$ and $c^i_{\sigma,l}$ are the Grassmann variables. The Hamiltonian $\widehat{H}_T$ due to tunneling of an electron between the two adjacent S layers is given in terms of the tunneling matrix element T_{ij} as

$$\widehat{H}_T = \sum_{\sigma,i\neq j}\left(T_{ij}\bar{c}^i_{\sigma,1}c^j_{\sigma,2} + h.c.\right). \tag{3.18}$$

To obtain the free energy, one may start with the BCS Hamiltonian for a two-gap superconductor and carry out a number of steps as discussed in appendix A. First, one may use the Nambu notation and Hubbard-Stratonovich transformation to simplify the partition function. Also, by using the Grassmann integrals to integrate the fermion fields, one can obtain the effective action for the system.

The free energy *F* of the system may be obtained from the effective action as

$$F = \frac{1}{\beta} S[\phi_k], \tag{3.19}$$

where ϕ_k is the Hubbard-Stratonovich field. Here the components of the auxiliary field

$$\bar{\phi}_k = (\bar{\phi}_k^s \quad \bar{\phi}_k^s) \quad \text{and} \quad \phi_k = \begin{pmatrix} \phi_k^s \\ \phi_k^d \end{pmatrix},$$

where $\phi_k^i = \Delta_k^i e^{i\theta^i}$. Using the effective action derived in appendix A, one can write the free energy

$$\begin{aligned} \beta F = \sum_l \Big\{ \int_0^\beta d\tau \left[\frac{|\Delta_l^s|^2}{g_{ss}} - \frac{|\Delta_l^d|^2}{g_{dd}} - \frac{2g_{sd}}{g_{ss}g_{dd}} \Delta_l^s \Delta_l^d \cos\chi_l \right] \\ + \int_0^\beta d\tau \sum_i \left[m_i \rho_s^i v_{s,l}^{i2} + \frac{1}{8\pi\mu_i^2} \left(\frac{\Phi_0}{2\pi} \frac{\partial \theta_l^i}{\partial \tau} + \varphi_l \right)^2 \right] \Big\} \Theta(\pm z) \\ + \left\{ \int_0^\beta \frac{d\tau}{8\pi} \left(\epsilon E_z^2 + B_y^2 \right) + \int_0^\beta \frac{d\tau}{d_s} \int_0^\beta d\tau' B_{\alpha\beta} \right\} \delta(z) \end{aligned} \tag{3.20}$$

where $\chi_l = \theta_l^d - \theta_l^s$ and $B_{\alpha\beta}$ is the second order tunneling contribution to free energy defined in appendix A. Also the phase difference between two S layers in the presence of an external magnetic field is

$$\tilde{\phi}^{ji} = \theta_2^j - \theta_1^i - 2eA_{2,1}^z, \tag{3.21}$$

and

$$\vec{v}_{s,l}^i = \frac{1}{2m_i} \left(\nabla\theta_l^i - \frac{2\pi}{\Phi_0} \vec{A}_l \right), \tag{3.22}$$

is superfluid velocity. For simplicity, one can make the local approximation for the integral kernel $\tilde{\beta}^{ji}(\tau - \tau')$ in $B_{\alpha\beta}$ by writing

$$\tilde{\beta}^{ji}(\tau - \tau') = -\tilde{J}^{ss}(\tau - \tau')\delta(\tau - \tau').$$

Within this local approximation, noting that the Ohmic quasi-particle contributions $\tilde{\alpha}^{ij}(\tau - \tau') \cos \phi_-^{ij}(r, \tau; r, \tau')$ in $B_{\alpha\beta}$ do not depend on the phases, one may write

$$\beta F = \sum_l \left\{ \int_0^\beta d\tau \left[\frac{|\Delta_l^s|^2}{g_{ss}} - \frac{|\Delta_l^d|^2}{g_{dd}} - \frac{2g_{sd}}{g_{ss}g_{dd}} \Delta_l^s \Delta_l^d \cos\chi_l \right] \right.$$

$$\left. + \int_0^\beta d\tau \sum_i \left[m_i \rho_s^i v_{s,l}^{i2} + \frac{1}{8\pi\mu_i^2} \left(\frac{\Phi_0}{2\pi} \frac{\partial \theta_l^i}{\partial \tau} + \varphi_l \right)^2 \right] \right\} \Theta(\pm z)$$

$$+ \left\{ \frac{1}{8\pi} \int_0^\beta d\tau \left(\epsilon E_z^2 + B_y^2 \right) + \frac{1}{d_s} \int_0^\beta d\tau \, B_\beta \right\} \delta(z). \quad (3.23)$$

Note that, under local approximation, $B_{\alpha\beta}$ becomes

$$B_{\alpha\beta} = B_\beta = J^{ss} \cos\tilde{\phi}^{ss} + J^{dd} \cos\tilde{\phi}^{dd} + J^{ds} \cos\tilde{\phi}^{ds} + J^{sd} \cos\tilde{\phi}^{sd}. \quad (3.24)$$

In the steady state, the free energy of the system in the absence of magnetic field is

$$F = \Theta(\pm z) \sum_l \left\{ \frac{|\Delta_l^s|^2}{g_{ss}} - \frac{|\Delta_l^d|^2}{g_{dd}} - \frac{2g_{sd}}{g_{ss}g_{dd}} \Delta_l^s \Delta_l^d \cos\chi_l \right.$$

$$\left. + \frac{1}{4m_s} \rho_s^s (\nabla\theta_l^s)^2 + \frac{1}{4m_d} \rho_s^d \left(\nabla\theta_l^d \right)^2 \right\} - B_{\beta 0} \, \delta(z), \quad (3.25)$$

where

$$B_{\beta 0} = J^{ss} \cos\phi^{ss} + J^{dd} \cos\phi^{dd} + J^{ds} \cos\left(\theta_2^d - \theta_1^s\right) + J^{sd} \cos\left(\theta_2^s - \theta_1^d\right), \quad (3.26)$$

$\phi^{ss} = \theta_2^s - \theta_1^s$ and $\phi^{dd} = \theta_2^d - \theta_1^d$. In the remainder of Chapter III, the phase configuration that minimizes the free energy is discussed. In the steady state, the phase part of the free energy $F_\theta = F - F_0$ of the LJJ based on two-gap superconductors is

$$F_\theta = -\bar{g}_{sd} (\cos\chi_1 + \cos\chi_2) - \bar{J}^{ss} (\cos\phi^{ss} + \cos\phi^{dd})$$

$$- \bar{J}^{sd} \left[\cos\left(\theta_2^s - \theta_1^d\right) + \cos\left(\theta_2^d - \theta_1^s\right) \right], \quad (3.27)$$

where $\bar{g}_{sd} = 2g_{sd}\Delta_l^s\Delta_l^d / g_{ss}g_{sd}$, $\chi_1 = \theta_1^d - \theta_1^s$, and $\chi_2 = \theta_2^d - \theta_2^s$. Note that one may set that $\bar{J}^{ss} = J^{ss}/d_s = J^{dd}/d_s$, and $\bar{J}^{sd} = J^{sd}/d_s = J^{ds}/d_s$ for simplicity. Here F_0 is the part of the free energy density which is independent of the θ's. Note that $g_{ss} = det(V)/V^{dd}$, $g_{dd} = det(V)/V^{ss}$, and $g_{sd} = det(V)\, V^{sd}/V^{dd}\, V^{ss}$, where V is given in Eq. (2.18). To examine the phase configurations which minimize the free energy density,

the first derivative of F_θ with respect to phase variables is set to zero. The extrema of the free energy function $F\left(\theta_1^s, \theta_1^d, \theta_2^s, \theta_2^d\right) = F(\chi_1, \chi_2, \phi^{ss}, \phi^{dd})$ may be found by using the two sets of conditions. The first set of conditions is

(i) $\phi^{dd} = \phi^{ss} + \chi_2 - \chi_1$

(ii) $\phi^{ss} + \frac{\chi_2 - \chi_1}{2} = n\pi,$

(iii) $\bar{g}_{sd} \sin(\frac{\chi_2+\chi_1}{2} - \frac{\chi_2-\chi_1}{2}) + (-1)^n \left(-\bar{J}^{ss} \sin\frac{\chi_2-\chi_1}{2} + \bar{J}^{sd} \sin\frac{\chi_2+\chi_1}{2}\right) = 0$.

The second set of conditions is

(i) $\phi^{dd} = \phi^{ss} + \chi_2 - \chi_1$,

(ii) $J^{ss}\cos\left(\frac{\chi_2-\chi_1}{2}\right) + J^{sd}\cos\left(\frac{\chi_2+\chi_1}{2}\right) = 0,$

(iii) $\bar{g}_{sd} \sin(\frac{\chi_2+\chi_1}{2} - \frac{\chi_2-\chi_1}{2}) - \cos(\phi^{ss} + \frac{\chi_2-\chi_1}{2}) \left(\bar{J}^{ss} \sin\frac{\chi_2-\chi_1}{2} - \bar{J}^{sd} \sin\frac{\chi_2+\chi_1}{2}\right) = 0$.

(See appendix A for a detailed discussion.) Using the conditions for minimum free energy, Eq. (3.59) is solved for z = 0 numerically. To study the phase frustration in the ground state of the LJJ, the free energy F_θ/J^{ss} is plotted in the Fig. 10 as a function of inter-band relative phase for (a) $g_{SD} = \bar{g}_{sd}/J^{ss} = 1.0$, $J_{SD} = \bar{J}^{sd}/J^{ss} = 1.0$, $\phi^{ss} = 0.0$ (b) $J_{SD} = 1.0$ $g_{SD} = -1$, $\phi^{ss} = 0.0$ and (c) $g_{SD} = -1.0$, $J_{SD} = 1.0$, $\phi^{ss} = 1.4$. Also, in Fig. 11, the free energy contours are plotted as a function of relative phase for the same set of parameters as used in Fig. 10. These free energy plots indicate that the value of relative phases (χ_1^o, χ_2^o) for the free energy minimum depends on ϕ^{ss}. From the free energy contour plot of Fig. 11, one can easily see that the ground state value for (χ_1^o, χ_2^o) is (0, 0), when the phase difference ϕ^{ss} across the two adjacent layers is zero (i.e., $\phi^{ss} = 0$). However, when $\phi^{ss} \neq 0$, the free energy minimum occurs for g_{SD}=-1.0 and

J_{SD}=1.0 at a non-zero value of (χ_1^o, χ_2^o), indicating the appearance of phase frustration in the ground state. This dependence on ϕ^{ss} may be seen easily in Fig. 10c. Similarly for g_{SD}= -1.0, J_{SD}=1.0, and ϕ^{ss}= 0.0, the free energy surface and contours in the (χ_1, χ_2) space is shown in Figs. 10b and 11b, respectively.

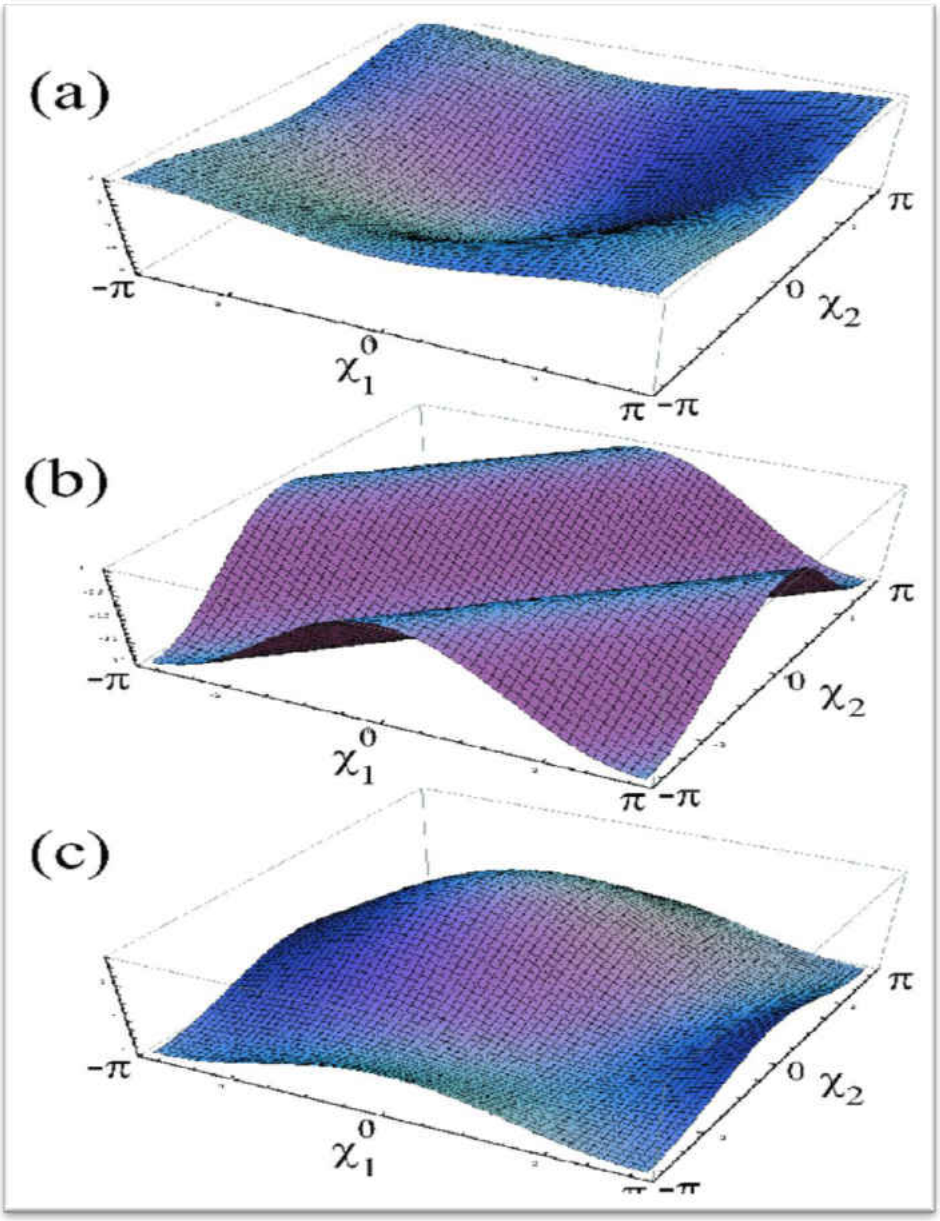

Figure 10. The free energy F_θ/J^{ss} is plotted as a function of inter-band relative phase difference χ_1 and χ_2 for (a) $g_{SD} = \bar{g}_{sd}/J^{ss} = 1.0$, $J_{SD} = \bar{J}^{sd}/J^{ss} = 1.0$, $\phi^{ss} = 0$ (b) $J_{SD} = 1.0$, $g_{SD} = -1$, $\phi^{ss} = 0$ and (c) $g_{SD} = -1.0$, $J_{SD} = 1.0$, $\phi^{ss} = 1.4$. These free energy surfaces illustrate the dependence of the ground state phase configuration on the parameters g_{SD}, J_{SD}, and ϕ^{ss}.

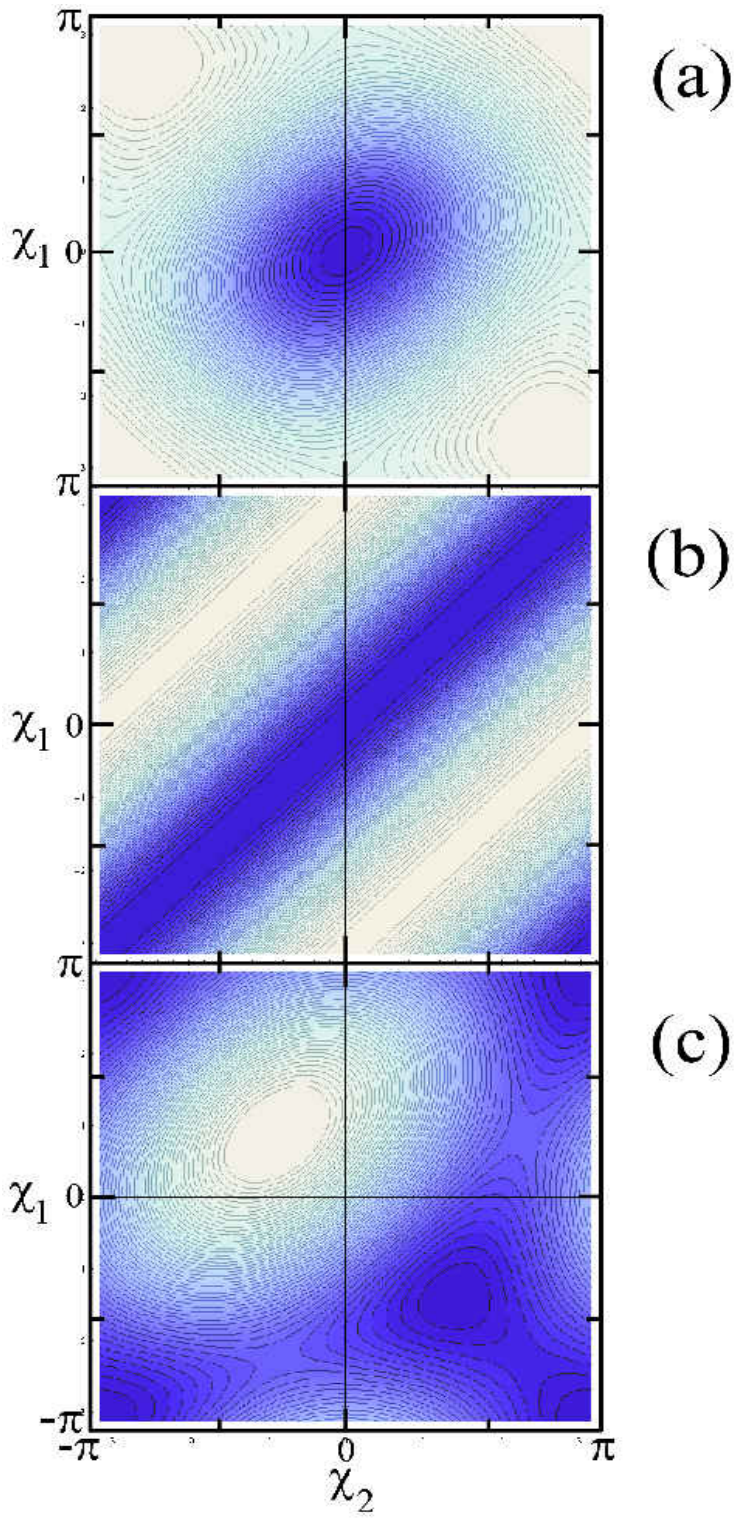

Figure 11: The free energy F_θ/J^{ss} is plotted as a function of inter-band relative phase difference χ_1 and χ_2 for (a) $g_{SD} = \bar{g}_{sd}/J^{ss} = 1.0$, $J_{SD} = \bar{J}^{sd}/J^{ss} = 1.0$, $\phi^{ss} = 0$ (b) $J_{SD} = 1.0$, $g_{SD} = -1$, $\phi^{ss} = 0$ and (c) $g_{SD} = -1.0$, $J_{SD} = 1.0$, $\phi^{ss} = 1.4$. These free energy contours illustrate the location of the minimum free energy and to estimate the coordinates (χ_1, χ_2) for given parameters g_{SD}, J_{SD}, and ϕ^{ss} .

One may estimate the phase frustration in the ground state from the phase equation of motion derived from the free energy of Eq. (3.27). One uses the Euler-Lagrange equations for different phase variables to obtain the equations of motion. For an example, for the θ_2^d variable, the equation of motion is given by

$$\frac{\hbar^2\rho_s^d}{2m_d}\nabla^2\theta_2^d - \frac{2g_{sd}}{g_{ss}g_{dd}}\Delta_2^s\Delta_2^d\sin\left(\theta_2^d-\theta_2^s\right) = \left[\frac{J^{dd}}{d_s}\sin\left(\theta_2^d-\theta_1^d\right)+\frac{J^{ds}}{d_s}\sin\left(\theta_2^d-\theta_1^s\right)\right]\delta(z). \quad (3.28)$$

Similar equations of motion can be obtained for the phase variables θ_2^s, θ_1^d, and θ_1^s. When the Euler-Lagrange equations for θ_2^d and θ_2^s are added, one can obtain

$$\nabla^2(\theta_2^d-\theta_2^s) - \frac{g_{sd}}{g_{ss}g_{dd}}\Delta_2^s\Delta_2^d\frac{4}{\hbar^2}\left(\frac{m_d}{\rho_s^d}+\frac{m_s}{\rho_s^s}\right)\sin\left(\theta_2^d-\theta_2^s\right)=0 \quad (3.29)$$

for $z>0$. Noting that $\chi_2=\theta_2^s-\theta_2^d$, one can write Eq. (3.30) as

$$\nabla^2\chi_2-\frac{1}{\lambda^2}\sin\chi_2=0, \quad (3.30)$$

where

$$\frac{1}{\lambda^2}=\frac{g_{sd}}{g_{ss}g_{dd}}\Delta_2^s\Delta_2^d 4\left(\frac{m_d}{\rho_s^d}+\frac{m_s}{\rho_s^s}\right).$$

A single-soliton solution to the sine-Gordon equation of Eq. (3.30) for the relative phase χ_2 is given by

$$\chi_2(z)=4\tan^{-1}\left(a_2e^{-\frac{z}{\lambda_2}}\right). \quad (3.31)$$

One can decompose Eq. (3.31) and obtain the expression for θ_2^d and θ_2^s as

$$\theta_2^d=\beta_2^0z+\theta_2^0+\pi-\frac{4\rho_s^sm_d}{\rho_s^dm_s+\rho_s^sm_d}\tan^{-1}\left(a_2e^{-\frac{z}{\lambda_2}}\right), \quad (3.32)$$

and

$$\theta_2^s=\beta_2^0z+\theta_2^0+\frac{4\rho_s^dm_s}{\rho_s^dm_s+\rho_s^sm_d}\tan^{-1}\left(a_2e^{-\frac{z}{\lambda_2}}\right), \quad (3.33)$$

respectively. Similarly, one may add the Euler-Lagrange equation for θ_1^d and θ_1^s to obtain the sine-Gordon equation for $\chi_1 = \theta_1^s - \theta_1^d$ (i.e., for $z < 0$). By following the decomposition approach for χ_2 , one can write the phase variables $\theta_1^d$and θ_1^s as

$$\theta_1^d = \beta_1^0 z + \theta_1^0 + \pi - \frac{4\rho_s^s m_d}{\rho_s^d m_s + \rho_s^s m_d} \tan^{-1}\left(a_1 e^{-\frac{z}{\lambda_1}}\right), \tag{3.34}$$

and

$$\theta_1^s = \beta_1^0 z + \theta_1^0 + \frac{4\rho_s^d m_s}{\rho_s^d m_s + \rho_s^s m_d} \tan^{-1}\left(a_1 e^{-\frac{z}{\lambda_1}}\right), \tag{3.35}$$

respectively. The current density $\tilde{J}_l^i = 2e\,(\partial F/\partial\theta_l^i)$ for l=1, 2 at $z = 0$ leads to

$$\tilde{J}_2^s = \frac{2e}{\hbar}\left[\frac{J^{ss}}{d_s}\sin(\theta_2^s - \theta_1^s) + \frac{J^{sd}}{d_s}\sin(\theta_2^s - \theta_1^d)\right], \tag{3.36}$$

and

$$\tilde{J}_1^s = \frac{2e}{\hbar}\left[-\frac{J^{ss}}{d_s}\sin(\theta_2^s - \theta_1^s) - \frac{J^{sd}}{d_s}\sin(\theta_2^d - \theta_1^s)\right], \tag{3.37}$$

Similar relation for $\tilde{J}_1^d$ and $\tilde{J}_1^s$ can be obtained easily. Also, noting that the current density is given by

$$\vec{J} \cong \frac{1}{\Lambda}\frac{\Phi_0}{2\pi}\nabla\theta = 2e\frac{dF}{d\theta},$$

one may write for

$$\begin{aligned}\tilde{J}_1^s &= 2e\frac{\hbar\rho_s^s}{m_s}\beta_1^0 + \frac{b_1 a_1}{\lambda_1(1+a_1)} \\ &= -\frac{J^{ss}}{d_s}\sin[\delta\theta^o + b_2(\tan^{-1}a_2 + \tan^{-1}a_1)] \\ &\quad -\frac{J^{sd}}{d_s}\sin[\delta\theta^o + \pi + b_2(\tan^{-1}a_2 + \tan^{-1}a_1)],\end{aligned} \tag{3.38}$$

where $\delta\theta^o = \theta_2^o - \theta_1^o$ denotes the relative phase constant which does not depend on position, $b_1 = 8e\rho_s^s\rho_s^d/(\rho_s^d m_s + \rho_s^s m_d)$ and $b_2 = 4\rho_s^d m_s\ /(\rho_s^d m_s + \rho_s^s m_d)$. For the simple case of $a_1 = 0$ and $a_2 = 0$, one can obtain

$$\frac{2e\rho_s^s}{m_s}\beta_1^0 = -\frac{J^{ss}}{d_s}\sin(\delta\theta^o) + \frac{J^{ds}}{d_s}\sin(\delta\theta^o). \tag{3.39}$$

This means that when $\beta_1^0 = 0$ and $\theta_2^0 = (0,\pi) = \theta_1^0$, the ground state is time-reversal symmetry invariant since $\tilde{J}_1^s = 0$ and $\tilde{J}_1^d = 0$. On the other hand, when $a_1 \neq 0$ and $a_2 \neq 0$, but both a_1 and a_2 are small, one may expand

$$\tan^{-1} a = a - \frac{a^3}{3} + \frac{a^5}{5} + \cdots .$$

and write Eq. (3.40) as

$$\frac{2e\rho_s}{m_s}\beta_1^0 + \frac{b_1 a_1}{\lambda_1} \cong$$

$$-\frac{J^{ss}}{d_s}\sin[\delta\theta^o + b_2\,(a_2 + a_1)\,] + \frac{J^{ds}}{d_s}\sin(\delta\theta^o + b_3 a_2 + b_2 a_1), \tag{3.40}$$

indicating the relations between the constants β_1^0, $\delta\theta^o$, a_1, and a_2.

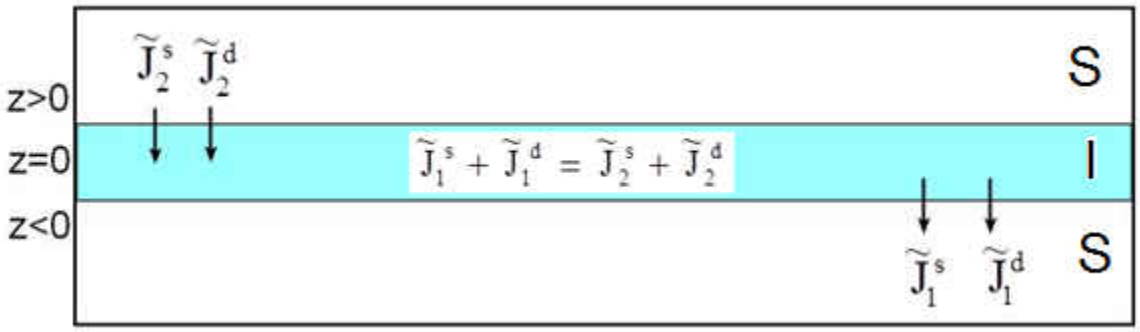

Figure 12. Boundary conditions for current density in the ground state of LJJ are schematically illustrated. A LJJ with two layers of two-gap superconductors which are separated by an insulator in the z-direction is shown. The *l=2* and *l*=1 superconductor layers are above ($z > 0$) and below ($z < 0$) the junction interface.

At the junction interface (i.e., z =0), the current density is conserved (Fig. 12). This boundary condition for the current densities may be summarized as

$$\tilde{J}_1^s + \tilde{J}_1^d = (\tilde{J}_2^s + \tilde{J}_2^d). \tag{3.41}$$

One may see how this boundary condition may lead to phase frustration by first evaluating the current densities at $z = 0$ as

$$\tilde{J}_2^s = 2e\frac{\partial F}{\partial \theta_2^s} = 2e\left[\frac{J^{ss}}{d_s}\sin(\theta_2^s - \theta_1^s) + \frac{J^{sd}}{d_s}\sin\left(\theta_2^s - \theta_1^d\right)\right], \tag{3.42}$$

$$\tilde{J}_2^d = 2e\frac{\partial F}{\partial \theta_2^d} = 2e\left[\frac{J^{dd}}{d_s}\sin(\theta_2^d - \theta_1^d) + \frac{J^{ds}}{d_s}\sin(\theta_2^d - \theta_1^s)\right], \tag{3.43}$$

$$\tilde{J}_1^s = 2e\frac{\partial F}{\partial \theta_1^s} = -2e\left[\frac{J^{ss}}{d_s}\sin(\theta_2^s - \theta_1^s) + \frac{J^{ds}}{d_s}\sin(\theta_2^d - \theta_1^s)\right], \tag{3.44}$$

and

$$\tilde{J}_1^d = 2e\frac{\partial F}{\partial \theta_1^d} = -2e\left[\frac{J^{dd}}{d_s}\sin(\theta_2^d - \theta_1^d) + \frac{J^{sd}}{d_s}\sin\left(\theta_2^s - \theta_1^d\right)\right]. \tag{3.45}$$

Now, one can impose the boundary condition of Eq. (3.44) at $z = 0$. Applying the boundary condition, one can show that $\tilde{J}_1^s = 0$ when $\beta_1^0 = 0$, $a_1 = a_2 = 0$ and $\theta_1^0 = (0, \pi) = \theta_2^0$. This means that $\tilde{J}_1^s = \tilde{J}_1^d = \tilde{J}_2^s = \tilde{J}_2^d$ =0, indicating that there is no net current flowing through the system in the ground state. This solution obeys the time-reversal symmetry. Another solution that satisfies the boundary condition at z = 0 may also be found. The solution $\tilde{J}_1^s + \tilde{J}_1^d = 0$ (and $\tilde{J}_2^s + \tilde{J}_2^d = 0$) indicates that the net current density is zero when $\tilde{J}_1^s = -\tilde{J}_1^d$ (and $\tilde{J}_2^s = -\tilde{J}_2^d$). This solution breaks time-reversal symmetry.

The appearance of the BTRS state in the ground state is indicated by the non-zero value of the relative phase constant $\delta\theta^o = \theta_2^0 - \theta_1^0$. This constant may be computed by evaluating the phases at the junction interface (i.e., z = 0). At z = 0, the phases can be obtained using Eqs. (3.37) and (3.38) as

$$\theta_l^d = \theta_l^0 + \pi - \frac{4\rho_s^s m_d}{\rho_s^d m_s + \rho_s^s m_d}\tan^{-1} a_l, \tag{3.46}$$

and

$$\theta_l^s = \theta_l^0 + \frac{4\rho_s^s m_d}{\rho_s^d m_s + \rho_s^s m_d} \tan^{-1} a_l. \tag{3.47}$$

Subtracting Eq. (3.46) from Eq. (3.47), one can obtain

$$\chi_l = \pi - 4 \tan^{-1} a_l. \tag{3.48}$$

Now, the relative phase constant $\delta\theta^o = \theta_2^0 - \theta_1^0$ indicating that the ground state breaks the time-reversal symmetry is obtained by imposing the boundary conditions $\tilde{J}_1^s = -\tilde{J}_1^d$ and $\tilde{J}_2^s = -\tilde{J}_2^d$. By using Eqs. (3.46) and (3.47), one can obtain

$$\delta\theta^o = \tan^{-1}\left\{\frac{\sin K_d(\chi_2^o - \chi_1^o) - \sin K_s(\chi_2^o - \chi_1^o) - \frac{J^{sd}}{J^{ss}}[\sin(K_s\chi_2^o - K_d\chi_1^o) - \sin(K_d\chi_2^o - K_s\chi_1^o)]}{\cos K_d(\chi_2^o - \chi_1^o) + \cos K_s(\chi_2^o - \chi_1^o) + \frac{J^{sd}}{J^{ss}}[\cos(K_s\chi_2^o - K_d\chi_1^o) + \cos(K_d\chi_2^o - K_s\chi_1^o)]}\right\}, \tag{3.49}$$

where χ_l^o is the relative phase of the two condensates of l-th S layer in the ground state where the system has minimum free energy. From Eq. (3.44) it is clear that $\theta_2^o - \theta_1^o = 0$ when the relative phases for both the S layers are zero. Similarly, when two relative phases are equal, but have opposite signs (i.e. $\chi_2^o = \chi^o$ and $\chi_1^o = -\chi^o$), one can obtain

$$\delta\theta^o = \tan^{-1}\left[\frac{\sin 2K_s\chi^o - \sin 2K_d\chi^o - \frac{2J^{sd}}{J^{ss}} \sin\chi^o(K_d - K_s)}{\cos 2K_s\chi^o + \cos 2K_d\chi^o + \frac{2J^{sd}}{J^{ss}} \cos\chi^0(K_d - K_s)}\right]. \tag{3.50}$$

To study the variation of phase constant $\delta\theta^o = \theta_2^0 - \theta_1^0$ as a function of ϕ^{ss}, the relative phases at the minimum free energy was obtained by plotting free energy as a function of relative phase as shown in Fig. 13. For a given value of ϕ^{ss}, the phase configuration (χ_1, χ_2) which corresponds to the ground state (χ_1^o, χ_2^o) is determined. This value is substituted into Eq. (3.50) to calculate $\delta\theta^o$ numerically. In Fig. 13, a plot of $\delta\theta^o$ versus ϕ^{ss} is shown to illustrate the dependence on K_s. The three lines corresponds to $K_s = 0.49$ (solid line), $K_s = 0.47$ (dashed line), and $K_s = 0.45$ (dot-dashed line). The curves in Fig. 13 show that the relative phase constant $\delta\theta^o$in the

ground state varies linearly with ϕ^{ss}. Also, one can see from Fig. 14 that the rate of variation $\delta\theta^o$ of for $K_s = 0.45$ is higher than that for $K_s = 0.47$ and $K_s = 0.49$. This dependence on K_s indicates that greater charge imbalance between the charge densities of the s and d-band present in the system leads to stronger frustration in the ground state phase configurations.

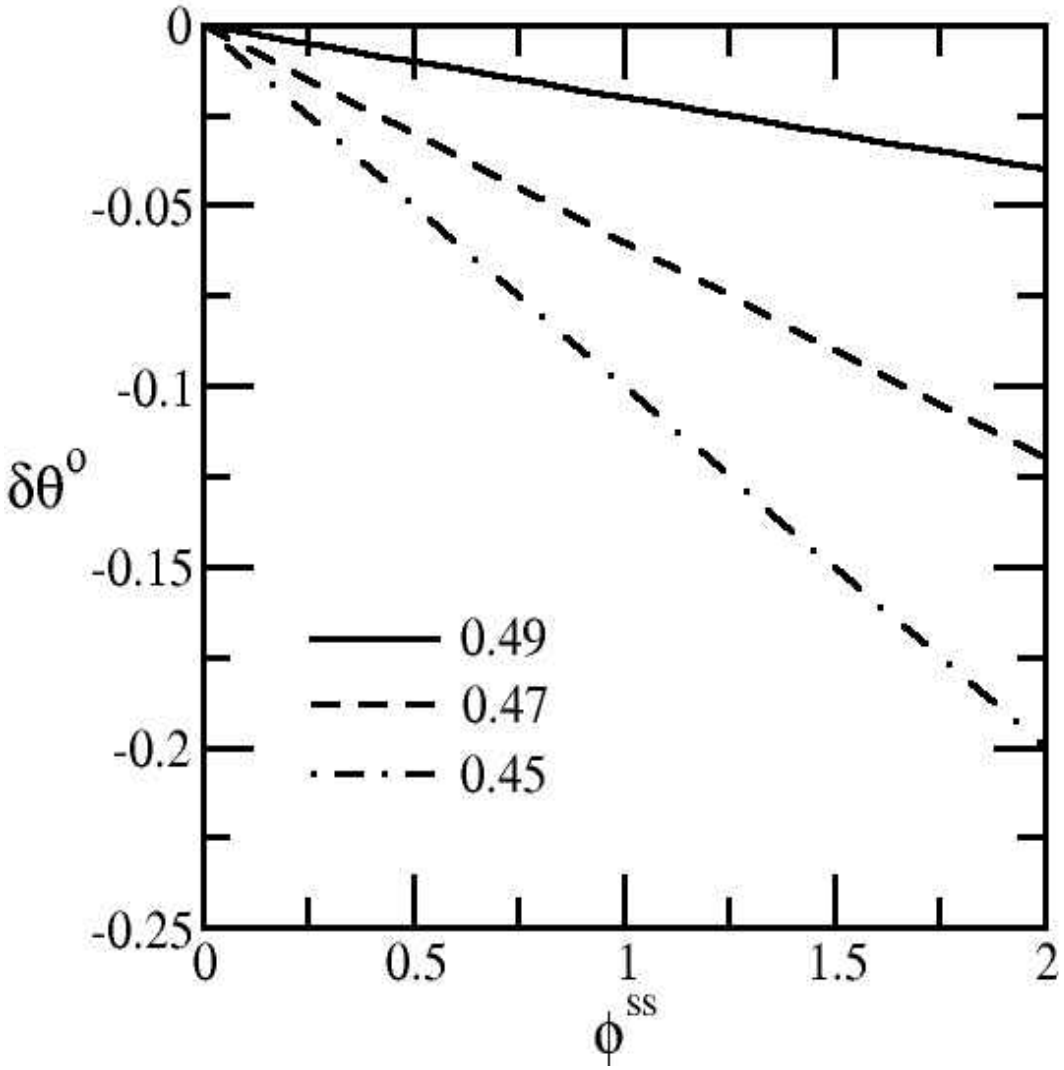

Figure 13. The phase constant $\delta\theta^o$ for the ground state is plotted as a function of ϕ^{ss} for three different values of $K_s = 0.49$ (solid line), 0.47 (dashed line), and 0.45 (dot-dashed line). These curves illustrate the effect of relative phase on the phase constant.

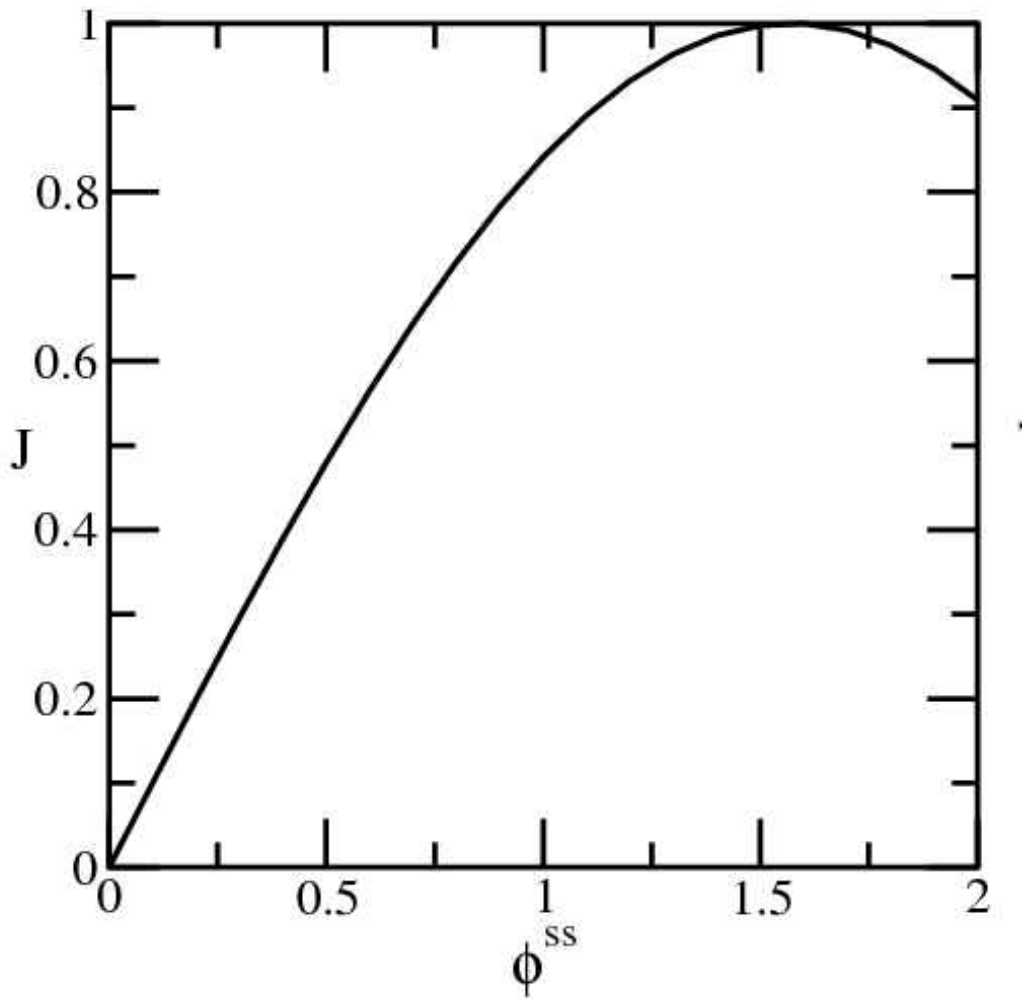

Figure 14: The current density J in the ground state is plotted as a function of ϕ^{ss}. The curve illustrates the effect of relative phase on the current density at the junction interface ($z = 0$).

In Fig. 14 the current density $J = |J_1^s|$ at the junction interface (i.e., z = 0) is plotted as a function of the phase difference ϕ^{ss}. The curve indicates clearly that current density varies as the sine function with the phase difference. The results of phase frustration in the ground state of the Josephson junction with two-gap superconductors and its consequences are discussed in Chapter V.

CHAPTER IV

FLUXON DYNAMICS IN TWO COUPLED LJJS

In this chapter, the equation of motion for a fluxon in the two-coupled LJJs with two-gap superconductors is derived from the microscopic Hamiltonian. This equation of motion can serve as a starting point for investigating the phase dynamics of two coupled LJJs in future work. As a way to derive the equation of motion, the effective action for a stack of LJJs is obtained by starting with the BCS model. Equations of motion for different phase variables in the LJJ are obtained by using Euler-Lagrange equations. These Euler-Lagrange equations are expressed as a set of coupled sine-Gordon equations.

4.1 Effective Action for Two-Coupled LJJs

A system of two vertically stacked LJJs that are based on two-gap superconductors will interact with each other via the charging effect and magnetic induction effect. These two coupled LJJs may have interesting phase dynamics due to the magnetic induction effect between junctions. In this junction, each superconducting layer is represented by two pseudo-order parameters $\psi_{0,l}^{s}\exp(i\theta_l^s)$ and $\psi_{0,l}^{d}\exp(i\theta_l^d)$. For the two coupled LJJs, there are three superconductor layers as shown schematically in Fig. 15. Here, L_x and L_y denote the dimensions in *x*- and *y*- direction, respectively. The external magnetic field B is applied in the y-direction. Here d_s and d_I denote the thickness of the superconductor

(S) and insulator (I) layer, respectively. In this LJJ system, there are three types of interactions: i) the conventional Josephson interaction between two adjacent S layers, ii) the inter-band Josephson effects between two condensates in the same S layer, and iii) the interaction between the Josephson vortices of the two LJJs via the magnetic induction effect.

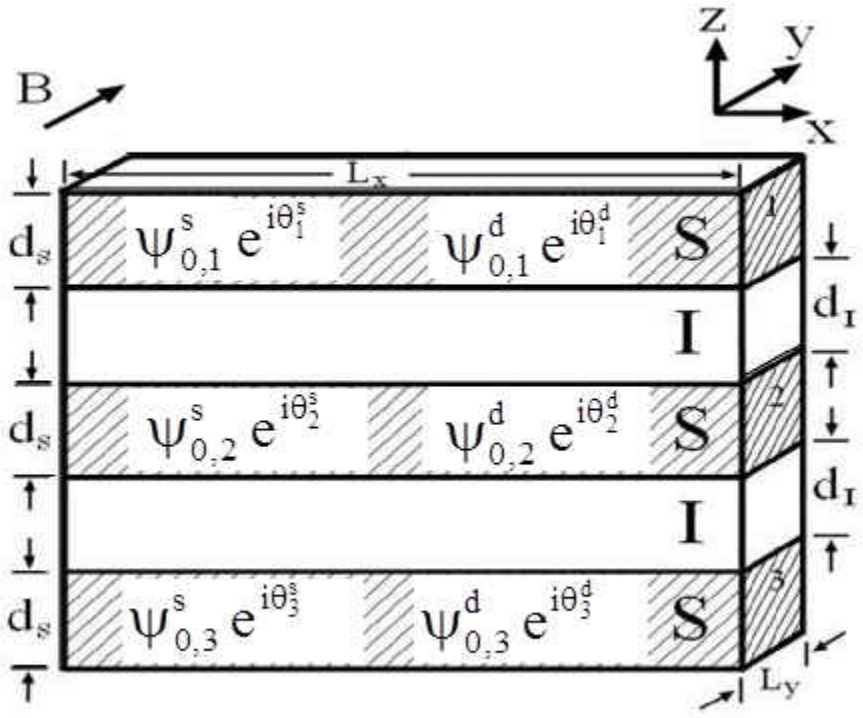

Figure 15. A Schematic diagram illustrating two coupled LJJ with two-gap superconductors is shown.

One may include these three types of interactions in the LJJ and examine the phase dynamics by using the functional integral approach. By using the BCS model for two-gap superconductors, one may write the partition function Z for the system of coupled LJJs. In this functional integral approach, the fermion fields are represented by

Grassmann variables due to its anti-commutation property. The partition function Z is given by

$$Z = \prod_{l,i} \int D[\bar{c}^i_{\sigma,l}, c^i_{\sigma l}] D\vec{A}_l D A^z_{l+1,l} D\varphi_l D\Delta^i_l e^{-S[\bar{c}^i_{\sigma,l}, c^i_{\sigma l}, \vec{A}_l, A^z_{l+1,l}, \varphi_l, \Delta^i_l]}, \tag{4.1}$$

where $A^z_{l+1,l} = \int_{l=1}^{l=2} A^z dz$, and A^z is the z-component of the vector potential in the insulator between the (l+1)-th and l-th S layers. Here, $\boldsymbol{A}^x_l$ and φ_l are the vector potential and scalar potential in the l-th S layer, respectively. The Euclidean action S includes three contributions: $S = S_{field} + S_{gap} + S_{matter}$. The action S_{field} accounts for the electromagnetic field contribution

$$S_{field} = \sum_l \int \partial\tau \int d\vec{r} \frac{d_I}{8\pi} \left[\epsilon \left(E^z_{l+1,l} \right)^2 + \left(B^y_{l+1,l} \right)^2 \right], \tag{4.2}$$

where the electric field $E^z_{l+1,l}$ and magnetic field $B^y_{l+1,l}$ in the I layer are given by

$$E^z_{l+1,l} = \frac{1}{d_I} \frac{\partial A^z_{l+1,l}}{\partial \tau} - \frac{\varphi_{l+1} - \varphi_l}{d_I}, \tag{4.3}$$

$$B^y_{l+1,l} = -\frac{1}{d_I} \frac{\partial A^z_{l+1,l}}{\partial x} - \frac{\boldsymbol{A}^x_{l+1} - \boldsymbol{A}^x_l}{d_I}. \tag{4.4}$$

The action S_{gap} which accounts for the gap energy contribution is given by

$$S_{gap} = \sum_l \int \partial\tau \int d\vec{r} \left[\frac{|\Delta^s_l|^2}{g_{ss}} + \frac{|\Delta^d_l|^2}{g_{dd}} - \frac{g_{sd} d_s}{g_{ss}\, g_{dd}} \left(\Delta^s_l \bar{\Delta}^d_l + \bar{\Delta}^s_l \Delta^d_l \right) \right]. \tag{4.5}$$

This action may be rewritten in terms of the phase as

$$S_{gap} = \sum_l \int \partial\tau \int d\vec{r} \left[\frac{|\Delta^s_l|^2}{g_{ss}} + \frac{|\Delta^d_l|^2}{g_{dd}} - \frac{2\, g_{sd}}{g_{ss}\, g_{dd}} \Delta^s_l \Delta^d_l \cos\left(\theta^d_l - \theta^s_l \right) \right], \tag{4.6}$$

where the first two terms of Eq. (4.6) are due to the energy gap contributions in the *s*- and *d*-band of l-th S layer. Here, $g_{ss} = det(V)/V^{dd}$, $g_{dd} = det(V)/V^{ss}$, $g_{sd} = det(V)\, V^{sd}/V^{dd}\, V^{ss}$, and the pairing matrix V is defined in Eq. (2.18). Note that the $\Delta^s_l \bar{\Delta}^d_l$ term accounts for the contribution from the process of a Cooper pair creation in the

d-band and a Cooper pair destruction in the *s*-band of *l*-th S layer. Similarly, the $\bar{\Delta}_l^s \Delta_l^d$ term describes the process of a Cooper pair creation in the *s*-band and Cooper pair destruction in the *d*-band of *l*-th S layer. Finally, the action S_{matter} accounts for the contributions from the matter field. The action S_{matter} for the two-gap superconductors based LJJ is given by

$$S_{matter} = \sum_{l,i} \int d\tau \int d\vec{r} \left\{ \bar{c}_{\sigma,l}^i (\partial\tau - ie\varphi_l) c_{\sigma l}^i - \bar{c}_{\sigma,l}^i \left[\frac{1}{2m} \left(\nabla - ie\vec{A}_l \right)^2 + \mu_l \right] c_{\sigma l}^i \right\}$$
$$+ \sum_{l,i} \int d\tau \int d\vec{r} \left[\bar{\Delta}_l^i c_{\sigma l}^i c_{\sigma' l}^i + \Delta_l^i \bar{c}_{\sigma,l}^i \bar{c}_{\sigma',l}^i \right]$$
$$+ \sum_{l,i,j} \int d\tau \int d\vec{r} \ \left(T_{l+1,l}^{ij} e^{ieA_{l+1,l}^z} \bar{c}_{\sigma,l+1}^i c_{\sigma l}^j + h.c. \right), \qquad (4.7)$$

where Δ_l^i annihilates and $\bar{\Delta}_l^i$ creates a Cooper pair in the *i*-band of *l*-th S layer. The first two terms of Eq. (4.7) represent the non-interacting Hamiltonian contribution. The pair interaction term, $\bar{\Delta}_l^i c_{\sigma l}^i c_{\sigma' l}^i$, denotes the destruction of two electrons while creating a Cooper pair in the same *i*-electronic band of *l*-th S layer. Similarly, the $\Delta_l^i \bar{c}_{\sigma,l}^i \bar{c}_{\sigma',l}^i$ term denotes the destruction of a Cooper pair while creating two electrons in the *i*-th electronic band of *l*-th S layer. The last two terms of Eq. (4.7) represent the contribution from tunneling between the two adjacent S layers. For example, the $\bar{c}_{\sigma,l+1}^i c_{\sigma l}^j$ term represents destruction of an electron in the *i*-band of *l*-th S layer and creation of an electron in the *j*-th band of (*l+1*)-th S layer. The hermitian conjugate of the $\bar{c}_{\sigma,l+1}^i c_{\sigma l}^j$ term represents destruction of an electron in the *i*-band of (*l+1*)-th S layer and creation of an electron in the *j*-band of *l*-th S layer of the system. Here, the tunneling matrix $T_{l+1,l}^{ij}$ describes the amplitude of electron tunneling between the two adjacent S layers.

The matter field contribution S_{matter} to the action S may be simplified by introducing the Nambu representation. In this representation, the fermion fields are written as

$$\bar{C}_k^i = \left(\bar{c}_{k,\uparrow}^i \;\; c_{-k,\downarrow}^i\right), \quad \text{and} \quad C_k^i = \begin{pmatrix} c_{k,\uparrow}^i \\ \bar{c}_{-k,\downarrow}^i \end{pmatrix}.$$

The pair fields $\bar{A}_k^i$ and A_k^i which represent creation and destruction of a Cooper pairs, respectively, are written as operators. These operators may be written in terms of the Pauli matrices as

$$\bar{A}_k^i = \bar{C}_k^i \tau_+ C_k^i, \tag{4.8}$$

$$A_k^i = \bar{C}_k^i \tau_- C_k^i, \tag{4.9}$$

where $\tau_\pm = \frac{1}{2}(\tau_1 \pm i\tau_2)$ and the three Pauli matrices are

$$\tau_1 = \begin{pmatrix} 0 & 1 \\ 1 & 0 \end{pmatrix},$$

$$\tau_2 = \begin{pmatrix} 0 & -i \\ i & 0 \end{pmatrix},$$

$$\tau_3 = \begin{pmatrix} 1 & 0 \\ 0 & -1 \end{pmatrix}.$$

By substituting $\bar{C}_k^i$, C_k^i, and Pauli matrices into Eqs. (4.8) and (4.9), one can show that

$$\bar{A}_k^i = \bar{c}_{k,\uparrow}^i \, \bar{c}_{-k,\downarrow}^i, \tag{4.10}$$

$$A_k^i = c_{-k,\downarrow}^i c_{k,\uparrow}^i. \tag{4.11}$$

Similarly, the Nambu representation may be expanded to include both *s*- and *d*-band electrons as

$$\bar{C} = \left(\bar{c}_{\uparrow l}^s \;\; c_{\downarrow,l}^s \; \bar{c}_{\uparrow l}^d \;\; c_{\downarrow,l}^d\right) \quad \text{and} \quad C = \begin{pmatrix} c_{\uparrow l}^s \\ \bar{c}_{\downarrow l}^s \\ c_{\uparrow,l}^d \\ \bar{c}_{\downarrow l}^d \end{pmatrix}.$$

By following Machida *et al*. [34], one can write the matter field contribution to the action in a matrix form as

$$S_{matter} = \sum_l \int d\tau \int d\vec{r}\,\{\bar{C}G^{-1}C\}. \tag{4.12}$$

The action S_{matter} may be written more explicitly as

$$S_{matter} = \sum_l \int d\tau \int d\vec{r} \left\{ \bar{C} \begin{pmatrix} \ddots & & & & & \\ & 0 & 0 & 0 & 0 & \\ & \hat{\mathrm{T}}_{l+2,l+1} & \mathrm{G}_{l+1}^{-1} & \hat{\mathrm{T}}_{l+1,l} & 0 & \\ & 0 & \hat{\mathrm{T}}_{l+1,l}^{*} & \mathrm{G}_{l}^{-1} & \hat{\mathrm{T}}_{l,l-1}^{*} & \\ & 0 & 0 & 0 & 0 & \\ & & & & & \ddots \end{pmatrix} C \right\}, \tag{4.13}$$

where the electron Green function G_l is given by

$$G_l^{-1} = \begin{pmatrix} g_l^{+s} & \Delta_l^s & 0 & 0 \\ \bar{\Delta}_l^s & g_l^{-s} & 0 & 0 \\ 0 & 0 & g_l^{+d} & \Delta_l^d \\ 0 & 0 & \bar{\Delta}_l^d & g_l^{-d} \end{pmatrix}. \tag{4.14}$$

Here, the matrix elements of the Green function $G_l^{-1}$are

$$g_l^{+s} = -\partial_\tau - ie\varphi_l + \frac{1}{2m}\left(\nabla_l - ie\vec{A}_l\right)^2 + \mu_l^s, \tag{4.15}$$

$$g_l^{-s} = -\partial_\tau + ie\varphi_l - \frac{1}{2m}\left(\nabla_l + ie\vec{A}_l\right)^2 - \mu_l^s, \tag{4.16}$$

$$g_l^{+d} = -\partial_\tau - ie\varphi_l + \frac{1}{2m}\left(\nabla_l - ie\vec{A}_l\right)^2 + \mu_l^d, \tag{4.17}$$

$$g_l^{-d} = -\partial_\tau + ie\varphi_l - \frac{1}{2m}\left(\nabla_l + ie\vec{A}_l\right)^2 - \mu_l^d, \tag{4.18}$$

and the μ_l^i's are the chemical potential of the *i*-band of the *l*-th S layer. Similarly, the tunneling matrix $\hat{T}_{l+1,l}$ for the electrons is given by

$$\widehat{T}_{l+1,l} = \begin{pmatrix} T^{s}_{l+1,l} e^{ieA^{z}_{l+1,l}} & 0 & 0 & 0 \\ 0 & -T^{*s}_{l+1,l}\, e^{-ieA^{z}_{l+1,l}} & 0 & 0 \\ 0 & 0 & T^{d}_{l+1,l} e^{ieA^{z}_{l+1,l}} & 0 \\ 0 & 0 & 0 & -T^{*d}_{l+1,l} e^{-ieA^{z}_{l+1,l}} \end{pmatrix}. \quad (4.19)$$

The fermion contribution in the S_{matter} must be integrated out to obtain the effective action S_{eff} which includes the phase contribution.

To obtain the effective action S_{eff}, one writes the partition function Z for the stack of two LJJs as

$$Z = \prod_{l,i} \int D[\bar{C}, C] D\vec{A}_l DA^{z}_{l+1,l} D\varphi_l D\Delta^{i}_{l} e^{-S[\bar{C}, C, \vec{A}_l, A^{z}_{+1,l}, \varphi_l, \Delta^{i}_{l}]}. \quad (4.20)$$

Integrating out the fermion degrees (i.e., $\bar{C}$, and C) in the functional integral by using Grassmann integration, one may simplify the partition function Z as

$$Z = \prod_{l,i} \int D\vec{A}_l DA^{z}_{l+1,l} D\varphi_l D\Delta^{i}_{l}\, e^{-T_r \ln G^{-1}} e^{-(S_{field}+S_{gap})}. \quad (4.21)$$

Equation (4.21) indicates that the effective action S_{eff} of the LJJ system may now be written as

$$S_{eff} = S_{field} + S_{gap} + T_r \ln G^{-1}. \quad (4.22)$$

To obtain an explicit expression for the effective action, one needs to evaluate the last term of Eq. (4.22). The trace of the logarithm of inverse Green's function (i.e.,$Tr\ \ln G^{-1}$) may be evaluated by making a unitary transformation (i.e., $G \rightarrow \widehat{U}_l G \widehat{U}_l^{-1}$). The unitary transformation matrix $\widehat{U}_l$ is written as

$$\widehat{U}_l = \begin{pmatrix} e^{-i\frac{\theta_l^s}{2}} & 0 & 0 & 0 \\ 0 & e^{i\frac{\theta_l^s}{2}} & 0 & 0 \\ 0 & 0 & e^{-i\frac{\theta_l^d}{2}} & 0 \\ 0 & 0 & 0 & e^{i\frac{\theta_l^d}{2}} \end{pmatrix}, \tag{4.23}$$

and the inverse of the transformation matrix is given by

$$\widehat{U}_l^{-1} = \begin{pmatrix} e^{i\frac{\theta_l^s}{2}} & 0 & 0 & 0 \\ 0 & e^{-i\frac{\theta_l^s}{2}} & 0 & 0 \\ 0 & 0 & e^{i\frac{\theta_l^d}{2}} & 0 \\ 0 & 0 & 0 & e^{-i\frac{\theta_l^d}{2}} \end{pmatrix}. \tag{4.24}$$

As the Green function G can be decomposed into the non-interacting part G_o and the interaction contribution δG, one may write $G^{-1} = G_0^{-1} + \delta G^{-1}$. By taking the trace of logarithm of G^{-1}, one may write the last term of Eq. (4.24) as

$$\begin{aligned} \mathrm{Tr}\ln G^{-1} &= \mathrm{Tr}\ \ln\left[\widehat{U}_l(G_0^{-1} + \delta G^{-1})\widehat{U}_l^{-1}\right] \\ &= \mathrm{Tr}\ln\left[\widehat{U}_l G_0^{-1}(1 + G_0\delta G^{-1})\right]\widehat{U}_l^{-1}, \end{aligned} \tag{4.25}$$

One can simplify Eq. (4.24) by expanding the logarithm of G^{-1} as

$$\begin{aligned} \ln G^{-1} = \mathrm{Tr}\ \ln\left(\widehat{U}_l G_0^{-1}\widehat{U}_l^{-1}\right) + \mathrm{Tr}\ \widehat{U}_l(G_0\delta G^{-1})\widehat{U}_l^{-1} \\ -\frac{1}{2}\mathrm{Tr}\left[\left(\widehat{U}_l G_0\widehat{U}_l^{-1}\widehat{U}_l\delta G^{-1}\widehat{U}_l^{-1}\right)\left(\widehat{U}_l G_0\widehat{U}_l^{-1}\widehat{U}_l\delta G^{-1}\widehat{U}_l^{-1}\right)\right]. \end{aligned} \tag{4.26}$$

Here one may write G_0^{-1} and δG^{-1} more explicitly as

$$G_0^{-1} = \begin{pmatrix} \ddots & & & & \\ & G_{l+2}^{-1} & & 0 & \\ & & G_{l+1}^{-1} & & \\ & & & G_l^{-1} & \\ & 0 & & G_{l-1}^{-1} & \\ & & & & \ddots \end{pmatrix} \tag{4.27}$$

and

$$\delta G^{-1} = \begin{pmatrix} \ddots & & & & & \\ & 0 & 0 & 0 & 0 & \\ & \hat{T}_{l+2,l+1} & 0 & \hat{T}_{l+1,l} & 0 & \\ & 0 & \hat{T}_{l+1,l} & 0 & \hat{T}_{l,l-1} & \\ & 0 & 0 & \hat{T}_{l,l-1} & 0 & \\ & & & & & \ddots \end{pmatrix}. \tag{4.28}$$

Multiplying these matrices, one can obtain the expression for the unitary transformation of G^{-1}as

$$\hat{U}_l G_0^{-1} \hat{U}_l^{-1} = \begin{pmatrix} \ddots & & & & 0 \\ & \hat{U}_{l+1} G_{l+1}^{-1} \hat{U}_{l+1}^{-1} & & & \\ & & \hat{U}_l G_l^{-1} \hat{U}_l^{-1} & & \\ & & & \hat{U}_{l-1} G_{l-1}^{-1} \hat{U}_{l-1}^{-1} & \\ 0 & & & & \ddots \end{pmatrix}. \tag{4.29}$$

Here, the matrix elements $\hat{U}_l G_l^{-1} \hat{U}_l^{-1}$ are obtained by carrying out simple matrix multiplications as

$$\hat{U}_l G_l^{-1} \hat{U}_l^{-1} = \begin{pmatrix} g_l^{+s} & \Delta_l^s & 0 & 0 \\ \bar{\Delta}_l^s & g_l^{-s} & 0 & 0 \\ 0 & 0 & g_l^{+d} & \Delta_l^d \\ 0 & 0 & \bar{\Delta}_l^d & g_l^{-d} \end{pmatrix} + \hat{U}_l G_0^{-1} \hat{U}_l^{-1},$$

the first term does not affect the phase dynamics. Here, $g_l^{\pm i}$ is given in Eq. (4.15)-Eq. (4.18). The second term of $\hat{U}_l G_l^{-1} \hat{U}_l^{-1}$ is given by

$$\widehat{U}_l G_0^{-1} \widehat{U}_l^{-1} = \begin{pmatrix} \mathrm{G1} & 0 & 0 & 0 \\ 0 & \mathrm{G2} & 0 & 0 \\ 0 & 0 & \mathrm{G3} & 0 \\ 0 & 0 & 0 & \mathrm{G4} \end{pmatrix} \text{ and } G_0 = \begin{pmatrix} \hat{G}_{0l+1} & \hat{0} \\ \hat{0} & \hat{G}_{0l} \end{pmatrix}, \tag{4.30}$$

where the diagonal elements of the matrix $\widehat{U}_l G_0^{-1} \widehat{U}_l^{-1}$ are

$$G1 = -i\frac{\pi}{\Phi_0} W^s - \frac{m\vec{v}_{sl}^{s2}}{2} + \vec{v}_{sl}^{s}.\vec{p},$$

$$G2 = i\frac{\pi}{\Phi_0} W^s + \frac{m\vec{v}_{sl}^{s2}}{2} + \vec{v}_{sl}^{s}.\vec{p},$$

$$G3 = -i\frac{\pi}{\Phi_0} W^d - \frac{m\vec{v}_{sl}^{s2}}{2} + \vec{v}_{sl}^{d}.\vec{p},$$

$$G4 = i\frac{\pi}{\Phi_0} W^d + \frac{m\vec{v}_{sl}^{s2}}{2} + \vec{v}_{sl}^{d}.\vec{p},$$

and $W^i = (\Phi_0/2\pi c)\,(\partial\theta_l^i/\partial\tau) + \varphi_{l.}$ Here, the superfluid velocity $\vec{v}_{sl}^{\,i}$ at the *i*-band is

$$\vec{v}_{sl}^{\,i} = -\frac{1}{2m}\left(\nabla\theta_l^i - \frac{2\pi\,\vec{A}_l}{\Phi_0}\right). \tag{4.31}$$

The non-interacting Green function G_{0l} is given by

$$G_{0l} = \frac{1}{D}\begin{pmatrix} m1 & m2 & 0 & 0 \\ m3 & m4 & 0 & 0 \\ 0 & 0 & m5 & m6 \\ 0 & 0 & m7 & m8 \end{pmatrix}, \tag{4.32}$$

where *D* is the determinant of the matrix G_0^{-1} which may be written as

$$D = (g_l^{+s} g_l^{-s} - \Delta_l^s \bar{\Delta}_l^s)\left(g_l^{+d} g_l^{-d} - \Delta_l^d \bar{\Delta}_l^d\right),$$

$$m1 = g_l^{+s} g_l^{+d} g_l^{-d} - g_l^{-s} \Delta_l^d \bar{\Delta}_l^d,$$

$$m2 = -\bar{\Delta}_l^s g_l^{-d} g_l^{+d} + \Delta_l^s \Delta_l^d \bar{\Delta}_l^d,$$

$$m3 = \bar{\Delta}_l^s \Delta_l^d \bar{\Delta}_l^d + \bar{\Delta}_l^s \Delta_l^d \bar{\Delta}_l^d,$$

$$m4 = g_l^{+s} g_l^{+d} g_l^{-d} - g_l^{+s} \Delta_l^d \bar{\Delta}_l^d,$$

$$m5 = g_l^{+s} g_l^{-s} g_l^{-d} - \Delta_l^s \bar{\Delta}_l^s g_l^{-d}.$$

$$m6 = -g_l^{+s} g_l^{-s} \Delta_l^d + \Delta_l^s \bar{\Delta}_l^s \Delta_l^d,$$

$$m7 = -g_l^{+s} g_l^{-s} \bar{\Delta}_l^d + \Delta_l^s \bar{\Delta}_l^s \bar{\Delta}_l^d,$$

and

$$m8 = g_l^{+s} g_l^{-s} g_l^{+d} - \Delta_l^s \bar{\Delta}_l^s g_l^{+d}.$$

Combining these results, one can obtain the explicit expression for the Tr $\ln\left(\hat{U}_l G_0^{-1} \hat{U}_l^{-1}\right)$ term as

$$\text{Tr } \ln\left(\hat{U}_l G_0^{-1} \hat{U}_l^{-1}\right) = m_s \rho_s^s d_s \vec{v}_{sl}^{s2} + m_s \rho_s^d d_s \vec{v}_{sl}^{d2} + \frac{d_s}{8\pi\mu_s^2}\left(\frac{\Phi_0}{2\pi}\frac{\partial\theta_l^s}{\partial\tau} + \varphi_{l.}\right)^2 + \frac{d_s}{8\pi\mu_d^2}\left(\frac{\Phi_0}{2\pi}\frac{\partial\theta_l^d}{\partial\tau} + \varphi_{l.}\right)^2. \quad (4.33)$$

Note that the calculation of both matrices, $\hat{U}_l G_0 \hat{U}_l^{-1}$ and $\hat{U}_l \delta G^{-1} \hat{U}_l^{-1}$, involve multiplications of 8×8 matrices since the $\hat{U}$ is a 8×8 unitary matrix. From the calculation, one can show that Tr $\hat{U}_l G_0 \hat{U}_l^{-1} \hat{U}_l \delta G^{-1} \hat{U}_l^{-1} = 0$. The last term of Eq. (4.25) may be computed as follows. First, one needs to calculate the matrix $\hat{U}_l G_0 \hat{U}_l^{-1} \hat{U}_l \delta G^{-1} \hat{U}_l^{-1}$ for time τ and τ'. Second, one needs to multiply the two matrices evaluated at different times. Finally, one needs to take the trace of the product of the two matrices. This procedure allows one to obtain the result

$$-\frac{1}{2}\text{Tr}\left[\left(\hat{U}_l G_0 \hat{U}_l^{-1} \hat{U}_l \partial G^{-1} \hat{U}_l^{-1}\right)_{(r,\tau)} \left(\hat{U}_l G_0 \hat{U}_l^{-1} \hat{U}_l \partial G^{-1} \hat{U}_l^{-1}\right)_{(r,\tau')}\right] =$$

$$+\tilde{\beta}^{ss}(\tau-\tau')\cos\left[\frac{\tilde{\phi}_{l+1,l}^{ss}(r,\tau)+\tilde{\phi}_{l+1,l}^{ss}(r,\tau')}{2}\right] - \tilde{\alpha}^{ss}(\tau-\tau')\cos\left[\frac{\tilde{\phi}_{l+1,l}^{ss}(r,\tau)-\tilde{\phi}_{l+1,l}^{ss}(r,\tau')}{2}\right]$$

$$+\tilde{\beta}^{sd}(\tau-\tau')\cos\left[\frac{\tilde{\phi}_{l+1,l}^{sd}(r,\tau)+\tilde{\phi}_{l+1,l}^{sd}(r,\tau')}{2}\right] - \tilde{\alpha}^{sd}(\tau-\tau')\cos\left[\frac{\tilde{\phi}_{l+1,l}^{sd}(r,\tau)-\tilde{\phi}_{l+1,l}^{sd}(r,\tau')}{2}\right]$$

$$+\tilde{\beta}^{ds}(\tau-\tau')\cos\left[\frac{\tilde{\phi}_{l+1,l}^{ds}(r,\tau)+\tilde{\phi}_{l+1,l}^{ds}(r,\tau')}{2}\right] - \tilde{\alpha}^{ds}(\tau-\tau')\cos\left[\frac{\tilde{\phi}_{l+1,l}^{ds}(r,\tau)-\tilde{\phi}_{l+1,l}^{ds}(r,\tau')}{2}\right]$$

$$+\tilde{\beta}^{dd}(\tau-\tau')\cos\left[\frac{\tilde{\phi}_{l+1,l}^{dd}(r,\tau)+\tilde{\phi}_{l+1,l}^{dd}(r,\tau')}{2}\right] - \tilde{\alpha}^{dd}(\tau-\tau')\cos\left[\frac{\tilde{\phi}_{l+1,l}^{dd}(r,\tau)-\tilde{\phi}_{l+1,l}^{dd}(r,\tau')}{2}\right], \quad (4.34)$$

where the derivation of the coefficients $\tilde{\beta}^{ij}(\tau-\tau')$ and $\tilde{\alpha}^{ij}(\tau-\tau')$ is discussed in appendix B. Hence the effective action S_{eff} is given by

$$S_{eff} = S_{field} + S_{gap} + \mathrm{Tr}\,\ln\left(\hat{U}_l G_0^{-1}\hat{U}_l^{-1}\right) + \mathrm{Tr}\,\hat{U}_l(G_0\partial G^{-1})\hat{U}_l^{-1} - \frac{1}{2}\mathrm{Tr}\left[\left(\hat{U}_l G_0\hat{U}_l^{-1}\hat{U}_l\partial G^{-1}\hat{U}_l^{-1}\right)\left(\hat{U}_l G_0\hat{U}_l^{-1}\hat{U}_l\partial G^{-1}\hat{U}_l^{-1}\right)\right]. \quad (4.35)$$

Substituting Eqs. (4.33) and (4.34) into Eq. (4.35), one may obtain the effective action S_{eff} as

$$S_{eff} = \sum_l \int d\tau \int d\vec{r}\left\{\frac{|\Delta_l^s|^2}{g_{ss}} + \frac{|\Delta_l^d|^2}{g_{dd}} - \frac{2\,g_{sd}}{g_{ss}\,g_{dd}}\Delta_l^s\Delta_l^d\cos\left(\theta_l^d-\theta_l^s\right) + \sum_i \int d\tau\left[m_s\rho_s^i d_s\vec{v}_{sl}^{\,i2} + \frac{d_s}{8\pi\mu_i^2}\left(\frac{\Phi_0}{2\pi}\frac{\partial\theta_l^i}{\partial\tau}+\varphi_l\right)^2\right] + \sum_{i,j}\int d\tau'\left[\tilde{\beta}^{ij}(\tau-\tau')\cos\phi_+^{ij} - \tilde{\alpha}^{ij}(\tau-\tau')\cos\phi_-^{ij}\right]\right\}, \quad (4.36)$$

where $\phi_\pm^{ij} = \phi_\pm^{ij}(r,\tau;r,\tau') = [\tilde{\phi}_{l+1,l}^{ij}(r,\tau) + \tilde{\phi}_{l+1,l}^{ij}(r,\tau')]/2$. Note that Eq. (4.36) includes both the Josephson current ($\tilde{\beta}^{ij}$) and the quasi-particle current ($\tilde{\alpha}^{ij}$) contribution in the junction. The effective action S_{eff} obtained for the system of coupled LJJs with two-gap superconductors can now be used to derive the equation of motion for the fluxon.

4.2 Equation of Motion for Two-Coupled LJJs

In this section, the equation of motion for the phases in the LJJ will be derived from the effective action S_{eff} discussed in the previous section. It is straightforward to obtain the equation of motion from the effective action S_{eff} by applying the calculus of variation. The variations of effective action S_{eff} with respect to different phase variables

are equivalent to the Euler-Lagrange equations. Noting that the effective action S_{eff} may be used to obtain the phase contribution S_{phase} and thereby the phase part of the Lagrange density L via the relation

$$S_{phase} = \int d\tau \int d\vec{r}\ L_{phase}\,,$$

one can obtain the phase contribution to the Lagrange density as

$$L_{phase} = \sum_l \left\{ -\frac{2\, g_{sd}}{g_{ss}\, g_{dd}} \Delta_l^s \Delta_l^d \cos\chi_l + \sum_i \left[m_s \rho_s^i d_s \vec{v}_{sl}^{\,i2} + \frac{d_s}{8\pi\mu_i^2} \left(\frac{\Phi_0}{2\pi} \frac{\partial \theta_l^i}{\partial \tau} + \varphi_l \right)^2 \right] \right.$$

$$\left. + \sum_{i,j} \int d\tau' \left[\tilde{\beta}^{ij}(\tau - \tau') \cos \phi_+^{ij} - \tilde{\alpha}^{ij}(\tau - \tau') \cos \phi_-^{ij} \right] \right\}, \qquad (4.37)$$

where $\chi_l = \theta_l^d - \theta_l^s$. One can minimize the action S_{eff} with respect to variation of the phase variable θ_l^i (i.e., $\delta S_{eff}/\delta\theta_l^i = 0$) to obtain the familiar equation of motion

$$\left(\frac{\partial}{\partial t} \frac{\partial}{\partial \dot{\theta}_l^i} - \frac{\partial}{\partial x} \frac{\partial}{\partial \theta_l'^i} - \frac{\partial}{\partial \theta_l^i} \right) L_{phase} = 0, \qquad (4.38)$$

where $\dot{\theta}_l^i$ and $\theta_l'^i$ denote the time and spatial derivative of θ_l^i, respectively. By following this approach, one can minimize the action with respect to the phase variable θ_l^s (i.e., $\delta S_{eff}/\delta\theta_l^s = 0$) and obtain the equation of motion for θ_l^s. The Euler-Lagrange equation for the phase variable θ_l^s may be written as

$$\left(\frac{\partial}{\partial t} \frac{\partial}{\partial \dot{\theta}_l^s} - \frac{\partial}{\partial x} \frac{\partial}{\partial \theta_l'^s} - \frac{\partial}{\partial \theta_l^s} \right) L_{phase} = 0. \qquad (4.39)$$

The Euler-Lagrange equation of the phase variable θ_l^s may be obtained as

$$\frac{d_s}{4\pi\lambda_s^2} \frac{\partial}{\partial x} \left(\frac{\Phi_0}{2\pi} \frac{\partial \theta_l^s}{\partial x} - A_l^x \right) - \frac{d_s}{4\pi\mu_s^2} \frac{\partial}{\partial t} \left(\frac{\Phi_0}{2\pi} \frac{\partial \theta_l^s}{\partial t} + \varphi_l \right) + J_{in} \sin\chi_l$$

$$+ J_{l+1,l}^{\beta,ss} - J_{l,l-1}^{\beta,ss} - J_{l+1,l}^{\alpha,ss} + J_{l,l-1}^{\alpha,ss} + J_{l+1,l}^{\beta,ds} - J_{l,l-1}^{\beta,sd} - J_{l+1,l}^{\alpha,ds} + J_{l,l-1}^{\alpha,sd} = 0\,. \qquad (4.40)$$

where $J_{in} = \left(2g_{sd}/g_{ss}\, g_{dd}\right)\Delta_l^s \Delta_l^d$ and

$$J_{l+1,l}^{\beta,ij} = -2e \int dt' \beta(t - t') \sin \frac{\phi_{l+1,l}^{ij}}{2}.$$

Similarly, the equation of motion for the phase variable θ_l^d can be obtained by taking $\delta S_{eff}/\delta\theta_l^d = 0$. This leads to the Euler-Lagrange equation for θ_l^d as

$$\left(\frac{\partial}{\partial t}\frac{\partial}{\partial \dot{\theta}_l^d} - \frac{\partial}{\partial x}\frac{\partial}{\partial \theta_l'^d} - \frac{\partial}{\partial \theta_l^d}\right) L_{phase} = 0\,. \tag{4.41}$$

The equation of motion for θ_l^d may be expressed as

$$\frac{d_s}{4\pi\lambda_d^2}\frac{\partial}{\partial x}\left(\frac{\Phi_0}{2\pi}\frac{\partial\theta_l^d}{\partial x} - A_l^x\right) - \frac{d_s}{4\pi m_d^2}\frac{\partial}{\partial t}\left(\frac{\Phi_0}{2\pi}\frac{\partial\theta_l^d}{\partial t} + \varphi_l\right) - J_{in}\sin\chi_l$$

$$+ J_{l+1,l}^{\beta,dd} - J_{l,l-1}^{\beta,dd} - J_{l+1,l}^{\alpha,dd} + J_{l,l-1}^{\alpha,dd} + J_{l+1,l}^{\beta,sd} - J_{l,l-1}^{\beta,ds} - J_{l+1,l}^{\alpha,sd} + J_{l,l-1}^{\alpha,ds} = 0, \tag{4.42}$$

where $J_{in} = 2d_s\, g_{sd}\Delta_l^s\Delta_l^s/g_{ss}g_{dd}$. The equation of motion for the phase variables θ_{l+1}^s and θ_{l+1}^d in the (l+1)-th S layer can be obtained by following the same procedure as above and by setting $\delta S_{eff}/\delta\theta_{l+1}^s = 0$ and $\delta S_{eff}/\delta\theta_{l+1}^d = 0$. By computing both $\delta S_{eff}/\delta\theta_{l+1}^s = 0$ and $\delta S_{eff}/\delta\theta_{l+1}^d = 0$, one can obtain the following equation of motion for the phase variables $\theta_{l+1}^s$and θ_{l+1}^d as

$$\frac{d_s}{4\pi\lambda_s^2}\frac{\partial}{\partial x}\left(\frac{\Phi_0}{2\pi}\frac{\partial\theta_{l+1}^s}{\partial x} - A_{l+1}^x\right) - \frac{d_s}{4\pi m_s^2}\frac{\partial}{\partial t}\left(\frac{\Phi_0}{2\pi}\frac{\partial\theta_{l+1}^s}{\partial t} + \varphi_{l+1}\right) - J_{in}\ \sin\chi_{l+1}$$

$$+ J_{l+2,l+1}^{\beta,ss} - J_{l+1,l}^{\beta,ss} - J_{l+2,l+1}^{\alpha,ss} + J_{l+1,l}^{\alpha,ss} + J_{l+2,l+1}^{\beta,ds} - J_{l+1,l}^{\beta,sd} - J_{l+2,l+1}^{\alpha,ds} + J_{l+1,l}^{\alpha,ds} = 0\,, \tag{4.43}$$

and

$$\frac{d_s}{4\pi\lambda_d^2}\frac{\partial}{\partial x}\left(\frac{\Phi_0}{2\pi}\frac{\partial\theta_{l+1}^d}{\partial x} - A_{l+1}^x\right) - \frac{d_s}{4\pi m_d^2}\frac{\partial}{\partial t}\left(\frac{\Phi_0}{2\pi}\frac{\partial\theta_{l+1}^d}{\partial t} + \varphi_{l+1}\right) - J_{in}\sin\chi_{l+1}$$

$$+ J_{l+2,l+1}^{\beta,dd} - J_{l+1,l}^{\beta,dd} - J_{l+2,l+1}^{\alpha,dd} + J_{l+1,l}^{\alpha,dd} + J_{l+2,l+1}^{\beta,sd} - J_{l+1,l}^{\beta,ds} - J_{l+2,l+1}^{\alpha,sd} + J_{l+1,l}^{\alpha,sd} = 0\,, \tag{4.44}$$

respectively. These four equations of motion (i.e., Eqs (4.40), (4.42), (4.43), and (4.44)) may be combined to obtain the equation for phase dynamics of the junction. To obtain the coupled equation of motion for the stacked LJJs, one computes

$$\frac{4\pi\lambda_s^2}{d_s d_I}\left(-\frac{\delta S_{eff}}{\delta\theta_l^s} + \frac{\delta S_{eff}}{\delta\theta_{l+1}^d}\right) + \left(-\frac{\delta S_{eff}}{\delta\theta_l^d} + \frac{\delta S_{eff}}{\delta\theta_{l+1}^d}\right)\frac{4\pi\lambda_d^2}{d_s d_I} = 0. \tag{4.45}$$

By substituting Eqs. (4.40) - (4.44) into Eq. (4.45), one may obtain the following equation of motion

$$-\sum_i\left(\frac{\Phi_0}{2\pi d_I}\frac{\lambda_i^2}{\mu_i^2}\frac{\partial\tilde{\phi}_{l+1,l}^{ii}}{\partial t^2}+\frac{\mathrm{a}_{\lambda\mu}\Phi_0}{2\pi d_I\mu_i^2}\frac{\partial\tilde{\phi}_{l+1,l}^{ii}}{\partial t^2}-\frac{\Phi_0}{2\pi d_I}\frac{\partial\tilde{\phi}_{l+1,l}^{ii}}{\partial x^2}+\frac{4\pi\mathrm{a}_{\lambda\mu}}{d_I}\frac{\partial\left(\rho_{l+1}^i-\rho_l^i\right)}{\partial t}\right)$$

$$+\frac{J_{in}4\pi\lambda_s^2}{d_sd_I}(\sin\chi_{l+1}-\sin\chi_l)-\frac{J_{in}4\pi\lambda_d^2}{d_sd_I}(\sin\chi_{l+1}-\sin\chi_l)$$

$$-8\pi J_8+\frac{4\pi\lambda_s^2}{d_sd_I}[J_5+J_9]+\frac{4\pi\lambda_d^2}{d_sd_I}[J_6+J_7]=0\,, \tag{4.46}$$

where $\mathrm{a}_{\lambda\mu}=(2\epsilon\mu_s^2\mu_d^2+\mu_d^2\lambda_s^2-\mu_s^2\lambda_d^2)/(\mu_d^2-\mu_s^2)$,

$$J_5=\left(J_{l+2,l+1}^{\beta,ss}+J_{l,l-1}^{\beta,ss}-2J_{l+1,l}^{\beta,ss}\right)-\left(J_{l+2,l+1}^{\alpha,ss}+J_{l,l-1}^{\alpha,ss}-2J_{l+1,l}^{\alpha,ss}\right). \tag{4.47}$$

$$J_6=J_{l+2,l+1}^{\beta,dd}+J_{l,l-1}^{\beta,dd}-2J_{l+1,l}^{\beta,dd}-\left(J_{l+2,l+1}^{\alpha,dd}+J_{l,l-1}^{\alpha,dd}-2J_{l+1,l}^{\alpha,dd}\right), \tag{4.48}$$

$$J_7=\left(J_{l+2,l+1}^{\beta,sd}+J_{l,l-1}^{\beta,ds}-J_{l+1,l}^{\beta,sd}-J_{l+1,l}^{\beta,ds}\right)-\left(J_{l+2,l+1}^{\alpha,sd}+J_{l,l-1}^{\alpha,ds}-J_{l+1,l}^{\alpha,sd}-J_{l+1,l}^{\alpha,ds}\right), \tag{4.49}$$

$$J_8=J_{l+1,l}^{\beta,ss}+J_{l+1,l}^{\beta,dd}+J_{l+1,l}^{\beta,sd}+J_{l+1,l}^{\beta,ds}+J_{l+1,l}^{\alpha,ss}+J_{l+1,l}^{\alpha,dd}+J_{l+1,l}^{\alpha,sd}+J_{l+1,l}^{\alpha,ds}, \tag{4.50}$$

and

$$J_9=J_{l+2,l+1}^{\beta,ds}+J_{l,l-1}^{\beta,sd}-J_{l+1,l}^{\beta,ds}-J_{l+1,l}^{\beta,sd}-\left(J_{l+2,l+1}^{\alpha,ds}+J_{l,l-1}^{\alpha,sd}-J_{l+1,l}^{\alpha,ds}-J_{l+1,l}^{\alpha,sd}\right). \tag{4.51}$$

One may now simplify the equation of motion of Eq. (4.45) by recognizing that

$$\tilde{\phi}_{l+1,l}^{dd}=\theta_{l+l}^d-\theta_l^d-2eA_{l+1,l}^{\mathrm{z}}=\tilde{\phi}_{l+1,l}^{ss}-\chi_{l+1}+\chi_l\,. \tag{4.52}$$

Note that χ_l denotes the relative phase between two condensates in the same S layer. By making use of the fact that the phase difference (i.e., $\tilde{\phi}_{l+1,l}^{dd}$) between the *d*-band of two adjacent S-layers can be expressed in terms of that between two *s*-bands (i.e., $\tilde{\phi}_{l+1,l}^{ss}$) via Eq. (4.52), one can write the sine-Gordon equation as

$$\frac{\epsilon\,\Phi_0\overline{\Lambda}}{2\pi d_sd_I^2}\frac{\partial^2}{\partial t^2}\left[\tilde{\phi}_{l+2,l+1}^{ss}+\tilde{\phi}_{l,l-1}^{ss}-\left(2+\frac{2d_sd_I}{\overline{\Lambda}}\right)\tilde{\phi}_{l+1,l}^{ss}\right]-\frac{\Phi_0}{2\pi d_I}\frac{\partial^2\tilde{\phi}_{l+1,l}^{ss}}{\partial x^2}-8\pi J_8$$

$$+\frac{\epsilon\,\Phi_0}{2\pi}\frac{\overline{\Lambda}}{\mu_d^2 d_s d_I^2}\frac{\partial^2}{\partial t^2}\left[\chi_{l+1}-\chi_{l+2}+\chi_{l-1}-\chi_l-\left(2+\frac{2d_I d_s}{\overline{\Lambda}}\right)(\chi_l-\chi_{l+1})\right]$$

$$+\frac{4\pi\lambda_s^2}{d_s d_I}(J_5+J_7)+\frac{4\pi\lambda_d^2}{d_s d_I}(J_6+J_9)-\frac{\Phi_0\Lambda}{2\pi d_I}\frac{\partial^2(\chi_l-\chi_{l+1})}{\partial t^2}$$

$$+\frac{\Phi_0}{2\pi d_I}\frac{\partial^2(\chi_l-\chi_{l+1})}{\partial x^2}-J_{in}\frac{4\pi\left(\lambda_d^2-\lambda_s^2\right)}{d_s d_I}(\sin\chi_{l+1}-\sin\chi_l)\;\cong 0, \qquad (4.53)$$

where $\overline{\Lambda}=[(\lambda_s^2/\mu_s^2)+(\lambda_d^2/\mu_d^2)]\,/\,(\mu_s^{-2}+\mu_d^{-2})$, $(\lambda_s^2\mu_s^{-2}-\lambda_d^2\mu_d^{-2})/(\mu_s^{-2}+\mu_d^{-2})$, and J_i' s are defined in Eqs. (4.47) - (4.51) The equation of motion of (4.51) for stacked LJJs with two-gap superconductors can now serve as the starting point for describing the phase dynamics of a two coupled LJJ.

CHAPTER V

RESULTS AND DISCUSSION

5.1 Single LJJ with Two-Gap Superconductors

In this dissertation work, the phase dynamics of a single LJJ with two-gap superconductors was studied. This investigation was carried out by extending the BCS Hamiltonian to describe the two-gap superconductivity. Also, the functional integral formalism had been applied to obtain the effective action for the LJJ system. This effective action approach allowed the derivation of the perturbed sine-Gordon equations for describing the dynamics of phase differences. The derivation of the equation of motion was carried out analytically. From this analysis, the phase dynamics of a two-gap superconductor based LJJ is found to be more complex than that for the usual LJJ with one-gap superconductors. The complexity of the two-gap superconductor based LJJ arises from the presence of an inter-band Josephson current which passes from one-band to the other band in the same S layer. This inter-band Josephson effect is found to yields a soliton-like excitation (i.e., *i*-soliton) representing a 2π-phase texture.

In the LJJ, a circulating current loop which extends within the superconductor (S) layer is modified by the inter-band Josephson current. The excitation induced by the inter-band Josephson effect can lead to a large stable variation of the relative phase between the two condensates. This large amplitude fluctuation in the relative phase is

described as soliton-like excitations. The soliton-like excitations in the S layer can lead to a spatial modulation in the critical current density between two adjacent S layers. Accounting for these excitations, one can find that the fluxon dynamics in the LJJ is influenced by the modulation of critical current density. The soliton-like phase texture plotted in Fig. 4 represents a single-kink solution of the unperturbed sine-Gordon equation. This plot illustrates the variation of phase of the order parameter as a function of the position along the I layer. The solitary wave represents a kink which changes the Josephson phase either from 0 to 2π (soliton) or from 2π to 0 (anti-soliton). The modulation of critical current within a region induced by the soliton-like excitations can lead to a modulation of the fluxon velocity. Hence, the fluxon can become accelerated and, as a result, it emits radiation during the deceleration phase of fluxon motion. However, when the moving fluxon is located beyond the range of critical current modulation, its velocity remains constant. Therefore, in this region, beyond the range of the critical current modulation, the moving fluxon emits no radiation.

To estimate the effects of bias current J^B/J_c^0 on the fluxon trajectories in the velocity-position phase plane, the fluxon trajectories were obtained by numerically integrating the equations representing velocity and position modulation. In Fig. 16, position X of the fluxon is plotted as a function of velocity v for $\Gamma_1 = \Gamma_2 = 0.1$. The solid curves represent the inter-band Josephson current density $J^{sd}/J^{ss} = 0.1$ for three different values of $J^B/J_c^0 = 0.01, 0.02,$ and 0.04. Similarly the dashed curves represent the inter-band Josephson current density $J^{sd}/J^{ss} = -0.1$ for three different values of $J^B/J_c^0 = 0.01, 0.02,$ and 0.04. Here, v_∞ is the uniform initial speed of the fluxon at a position far

away from the region of 2π −phase texture which is centered at *X=0.* The values of υ_∞ depends on J^B/J_c^0.

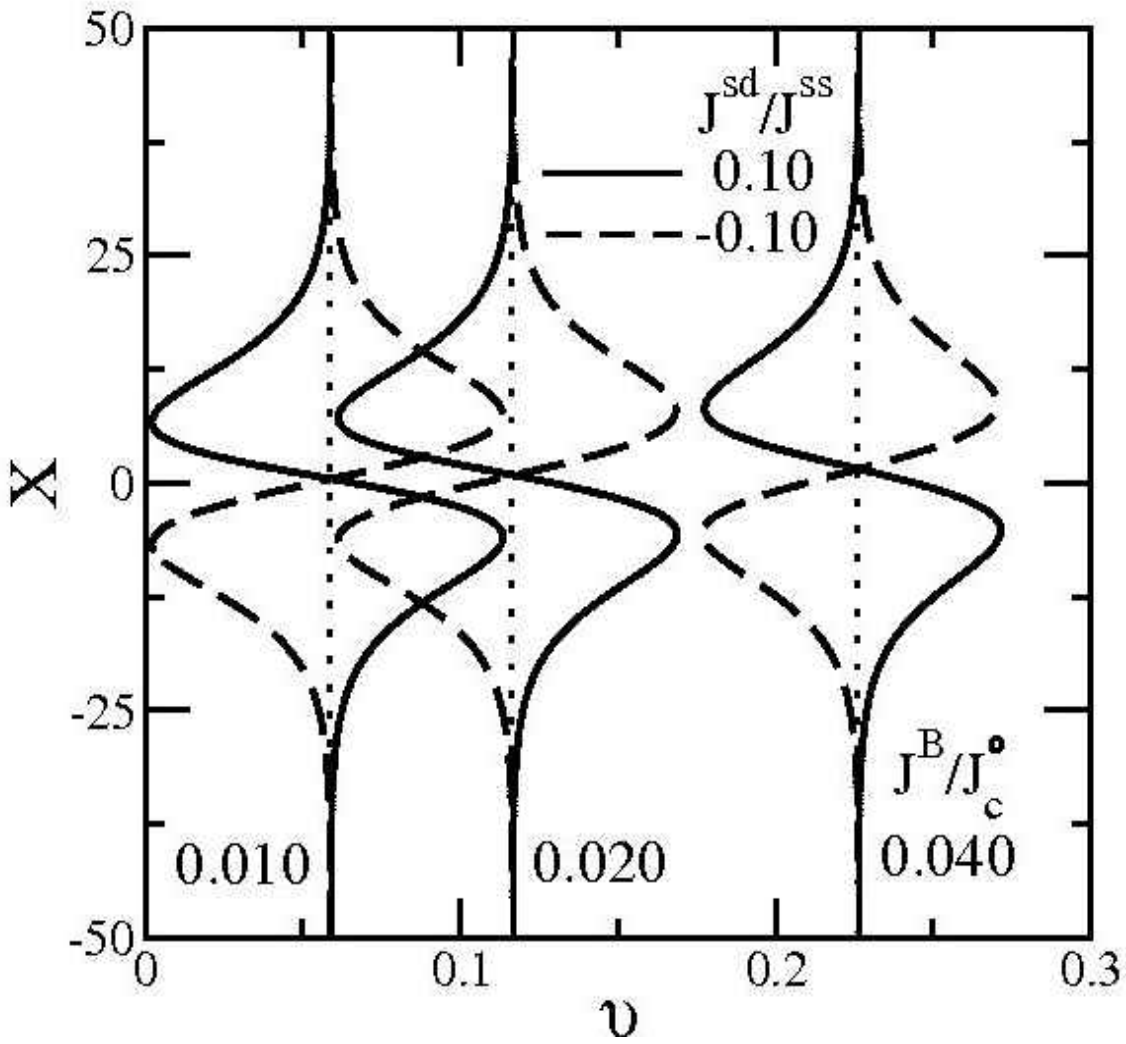

Figure 16. Fluxon trajectories in the $(\upsilon,\ X)$ phase plane for, $\Gamma_1 = 0.1,$ and $\Gamma_2 = 0.1$ are plotted to illustrate their dependence on the strength of both the bias current J^B/J_C and Josephson current J^{sd}/J^{ss}. Three curves, from left to right, correspond to $J^B/J_C = 0.01,\ 0.02,$ and 0.04 for $J^{sd}/J^{ss} = 0.1$ (solid) and $J^{sd}/J^{ss} = -0.1$ (dashed). The vertical dotted lines represent the uniform fluxon speed in the absence of critical current modulation.

From Fig. 16, it is clear that the curves show that when the bias current is small, the fluxon almost becomes pinned due to pinning effects of the critical current modulation.

For $J^B/J_C < 0.01$ speed becomes zero at $X \approx 6.5$ for $J^{sd}/J^{ss} = 0.1$ and $X \approx -6.5$ for $J^{sd}/J^{ss} = -0.1$. However, for the higher value of the bias current, $J^B/J_C > 0.01$ the driving force for the fluxon becomes stronger than the pinning force due to critical current modulation. This indicates that with a high bias current the fluxon can absorb this energy and can be accelerated. However, the fluxon can radiate energy during the decelerate phase of the motion. The curves also show that the variation in fluxon speed decreases with the increase of bias current density. The variation of fluxon speed from the vertical straight line also depends on the Josephson current density J^{sd}/J^{ss}. The curves show that the variation of fluxon speed increases with increasing J^{sd}/J^{ss}. When there is no current density (i.e., $J^{sd}/J^{ss} = 0$), there is no critical current modulation. Hence, the speed remains constant. From Eq. (2.61), one may see clearly that the bias current in a LJJ depends on the Josephson current and on the dissipation parameters $\Gamma_1$and Γ_2. It indicates that for a given value of parameters, there exists a certain cut-off for the bias current. This indicates that the bias current density must be larger than the threshold value J_{th}^B in order for the fluxon to pass through the region of critical current modulation.

The variation of the velocity (i.e., voltage) of a single fluxon with the bias current depends on the modulation of the critical current density and dissipation parameters $\Gamma_1$and Γ_2. However, the cut-off current density is the same for a given value of J^{sd}/J^{ss}. In Fig. 17, the bias current is plotted as a function of voltage for J^{sd}/J^{ss} = 0.1 (dotted line) and $J^{sd}/J^{ss} = 0.2$ (solid line) to illustrate the dependence of the threshold bias current J_{th}^B on the Josephson current J^{sd}/J^{ss}. Here the dissipation parameters are set as $\Gamma_1 = \Gamma_2 = 0.1$. The curves show that the threshold bias current increases with J^{sd}/J^{ss}.

As the critical current modulation plays the role of an effective potential for the fluxon, a larger bias current needed to overcome the pinning effect as J^{sd}/J^{ss} increases. Hence the threshold bias current is similar to the minimum current density needed to overcome the pinning force. From Fig. 17 it is clear that the voltage increases steadily with increasing bias current.

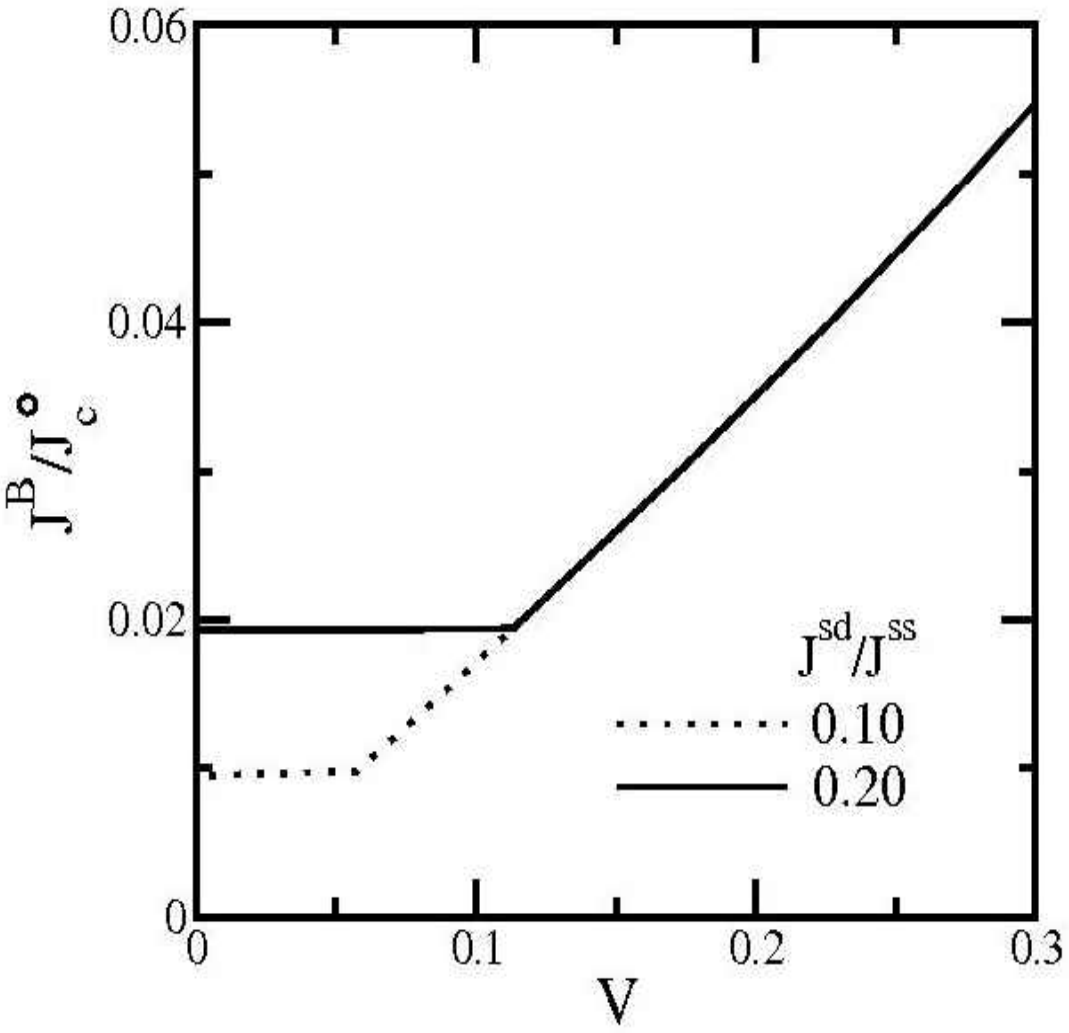

Figure 17. The current-voltage curves for J^{sd}/J^{ss}= 0.1 (dotted line) and J^{sd}/J^{ss} =0.2 (solid line) illustrate the dependence of the threshold bias current on the Josephson current. Here, the dissipation parameters are Γ_1 = 0.1, and Γ_2= 0.1.

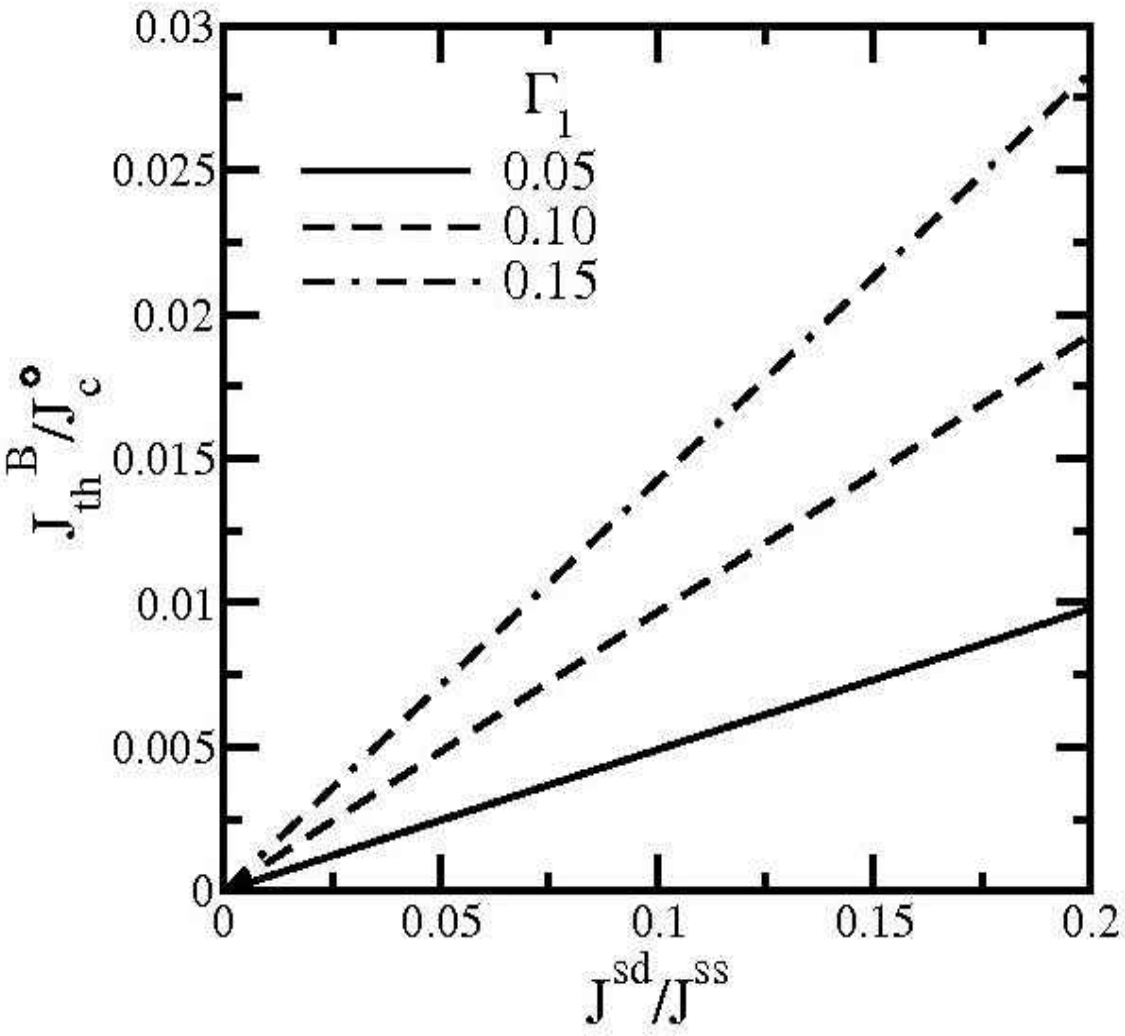

Figure 18. Variation of threshold bias current density as a function of the inter-band Josephson current density (j^{sd}) for $\Gamma_1 = 0.05, 0.07, 0.1$ (dark-solid line, dashed line, light solid, respectively) for $\Gamma_2 = 0.1, 0.07, 0.05, 0.03$, to illustrate the minimum bias current density necessary to overcome the pinning effect of the critical current modulation.

To illustrate the dependence of the threshold bias current on the inter-band Josephson effect the threshold bias current is plotted as a function of Josephson current density in Fig. 18. The curves indicate that the threshold bias current increases linearly with the Josephson current. This indicates that, as the critical current modulation increases, a

stronger driving force must be provided by the bias current density to pass the fluxon through the region of an *i*-soliton excitation.

5.2 Phase Frustration and Broken Time Reversal-Symmetry State

To understand the time-reversal symmetry invariant (TRSI) and broken time-reversal symmetry (BTRS) state in a Josephson junction with two-gap superconductors, the ground state phase configuration was investigated. The ground state phase configuration was obtained by minimizing the free energy of the LJJ with respect to phase variables in the absence of an external magnetic field. The boundary conditions were obtained at the junction interface. Applying the boundary conditions, the conditions for TRSI and BTRS state were obtained. When the current density in the *s* and *d* electronic bands in the ground state are zero, the ground state corresponds to TRSI state. In this case, the relative phase constants attain the values either 0 or π. Although the net current density in the ground state is zero, the individual currents can be non-zero. In this case, $\tilde{J}_l^s = -\tilde{J}_l^d$ and the relative phase constants are different than either 0 or π. This solution breaks time-reversal symmetry. The relative phase in the ground state was numerically calculated. The phase configuration of the ground state was determined from the free energy calculation as a functions of relative phases (χ_1, χ_2) for different values of inter-band current and Josephson current. When the ground state corresponds to the BTRS, the relative phase constant $\delta\theta^o$ computed as a function of phase difference ϕ^{ss} showed linearly dependence. The variation of current density $\lfloor J_1^s \rfloor$ with the phase difference ϕ^{ss} behaves as the sine-curve.

5.3 Two Coupled LJJ with Two-Gap Superconductors

The system of two coupled long Josephson junctions that are based on two-gap superconductors has interesting phase dynamics due to the magnetic induction effect between junctions. For the two coupled LJJs, there are three superconductor (S) separated by insulators. In this LJJ system, there are three types of tunneling interactions: i) the conventional Josephson interaction between the adjacent superconducting layers, ii) the inter-band Josephson effects between the two condensates of the same S layer, and iii) the interaction between the Josephson vortices of the two LJJs. The phase dynamics of two coupled LJJs that are based on the two-gap superconductors are studied by deriving the equation of motion. As a way to obtain the equation of motion, the effective action was obtained starting with the BCS model. Equations of motion for different variables were obtained by using Euler-Lagrange equations, which are expressed as a set of two coupled sine-Gordon equations. The coupled sine-Gordon equation for the two coupled LJJ based on two-gap superconductor shows that the dynamics of the fluxon in such a system is influenced by the inter-band Josephson effect in the superconducting layers.

CHAPTER VI

CONCLUSION

The present dissertation work is focused on the following three aspects of long Josephson junction (LJJ) with two-gap superconductors: i) inter-band Josephson effect and excitation of *i*-soliton, ii) the ground state which breaks the time-reversal symmetry, and iii) the equation of motion for the two-coupled LJJ stack.

The present investigation shows that the fluxon dynamics of LJJ with two-gap superconductors is influenced by the inter-band Josephson current. Due to the presence of two superconducting pseudo-order parameters, when the fluctuations in the relative phases become large, a 2π-phase texture may appear in each S layer. Accounting for the charge imbalance effect between two electronic bands, the equation of motion expressed as the sine-Gordon equation for relative phase was obtained for the large amplitude fluctuations. This equation is similar to that describing the motion of fluxon in the LJJ. The single-kink solution (*i*-soliton) for the equation of motion for the relative phase and the usual fluxon solution have the same functional form. However, they have a different physical interpretation because only the fluxon can carry a magnetic flux quantum. Excitation of an *i*-soliton which represents a large stable fluctuation in the relative phase can lead to a modulation of the critical current density in a LJJ. A modulation of critical current behaves as an effective pinning potential for the fluxon, modifying the fluxon

trajectories. When the bias current is applied to drive the fluxon in a dissipative environment, the fluxon motion was found to be uniform far away from the region of critical current modulation. However, the motion of a fluxon becomes non-uniform in the critical current modulation region. This allows the fluxon to be accelerated and then decelerated. During the deceleration phase of the motion, the fluxon can emit EM radiation. However, if the applied bias current is less than the threshold value, the speed of the fluxon may reduce to zero, thereby trapping the fluxon. The threshold value for the bias current density increases with increasing the inter-band Josephson current.

In the ground state of LJJ, phase frustration and broken time-reversal symmetry state are closely related and are an interesting property of LJJs with two-gap superconductors. Minimizing the steady state free energy with respect to phase variables, one can compute the current density associated with the *s*- and *d*-condensates at the junction interface as a function of parameters such as ϕ^{ss} and K_s. From both analytical and numerical calculations, the possibility of the phase frustration in the LJJ was studied. The conditions at which the solution breaks the time-reversal symmetry were obtained. The computed free energy as a function of relative phase indicates that the ground state phase configurations can have frustration, similar to a frustrated spin system. When the phase variables in a LJJ are frustrated, the relative phases which minimize the free energy can leads to the TRSB state. The numerically computed relative phase constant in the ground state varies linearly with relative the phase difference ϕ^{ss}. Also the ground state current density contribution from either *s*- or *d*-condensates at the junction interface satisfies that there is no net current but varies with the relative phase as a sine-function.

Also, the equation of motion for studying the phase dynamics of two coupled LJJs that are based on two-gap superconductors was derived. As a way to derive this equation of motion, the effective action was obtained from the BCS model and obtained through Euler-Lagrange equations for the phase variables equations, which are in turn expressed as a set of two coupled sine-Gordon equations. The coupled sine-Gordon for the two coupled LJJs based on a two-gap superconductor indicates that the dynamics of the fluxon can be influenced by the inter-band Josephson effect. This suggests that the nature of bunched fluxons in a coupled LJJs, originally is investigated for a single-gap superconductor, is modified. Hence, the inter-band Josephson effect studied in the present work can affect the collective excitation of fluxons in the intrinsic Josephson junction as well as the "Cherenkov" radiation emitted by the fluxon.

As shown in the present dissertation work, the fluxon dynamics of a LJJ with two-gap superconductors leads to a more interesting junction property than that with one-gap superconductors. Similarly, fluxon dynamics of LJJs with three-gap superconductors may even lead to an even more interesting junction property than that described in this dissertation work. Although the present research work shows that an unexpected property such as the BTRS state in the ground state can appear in a LJJ with two-gap superconductors, further investigation in clearly needed in future. Many other interesting properties of two-gap superconductors based LJJ, such as the presence of in-gap state at the junction interface and a formation of fractional fluxon has, not been investigated. A derivation of the equation of motion for the two-coupled LJJs with two-gap superconductors presented in the current dissertation work and can be taken as an excellent starting point for future research.

APPENDICES

APPENDIX A

Ginzburg-Landau Free Energy

The BCS model Hamiltonian for a long Josephson junction (LJJ) with two-gap superconductors may be expressed as the sum of two contributions: $\widehat{H} = \widehat{H}_{TB,l} + \widehat{H}_T$. Here, the Hamiltonian $\widehat{H}_{TB,l}$ accounts for the interacting electrons in the two-gap superconductor, and $\widehat{H}_T$ accounts for electron tunneling between the two adjacent superconducting (S) layers. Starting with the BCS Hamiltonian one can obtain the partition function and effective action as discussed in Chapter III. In using the Nambu notation in Grassmann variables and passing through the Hubbard-Stratonovich identity one may write the partition function Z to

$$Z = \int D[\bar{C}, C] D[\bar{\phi}, \phi] e^{-S[\bar{C}, C, \bar{\phi}, \phi]}, \tag{A.1}$$

where the action S is given by

$$S = \int_0^\beta d\tau \left\{ \sum_k \left[\bar{C}_k^s (\partial_\tau I + \varepsilon_k^s \tau_3) C_k^s + \bar{C}_k^d \left(\partial_\tau I + \varepsilon_k^d \tau_3 \right) C_k^d \right] \right.$$
$$\left. - \sum_{kk'} [\bar{\phi}_k V^{-1} \phi_{k'} + \bar{A}_k V^{-1} A_{k'}] \right\} \tag{A.2}$$

By shifting the auxiliary fields ϕ_k and $\bar{\phi}_k$, $\bar{\phi}_k \to \bar{\phi}_k + \bar{A}_{k'} V$ and $\phi_k \to \phi_k + V A_{k'}$ one may simplify the action S as

$$S = \int_0^\beta d\tau \left[\sum_{i,k} \bar{C}_k^i \left(\partial_\tau I + \varepsilon_k^i \tau_3 \right) C_k^i + \sum_{k,k'} \left(\bar{\phi}_k \frac{1}{V} \phi_{k'} + \bar{A}_k \phi_k + \bar{\phi}_k A_{k'} \right) \right], \tag{A.3}$$

where $\bar{\phi}_k$ and ϕ_k are the two component auxiliary field

$$\bar{\phi}_k = (\bar{\phi}_k^s \quad \bar{\phi}_k^d) \text{ and } \phi_k = \begin{pmatrix} \phi_k^s \\ \phi_k^d \end{pmatrix}.$$

The inverse of the pair interaction matrix V is given by

$$V^{-1} = \frac{1}{V^{ss}V^{dd} - (V^{sd})^2} \begin{pmatrix} V^{dd} & -V^{sd} \\ -V^{sd} & V^{ss} \end{pmatrix}, \tag{A.4}$$

where $det(V) = 1/V^{ss}V^{dd} - (V^{sd})^2$ is the determinant of V. The $\bar{\phi}_k V^{-1} \phi_{k'}$ term can be expressed as

$$\bar{\phi}_k V^{-1} \phi_{k'} = \frac{V^{dd}}{det(V)} \bar{\phi}_k^s \phi_{k'}^s + \frac{V^{ss}}{det(V)} \bar{\phi}_k^d \phi_{k'}^d - \frac{V^{sd}}{det(V)} \left(\bar{\phi}_k^s \phi_{k'}^d + \bar{\phi}_k^d \phi_{k'}^s \right) \tag{A.5}$$

$$= \frac{\bar{\phi}_k^s \phi_{k'}^s}{g_{ss}} + \frac{\bar{\phi}_k^d \phi_{k'}^d}{g_{dd}} - \frac{g_{sd}}{g_{ss} g_{dd}} \left(\bar{\phi}_k^s \phi_{k'}^d + \bar{\phi}_k^d \phi_{k'}^s \right), \tag{A.6}$$

where $g_{ss} = det(V)/V^{dd}$, $g_{dd} = det(V)/V^{ss}$, and $g_{sd} = det(V)\, V^{sd}/V^{dd}\, V^{ss}$. By substituting Eq. (A.6) into Eq. (A.3) and by removing the fermion fields via the Grassmann integration of the fermion part, one obtains the effective action S as

$$S = \int_0^\beta \sum_{k,k'} \left[\sum_i \frac{\bar{\phi}_k^i \phi_{k'}^i}{g_i} - \frac{g_{sd}}{g_{ss} g_{dd}} \left(\bar{\phi}_k^s \phi_{k'}^d + \bar{\phi}_k^d \phi_{k'}^s \right) \right] - \sum_i \mathrm{Tr}\, ln G_i^{-1},$$

(A.7)

where the inverse Green function $G_i^{-1} = G_s^{-1}$ or G_d^{-1} is given by

$$G_s^{-1} = \begin{pmatrix} \partial_\tau + \varepsilon_k^s & \phi_l^s \\ \bar{\phi}_l^s & \partial_\tau - \varepsilon_k^s \end{pmatrix},$$

$$G_d^{-1} = \begin{pmatrix} \partial_\tau + \varepsilon_k^d & \phi_l^d \\ \bar{\phi}_l^d & \partial_\tau - \varepsilon_k^d \end{pmatrix}. \tag{A.8}$$

After Grassmann integration, the partition function Z of the system is given by

$$Z = \prod_i det G_i^{-1} \int D[\bar{\phi}, \phi] \sum_{kk'} e^{-\int_0^\beta \left[\frac{\bar{\phi}_k^s \phi_{k'}^s}{g_{ss}} + \frac{\bar{\phi}_k^d \phi_{k'}^d}{g_{dd}} - \frac{g_{sd}}{g_{ss} g_{dd}} \left(\bar{\phi}_k^s \phi_{k'}^d + \bar{\phi}_k^d \phi_{k'}^s \right) \right]}, \tag{A.9}$$

where $G_i^{-1} = \exp[Tr \ln G_i^{-1}]$. The partition function of the system can be expressed in terms of the effective thermodynamic potential as

$$Z = \int D[\bar{\phi}, \phi] e^{-\beta\Omega[\bar{\phi},\phi]}. \tag{A.10}$$

From Eq. (A.9) and Eq. (A.10) it is clear that effective thermodynamic potential Ω is given by the relation

$$\beta\Omega[\bar{\phi}, \phi] = \int_0^\beta d\tau \left[\frac{\bar{\phi}_k^s \phi_k^s}{g_{ss}} + \frac{\bar{\phi}_k^d \phi_k^d}{g_{dd}} - \frac{g_{sd}}{g_{ss} g_{dd}} \left(\bar{\phi}_k^s \phi_k^d + \bar{\phi}_k^d \phi_k^s\right)\right]$$
$$-\mathrm{Tr} \ln G_s^{-1} - \mathrm{Tr} \ln G_d^{-1} \tag{A.11}$$

One can now simplify Ω of Eq. (A.10) by writing the pairing fields as

$$\phi_k^s = \Delta_k^s e^{i\theta^s}, \phi_k^d = \Delta_k^d e^{i\theta^d},$$
$$\bar{\phi}_k^s = \Delta_k^s e^{-i\theta^s}, \bar{\phi}_k^d = \Delta_k^d e^{-i\theta^d}.$$

Noting that $\bar{\phi}_k^s \phi_k^s = |\Delta_k^s|^2$, $\bar{\phi}_k^d \phi_k^d = |\Delta_k^d|^2$, and $\bar{\phi}_k^s \phi_k^d + \bar{\phi}_k^d \phi_k^s = 2\Delta_k^s \Delta_k^d \cos(\theta^s - \theta^d)$, one can obtain the effective thermodynamic potential as

$$\Omega = \frac{1}{\beta} \int_0^\beta d\tau \left[\frac{|\Delta_k^s|^2}{g_{ss}} + \frac{|\Delta_k^d|^2}{g_{dd}} - \frac{2g_{sd}}{g_{ss} g_{dd}} \Delta_k^s \Delta_k^d \cos(\theta^s - \theta^d)\right] - \frac{1}{\beta} \sum_i \mathrm{Tr} \ln G_i^{-1} \tag{A.12}$$

Note that the last two terms of Eq. (A.12) can be evaluated by expanding them as

$$\mathrm{Tr} \ln G_d^{-1} = \mathrm{Tr} \ln \left[\begin{pmatrix} \partial_\tau + \varepsilon_k^d & \phi_k^d \\ \bar{\phi}_k^d & \partial_\tau - \varepsilon_k^d \end{pmatrix}\right]$$
$$= \mathrm{Tr} \ln \left[G_d^{0-1} + \begin{pmatrix} 0 & \phi_k^d \\ \bar{\phi}_k^d & 0 \end{pmatrix}\right] .$$

Here, the inverse of the non-interacting Green function G_d^{0-1} has been factored out. In the expansion, it is useful to know that

$$\mathrm{Tr}\, G_d^0 \begin{pmatrix} 0 & \phi_k^d \\ \bar{\phi}_k^d & 0 \end{pmatrix} = 0 .$$

This allows one to simplify the expansion as

$$\mathrm{Tr} \ln G_d^{-1} = \mathrm{Tr} \ln G_d^{0-1} - \frac{1}{2} \mathrm{Tr} \left[G_d^0 \begin{pmatrix} 0 & \phi_k^d \\ \bar{\phi}_k^d & 0 \end{pmatrix}\right]^2 + \cdots. \tag{A.13}$$

where

$$G_d^{0-1} = \begin{pmatrix} \partial_\tau + \varepsilon_k^d & 0 \\ 0 & \partial_\tau - \varepsilon_k^d \end{pmatrix} = \begin{pmatrix} \left[G_d^{0,p}\right]^{-1} & 0 \\ 0 & \left[G_d^{0,h}\right]^{-1} \end{pmatrix}.$$

Here, the superscripts p and h denote particle and hole, respectively. The second term of Eq. (A.11) is evaluated as

$$\tilde{G}_2 = \mathrm{Tr}\left[G_d^0 \begin{pmatrix} 0 & \phi_k^d \\ \bar{\phi}_k^d & 0 \end{pmatrix}\right]^2 = \mathrm{Tr}\begin{pmatrix} G_d^{0,p}\phi_k^d G_d^{0,h}\bar{\phi}_k^d & 0 \\ 0 & G_d^{0,h}\bar{\phi}_k^d G_d^{0,p}\phi_k^d \end{pmatrix}. \qquad \text{(A.14)}$$

A further simplification of Eq. (A.14) may be made by assuming that the pairing field is time independent and by using the momentum variables $\vec{p} = \left(\vec{k} + \vec{k}'\right)/2$, and $\vec{q} = \vec{k} - \vec{k}'$ (i.e., $\vec{k} = \vec{p} + \vec{q}/2$, and $\vec{k}' = \vec{p} - \vec{q}/2$). These simplifications lead to

$$\tilde{G}_2 = -\frac{1}{\beta V_o}\sum_{\mu,\vec{q}}\sum_{\vec{p}}|\phi_{kk'}^d|^2 \frac{1}{\omega_\mu^2 + \left(\varepsilon_p^d\right)^2}\left[\frac{\hbar^2\vec{q}^2}{8m}\left(\frac{1}{i\omega_\mu - \varepsilon_p^d} - \frac{1}{i\omega_\mu + \varepsilon_p^d}\right)\right.$$
$$\left. + 1 + \frac{1}{4m^2}(\vec{p}\cdot\vec{q})^2\left(\frac{1}{\left(i\omega_\mu - \varepsilon_p^d\right)^2} + \frac{1}{\left(i\omega_\mu + \varepsilon_p^d\right)^2} - \frac{1}{\omega_\mu^2 + \left(\varepsilon_p^d\right)^2}\right) + \cdots\right] \qquad \text{(A.15)}$$

where the $\vec{q}^2/8m)\left[\left(i\omega_\mu - \varepsilon_p^d\right)^{-1} - \left(i\omega_\mu + \varepsilon_p^d\right)^{-1}\right]/[\omega_\mu^2 + \left(\varepsilon_p^d\right)^2]$ term can be neglected in the high density limit. Therefore, by noting $(\vec{p}\cdot\vec{q})^2 = \sum_{ij} p_i p_j\, q_i q_j$, and by taking the angular average of $p_i p_j = \delta_{ij}\vec{p}^2/3$, one may write $(\vec{p}\cdot\vec{q})^2 = \vec{p}^2\,\vec{q}^2/3$. This result may be used to rewrite Eq. (A.33) a

$$\tilde{G}_2 = -\frac{1}{\beta V_o}\sum_{\mu,\vec{q}}\sum_{\vec{p}}\frac{|\phi_q^d|^2}{\omega_\mu^2 + \left(\varepsilon_p^d\right)^2}\left\{1 + \frac{\vec{p}^2\,\vec{q}^2}{12m^2}\left[\frac{1}{\left(i\omega_\mu - \varepsilon_p^d\right)^2} + \frac{1}{\left(i\omega_\mu + \varepsilon_p^d\right)^2} - \frac{1}{\omega_\mu^2 + \left(\varepsilon_p^d\right)^2}\right]\right\}. \qquad \text{(A.16)}$$

One may now convert the summation over $\vec{p}$ into an integral and obtain the following result:

$$\frac{1}{\beta}\sum_\mu \int \frac{d^3\vec{p}}{(2\pi)^3}\frac{1}{\omega_\mu^2 + \left(\varepsilon_p^d\right)^2} = \rho_d \ln\frac{2\beta\tilde{\Lambda}e^{-\Upsilon}}{\pi}, \qquad \text{(A.17)}$$

$$\frac{1}{\beta}\sum_{\mu}\int\frac{d^3\vec{p}}{(2\pi)^3}\frac{1}{\left(\omega_{\mu}^2+\left(\varepsilon_p^d\right)^2\right)^2}=\rho_d\ln\frac{\eta\tilde{\zeta}}{8\pi^2T^2}, \tag{A.18}$$

$$\int_{-\infty}^{\infty}d\varepsilon_p^d\ \frac{1}{\left(\omega_{\mu}^2+\left(\varepsilon_p^d\right)^2\right)^2}=\frac{\pi}{2|\omega_{\mu}|^3}, \tag{A.19}$$

and

$$\int_{-\infty}^{\infty}d\varepsilon_p^d\ \frac{\left(\varepsilon_p^d\right)^2}{\left(\omega_{\mu}^2+\left(\varepsilon_p^d\right)^2\right)^3}=\frac{\pi}{8|\omega_{\mu}|^3}, \tag{A.20}$$

where $\rho_d = m\ k_F/2\pi^2$ and $\beta = 1/T$. These results allow one to simplify the express for $\tilde{G}_2$ as

$$\tilde{G}_2=-\rho_d\ln\frac{2\beta\tilde{\Lambda}e^{-\Upsilon}}{\pi}\sum_q\left|\phi_q^d\right|^2+\rho_d\frac{\eta\,\tilde{\zeta}\,{k_F}^2}{48m^2\pi^2T^2}\sum_q\vec{q}^2\left|\phi_q^d\right|^2. \tag{A.21}$$

Also, noting that

$$\sum_q\left|\phi_q^d\right|^2=\frac{1}{V_o}\int d^3\vec{x}\left|\phi_q^d\right|^2=|\phi^d|^2$$

and

$$\sum_q\vec{q}^2\left|\phi_q^d\right|^2=\frac{1}{V_o}\int d^3\vec{x}\left|\nabla\phi_q^d\right|^2,$$

where V_0 is the volume of the junction. One may write

$$\tilde{G}_2=-\rho_d\ln\frac{2\beta\tilde{\Lambda}e^{-\Upsilon}}{\pi}|\phi^d|^2+\rho_d\frac{\eta\,\tilde{\zeta}\,{k_F}^2}{48m^2\pi^2T^2}\int d^3\vec{x}\left|\nabla\phi_q^d\right|^2. \tag{A.22}$$

Combining the result, one can again rewrite Eq. (A.13) as

$$\mathrm{Tr}\ln G_d^{-1}=\mathrm{Tr}\ln G_d^{0-1}+\sum_{n=1}^{\infty}\frac{(-1)^{n+1}}{n}\ \mathrm{Tr}\left[G_d^0\begin{pmatrix}0 & \phi_k^d\\ \bar{\phi}_k^d & 0\end{pmatrix}\right]^n. \tag{A.23}$$

The fourth order contribution for the uniform pairing field ϕ_k^d may be written as

$$\frac{\tilde{G}_4}{4\beta V_o}=\frac{1}{4\beta V_o}\mathrm{Tr}\left[G_d^0\begin{pmatrix}0 & \phi_k^d\\ \bar{\phi}_k^d & 0\end{pmatrix}\right]^4$$

$$= \frac{|\bar{\phi}^d|^4}{2}\frac{1}{\beta}\sum_\mu \int \frac{d^3\vec{k}}{(2\pi)^3}\frac{1}{\left[\omega_\mu^2+\left(\varepsilon_p^d\right)^2\right]^2} = \frac{\eta\ \tilde{\varsigma}\ \rho_d k_F^2}{8m^2\pi^2T^2}\frac{|\bar{\phi}^d|^4}{2}. \quad \text{(A.24)}$$

The thermodynamic potential in the normal state Ω_n is given by

$$\Omega_n = -\frac{1}{\beta}\mathrm{Tr}\ln G_s^{0,-1} - \frac{1}{\beta}\mathrm{Tr}\ln G_d^{0,-1}. \quad \text{(A.25)}$$

This indicates that the Ginzburg-Landau free energy of the system may be written as

$$\Omega - \Omega_n = \frac{1}{V_o}\int d^3\vec{x}\left[\frac{\bar{\phi}_k^s\phi_k^s}{g_{ss}} + \frac{\bar{\phi}_k^d\phi_k^d}{g_{dd}} - \frac{g_{sd}}{g_{ss}g_{dd}}\left(\bar{\phi}_k^s\phi_k^d + \bar{\phi}_k^d\phi_k^s\right)\right]$$
$$+\frac{1}{\beta}\mathrm{Tr}\left[G_s^0\begin{pmatrix}0 & \phi_k^s\\ \bar{\phi}_k^s & 0\end{pmatrix}\right]^2 + \frac{1}{4\beta}\mathrm{Tr}\left[G_s^0\begin{pmatrix}0 & \phi_k^s\\ \bar{\phi}_k^s & 0\end{pmatrix}\right]^4$$
$$+\frac{1}{\beta}\mathrm{Tr}\left[G_d^0\begin{pmatrix}0 & \phi_k^d\\ \bar{\phi}_k^d & 0\end{pmatrix}\right]^2 + \frac{1}{4\beta}\mathrm{Tr}\left[G_d^0\begin{pmatrix}0 & \phi_k^d\\ \bar{\phi}_k^d & 0\end{pmatrix}\right]^4 \quad \text{(A.26)}$$

Now by combining the result into Eq. (A.26), one can obtain the Ginzburg-Landau free energy of the system as

$$\Omega - \Omega_n = \frac{1}{V_o}\int d^3\vec{x}\left\{\sum_i\left[a_i|\phi^s(x)|^2 + \frac{\eta\ \tilde{\varsigma}\ k_F^2\rho_s}{16m^2\pi^2T^2}\left|\phi^i(x)\right|^4 + \frac{\eta\ \tilde{\varsigma}\ k_F^2\rho_s}{48m_i^2\pi^2T^2}\left|\nabla\phi^i(x)\right|^2\right]\right.$$
$$\left. - \frac{g_{sd}}{g_{ss}g_{dd}}\left[\bar{\phi}^s(x)\phi^d(x) + \bar{\phi}^d(x)\phi^s(x)\right]\right\}. \quad \text{(A.27)}$$

where $a_i = (1/g_{ii}) - \rho_s\ln\left[(2\beta\tilde{\Lambda}\exp(-\Upsilon)/\pi)\right]$.

Similarly, one may consider a LJJ with two layers of two-gap superconductors separated by an insulator in the z-direction. Assuming that *l=2* layer of superconductor is above the junction ($z > 0$) and *l=1* layer is below the junction ($z < 0$). Therefore the Ginsburg-Landau free energy for such a system may be written as

$$F = \frac{1}{\beta}S[\phi_k], \quad \text{(A.28)}$$

and then

$$F = \Theta(\pm z)\frac{1}{\beta}\sum_{l=1,2}\left\{\int_0^\beta d\tau\left[\frac{|\Delta_l^s|^2}{g_{ss}} - \frac{\left|\Delta_l^d\right|^2}{g_{dd}} - \frac{2g_{sd}}{g_{ss}g_{dd}}\Delta_l^s\Delta_l^d\cos\left(\theta_l^d - \theta_l^s\right)\right]\right.$$

$$\left. + \int_0^\beta d\tau\left[m_s\rho_s^s\left(\upsilon_{s,l}^s\right)^2 + \frac{1}{8\pi\mu_s^2}\left(\frac{\Phi_0}{2\pi}\frac{\partial\theta_l^s}{\partial\tau} + \varphi_l\right)^2 + m_d\rho_s^d\left(\upsilon_{s,l}^d\right)^2 + \frac{1}{8\pi\mu_d^2}\left(\frac{\Phi_0}{2\pi}\frac{\partial\theta_l^d}{\partial\tau} + \varphi_l\right)^2\right]\right\}$$

$$+\left\{\int_0^\beta \frac{d\tau}{8\pi}\left(\epsilon E_z^2 + B_y^2\right) + \int_0^\beta \frac{d\tau}{d_s}\int_0^\beta d\tau'\left(A_{\alpha\beta} + B_{\alpha\beta}\right)\right\}\delta(z) \qquad \text{(A.29)}$$

where

$$B_{\alpha\beta} = \tilde{\beta}^{ss}(\tau - \tau')\cos\phi_+^{ss}(r,\tau;r,\tau') - \tilde{\alpha}^{ss}(\tau - \tau')\cos\phi_-^{ss}(r,\tau;r,\tau')$$

$$+ \tilde{\beta}^{sd}(\tau - \tau')\cos\phi_+^{sd}(r,\tau;r,\tau') - \tilde{\alpha}^{sd}(\tau - \tau')\cos\phi_-^{sd}(r,\tau;r,\tau')$$

$$+ \tilde{\beta}^{ds}(\tau - \tau')\cos\phi_+^{ds}(r,\tau;r,\tau') - \tilde{\alpha}^{ds}(\tau - \tau')\cos\phi_-^{ds}(r,\tau;r,\tau')$$

$$+ \tilde{\beta}^{dd}(\tau - \tau')\cos\phi_+^{dd}(r,\tau;r,\tau') - \tilde{\alpha}^{dd}(\tau - \tau')\cos\phi_-^{dd}(r,\tau;r,\tau'), \qquad \text{(A.30)}$$

where $\phi_\pm^{ij}(r,\tau;r,\tau') = [\tilde{\phi}_{l+1,l}^{ss}(r,\tau) \pm \tilde{\phi}_{l+1,l}^{ss}(r,\tau')]/2$. Here, the coefficients $\tilde{\beta}^{ij}$ and $\tilde{\alpha}^{ij}$ are given is given by

$$\tilde{\alpha}^{ss}(\tau - \tau') = \frac{|T_{l+1,l}^{ss}|^2}{A_l A_{l+1}}\left(g_l^{-s}g_{l+1}^{-s} + g_l^{+s}g_{l+1}^{+s}\right),$$

$$\tilde{\alpha}^{dd}(\tau - \tau') = \frac{|T_{l+1,l}^{dd}|^2}{B_l B_{l+1}}\left(g_l^{-d}g_{l+1}^{-d} + g_{l+1}^{+d}\right),$$

$$\tilde{\alpha}^{sd}(\tau - \tau') = \frac{\left|T_{l+1,l}^{sd}\right|^2}{B_l A_{l+1}}$$

$$\tilde{\alpha}^{ds}(\tau - \tau') = \frac{|T_{l+1,l}^{ds}|^2}{A_l B_{l+1}}\left(g_{l+1}^{-d}g_l^{-s}g_{l+1}^{+d}g_l^{+s}\right)$$

$$\tilde{\beta}^{dd}(\tau - \tau') = \frac{T_{l+1,l}^{*dd\,2}\bar{\Delta}_l^{0d}\Delta_{l+1}^{0d}}{B_l B_{l+1}},$$

$$\tilde{\beta}^{sd}(\tau - \tau') = \frac{T_{l+1,l}^{*sd\,2}\bar{\Delta}_l^{0d}\Delta_{l+1}^{0s}}{B_l A_{l+1}},$$

$$\tilde{\beta}^{ss}(\tau - \tau') = \frac{T_{l+1,l}^{*ss\,2}\bar{\Delta}_l^{0s}\Delta_{l+1}^{0s}}{A_l A_{l+1}},$$

and

$$\tilde{\beta}^{ds}(\tau-\tau') = \frac{T^{*ds}_{l+1,l}{}^{2}\bar{\Delta}^{0s}_{l}\Delta^{0d}_{l+1}}{A_l B_{l+1}}.$$

The free energy density which depends on the θ's is given by

$$\begin{aligned} F_\theta = &-\frac{2g_{sd}}{g_{ss}g_{sd}}\Delta^s_1\Delta^d_1\cos\left(\theta^d_1-\theta^s_1\right)-\frac{2g_{sd}}{g_{ss}g_{sd}}\Delta^s_2\Delta^d_2\cos\left(\theta^d_2-\theta^s_2\right) \\ &-\frac{J^{ss}}{d_s}\cos(\theta^s_2-\theta^s_1)-\frac{J^{dd}}{d_s}\cos\left(\theta^d_2-\theta^d_1\right) \\ &-\frac{J^{sd}}{d_s}\cos\left(\theta^s_2-\theta^d_1\right)-\frac{J^{ds}}{d_s}\cos\left(\theta^d_2-\theta^s_1\right). \end{aligned} \quad \text{(A.31)}$$

To examine the phase configurations which minimize the free energy density, first the derivative of F_θ with respect to phase variables is set to yield

$$\begin{aligned} &-g'_{sd}\sin\left(\theta^d_1-\theta^s_1\right)-\frac{J^{ss}}{d_s}\sin(\theta^s_2-\theta^s_1)-\frac{J^{ds}}{d_s}\sin\left(\theta^d_2-\theta^s_1\right)=0, \\ &g'_{sd}\sin\left(\theta^d_1-\theta^s_1\right)-\frac{J^{dd}}{d_s}\sin\left(\theta^d_2-\theta^d_1\right)-\frac{J^{sd}}{d_s}\sin(\theta^s_2-\theta^s_1)=0, \\ &-g'_{sd}\sin\left(\theta^d_2-\theta^s_2\right)+\frac{J^{ss}}{d_s}\sin(\theta^s_2-\theta^s_1)+\frac{J^{sd}}{d_s}\sin\left(\theta^s_2-\theta^d_1\right)=0, \\ &g'_{sd}\sin\left(\theta^d_2-\theta^s_2\right)+\frac{J^{dd}}{d_s}\sin\left(\theta^d_2-\theta^d_1\right)+\frac{J^{ds}}{d_s}\sin\left(\theta^d_2-\theta^s_1\right)=0, \end{aligned} \quad \text{(A.32)}$$

where we denote $g'_{sd}=\frac{2g_{sd}}{g_{ss}g_{sd}}\Delta^s_l\Delta^d_l$, $\theta^d_l-\theta^s_l=\chi_l$, $\theta^i_2-\theta^i_1=\phi^i$, $\phi^d+\chi_1=\phi^s+\chi_2$, and $\phi^d=\phi^s-\chi_2-\chi_1$. Substituting these to Eq. (3.32), one can get a set of four equations. Next subtracting the third part of Eq. (3.32) from the fourth part, one can obtain the following relation

$$\frac{J^{dd}}{d_s}\sin(\phi^s-\chi_2-\chi_1)+\frac{J^{ds}}{d_s}\sin(\phi^s+\chi_2)+\frac{J^{sd}}{d_s}\sin(\phi^s-\chi_1)+\frac{J^{ss}}{d_s}\sin\phi^s=0. \quad \text{(A.33)}$$

One can write a set of three equations in the exponential form using the relation $\sin X = \mathrm{Im}\, e^{iX}$ as

$$\mathrm{Im}\left[g'_{sd}e^{i\chi_1} - \frac{J^{dd}}{d_s}e^{i(\phi^s-\chi_2-\chi_1)-\frac{J^{sd}}{d_s}e^{i(\phi^s-\chi_1)}}\right] = 0, \quad \text{(A.34)}$$

$$\mathrm{Im}\left[g'_{sd}e^{i\chi_1} + \frac{J^{ss}}{d_s}e^{i\phi^s} + \frac{J^{ds}}{d_s}e^{i(\phi^s+\chi_2)}\right] = 0, \quad \text{(A.35)}$$

$$\mathrm{Im}\left[\left(\frac{J^{dd}}{d_s}e^{i(\chi_2-\chi_1)} + \frac{J^{ds}}{d_s}e^{i\chi_2} + \frac{J^{sd}}{d_s}e^{-i\chi_1} + \frac{J^{ss}}{d_s}\right)e^{i\phi^s}\right] = 0. \quad \text{(A.36)}$$

Suppose one write Eq. (A.37) as

$$\mathrm{Im}\left[e^{i(\frac{\chi_2-\chi_1}{2}+\phi^s)}\left(J^{dd}e^{i\frac{\chi_2-\chi_1}{2}} + J^{ds}e^{i\frac{\chi_2-\chi_1}{2}} + J^{sd}e^{-i\frac{\chi_2-\chi_1}{2}} + J^{ss}e^{-i\frac{\chi_2-\chi_1}{2}}\right)\right] = 0, \quad \text{(A.37)}$$

One can consider a simple case in which $J^{dd} = J^{ss}$ and $J^{ds} = J^{sd}$. By taking the $\exp[i\phi^s + i(\chi_2 - \chi_1)/2]$ factor out of Eq. (A.37), one can write

$$\sin\left(\phi^s + \frac{\chi_2-\chi_1}{2}\right)\left[J^{dd}\cos\left(\frac{\chi_2-\chi_1}{2}\right) + J^{sd}\cos\left(\frac{\chi_2+\chi_1}{2}\right)\right] = 0. \quad \text{(A.38)}$$

If $J^{dd}\cos\left(\frac{\chi_2-\chi_1}{2}\right) + J^{sd}\cos\left(\frac{\chi_2+\chi_1}{2}\right) \neq 0$ then the following condition must be satisfied:

$$\sin\left(\phi^s + \frac{\chi_2-\chi_1}{2}\right) = 0\ .$$

This implies that $\phi^s + (\chi_2 - \chi_1)/2 = n\pi(n = 0, \pm 1)$. Now, by adding Eqs. (A.35) and (A.36), one can obtain

$$g'_{sd}\sin\chi_2 + (-1)^n\left(-\frac{J^{ss}}{d_s}\sin\frac{\chi_2-\chi_1}{2} + \frac{J^{sd}}{d_s}\sin\frac{\chi_2+\chi_1}{2}\right) = 0. \quad \text{(A.39)}$$

Thus for the minimum of the free energy, the free energy function $F\left(\theta_1^s, \theta_1^d, \theta_2^s, \theta_2^d\right) = F(\chi_1, \chi_2, \phi^s, \phi^d)$ satisfies the following two set of conditions. The first set of conditions is given by

(i) $\phi^d = \phi^s + \chi_2 - \chi_1$

(ii) $\phi^s + \frac{\chi_2-\chi_1}{2} = n\pi,$

(iii) $g'_{sd}\sin(\frac{\chi_2+\chi_1}{2} - \frac{\chi_2-\chi_1}{2}) +$

$$+ (-1)^n \left(-\frac{J^{ss}}{d_s} \sin\frac{\chi_2 - \chi_1}{2} + \frac{J^{sd}}{d_s} \sin\frac{\chi_2 + \chi_1}{2} \right) = 0.$$

The second set of conditions is given by

(i) $\phi^d = \phi^s + \chi_2 - \chi_1$,

(ii) $\frac{J^{ss}}{d_s} \cos\frac{\chi_2 - \chi_1}{2} + \frac{J^{sd}}{d_s} \cos\frac{\chi_2 + \chi_1}{2} = 0,$

(iii) $g'_{sd} \sin(\frac{\chi_2 + \chi_1}{2} - \frac{\chi_2 - \chi_1}{2})$

$$+ \cos(\phi^s + \frac{\chi_2 - \chi_1}{2}) \left(-\frac{J^{ss}}{d_s} \sin\frac{\chi_2 - \chi_1}{2} + \frac{J^{sd}}{d_s} \sin\frac{\chi_2 + \chi_1}{2} \right) = 0 \quad .$$

These are the conditions for the minimum free energy of the system. This is useful to estimate phase configuration of the ground state of the system.

APPENDIX B

Two Coupled LJJs With Two-Gap Superconductors

In this appendix, a derivation of the equation of motion from the effective action S_{eff} for the system of two coupled LJJs with two-gap superconductors is discussed. The effective action obtained from the functional integral representation of the partition function after integrating out the fermion field is given by

$$\begin{aligned} S_{eff} = \;& S_{field} + S_{gap} + T_r \ln G^{-1} \\ =\; & S_{field} + S_{gap} + T_r \ln\left(\widehat{U}_l G_0^{-1} \widehat{U}_l^{-1}\right) + T_r\, \widehat{U}_l (G_0 \partial G^{-1}) \widehat{U}_l^{-1} \\ & - \tfrac{1}{2} T_r\left(\widehat{U}_l G_0 \widehat{U}_l^{-1} \widehat{U}_l \partial G^{-1} \widehat{U}_l^{-1}\right)\left(\widehat{U}_l G_0 \widehat{U}_l^{-1} \widehat{U}_l \partial G^{-1} \widehat{U}_l^{-1}\right), \end{aligned} \tag{B.1}$$

From the discussion presented in Chapter IV, it is useful note that

$$T_r \ln\left(\widehat{U}_l G_0^{-1} \widehat{U}_l^{-1}\right) = \sum_i \left[m_i \rho_s^i d_s \vec{v}_{sl}^{\,i2} + \frac{d_s}{8\pi\mu_i^2}\left(\frac{\Phi_0}{2\pi}\frac{\partial \theta_l^i}{\partial \tau} + \varphi_{l.}\right)^2 \right], \tag{B.2}$$

and

$$G_0 \widehat{U}_l^{-1} \widehat{U}_l \partial G^{-1} \widehat{U}_l^{-1} = 0. \tag{B.3}$$

Also, it is useful to note that the second order terms in the expansion may be written as

$$\begin{aligned} & -\tfrac{1}{2} T_r\left(\widehat{U}_l G_0 \widehat{U}_l^{-1} \widehat{U}_l \partial G^{-1} \widehat{U}_l^{-1}\right)\left(\widehat{U}_l G_0 \widehat{U}_l^{-1} \widehat{U}_l \partial G^{-1} \widehat{U}_l^{-1}\right) = \\ & \qquad \tilde{\beta}^{ss}(\tau - \tau') \cos \phi_+^{ss}(r, \tau; r, \tau') - \tilde{\alpha}^{ss}(\tau - \tau') \cos \phi_-^{ss}(r, \tau; r, \tau') \\ & + \tilde{\beta}^{sd}(\tau - \tau') \cos \phi_+^{sd}(r, \tau; r, \tau') - \tilde{\alpha}^{sd}(\tau - \tau') \cos \phi_-^{sd}(r, \tau; r, \tau') \\ & + \tilde{\beta}^{ds}(\tau - \tau') \cos \phi_+^{ds}(r, \tau; r, \tau') - \tilde{\alpha}^{ds}(\tau - \tau') \cos \phi_-^{ds}(r, \tau; r, \tau') \end{aligned}$$

$$+\tilde{\beta}^{dd}(\tau-\tau')\cos\phi_{+}^{dd}(r,\tau;r,\tau')-\tilde{\alpha}^{dd}(\tau-\tau')\cos\phi_{-}^{dd}(r,\tau;r,\tau') \quad \text{(B.4)}$$

where $\phi_{\pm}^{ij}(r,\tau;r,\tau')=[\tilde{\phi}_{l+1,l}^{ss}(r,\tau)\pm\tilde{\phi}_{l+1,l}^{ss}(r,\tau')]/2$. Here, the coefficients $\tilde{\beta}^{ij}$ and $\tilde{\alpha}^{ij}$ are given is given by

$$\tilde{\alpha}^{ss}(\tau-\tau')=\frac{2}{S}\sum_{k,k'}\frac{|T_{l+1,l}^{ss}|^2}{A_lA_{l+1}}(g_l^{-s}g_{l+1}^{-s}+g_l^{+s}g_{l+1}^{+s}),$$

$$\tilde{\alpha}^{dd}(\tau-\tau')=\frac{2}{S}\sum_{k,k'}\frac{|T_{l+1,l}^{dd}|^2}{B_lB_{l+1}}\left(g_l^{-d}g_{l+1}^{-d}+g_{l+1}^{+d}\right),$$

$$\tilde{\alpha}^{sd}(\tau-\tau')=\frac{2}{S}\sum_{k,k'}\frac{\left|T_{l+1,l}^{sd}\right|^2}{B_lA_{l+1}}\left(g_{l+1}^{-s}g_l^{-d}+g_{l+1}^{+s}g_l^{+d}\right)$$

$$\tilde{\alpha}^{ds}(\tau-\tau')=\frac{2}{S}\sum_{k,k'}\frac{|T_{l+1,l}^{ds}|^2}{A_lB_{l+1}}\left(g_{l+1}^{-d}g_l^{-s}+g_{l+1}^{+d}g_l^{+s}\right)$$

$$\tilde{\beta}^{dd}(\tau-\tau')=\frac{2}{S}\sum_{k,k'}\frac{T_{l+1,l}^{*dd\,2}\bar{\Delta}_l^{0d}\Delta_{l+1}^{0d}}{B_lB_{l+1}},$$

$$\tilde{\beta}^{sd}(\tau-\tau')=\frac{2}{S}\sum_{k,k'}\frac{T_{l+1,l}^{*sd\,2}\bar{\Delta}_l^{0d}\Delta_{l+1}^{0s}}{B_lA_{l+1}},$$

$$\tilde{\beta}^{ss}(\tau-\tau')=\frac{2}{S}\sum_{k,k'}\frac{T_{l+1,l}^{*ss\,2}\bar{\Delta}_l^{0s}\Delta_{l+1}^{0s}}{A_lA_{l+1}},$$

and

$$\tilde{\beta}^{ds}(\tau-\tau')=\frac{2}{S}\sum_{k,k'}\frac{T_{l+1,l}^{*ds\,2}\bar{\Delta}_l^{0s}(k,\tau)\Delta_{l+1}^{0d}(k',\tau')}{A_lB_{l+1}}. \quad \text{(B.5)}$$

Hence, the effective action is given by

$$\begin{aligned}S_{eff}=\sum_l\int\partial\tau\int d\vec{r}\,\Bigg\{&\left[\frac{|\Delta_l^s|^2}{g_{ss}}+\frac{\left|\Delta_l^d\right|^2}{g_{dd}}-\frac{2\,g_{sd}}{g_{ss}\,g_{dd}}\Delta_l^s\Delta_l^d\cos\left(\theta_l^d-\theta_l^s\right)\right]\\&+\sum_i\left[m_s\rho_s^d d_s\vec{v}_{sl}^{d2}+\frac{d_s}{8\pi\mu_s^2}\left(\frac{\Phi_0}{2\pi}\frac{\partial\theta_l^s}{\partial\tau}+\varphi_{l.}\right)^2\right] \quad \text{(B.6)}\\&+\sum_{ij}\int d\tau'\left[\tilde{\beta}^{ij}(\tau-\tau')\cos\phi_{+}^{ij}-\tilde{\alpha}^{ij}(\tau-\tau')\cos\phi_{-}^{ij}\right]\Bigg\}.\end{aligned}$$

One may now use the effective action to find the equation of motion by finding the minimum of free energy with respect to a variation in the phase variable. One can find to minimum of the action by setting $\delta S_{eff}/\delta\theta_l^s = 0$. This yields the Euler-Lagrage equation of

$$\frac{\partial}{\partial t}\frac{\partial L}{\partial \theta_l^s} - \frac{\partial}{\partial t}\frac{\partial L}{\partial \theta\prime_l^s} - \frac{\partial L}{\partial \theta_l^s} = 0\ . \tag{B.7}$$

By using the Lagrange density *L* obtained from the effective action, the Euler-Lagrange equation of Eq. (B.7) for the phase variable θ_l^s may be obtained as

$$\frac{d_s}{4\pi\lambda_s^2}\frac{\partial}{\partial x}\left(\frac{\Phi_0}{2\pi}\frac{\partial\phi_l^s}{\partial x} - A_l^x\right) - \frac{d_s}{4\pi m_s^2}\frac{\partial}{\partial t}\left(\frac{\Phi_0}{2\pi}\frac{\partial\phi_l^s}{\partial t} + \varphi_l\right) + \ J_{in}\sin\chi$$

$$+ J_{l+1,l}^{\beta,ss} - J_{l,l-1}^{\beta,ss} - J_{l+1,l}^{\alpha,ss} + J_{l,l-1}^{\alpha,ss} + \ \ J_{l+1,l}^{\beta,ds} - J_{l,l-1}^{\beta,sd} - J_{l+1,l}^{\alpha,ds} + J_{l,l-1}^{\alpha,sd} = 0\ . \tag{B.8}$$

where $\chi_l = \theta_l^s - \theta_l^d$ denotes the relative phase of the condensates and $J_{in} = 2d_s g_{sd}\Delta_l^s\Delta_l^d/g_{ss}g_{ss}$ is the inter-band current density. The electric field of $\vec{E} = -\vec{\nabla}\varphi - (1/c)\,\partial A/\partial\tau$ may be written as

$$\vec{E} = -4\pi\sum_a(\rho_{l+1}^a - \rho_l^a) - \left[(\rho_{l+1}^a - \rho_l^a) + \frac{\partial A_{l+1,l}^z}{\partial\tau}\right]\left(\frac{1}{m_s^2} + \frac{1}{m_d^2}\right). \tag{B.9}$$

Similarly, one may find the minimum of the action with respect to a variation of the phase variable θ_l^d from the condition $\delta S_{eff}/\delta\theta_l^d = 0$. This condition yields the Euler-Lagrange equation for θ_l^d which may be written as

$$\frac{d_s}{4\pi\lambda_d^2}\frac{\partial}{\partial x}\left(\frac{\Phi_0}{2\pi}\frac{\partial\phi_l^d}{\partial x} - A_l^x\right) - \frac{d_s}{4\pi m_d^2}\frac{\partial}{\partial t}\left(\frac{\Phi_0}{2\pi}\frac{\partial\phi_l^d}{\partial t} + \varphi_l\right) + \ J_{in}\ \sin\chi$$

$$+ J_{l,l-1}^{\beta,dd} - J_{l+1,l}^{\alpha,dd} + J_{l,l-1}^{\alpha,dd} + \ \ J_{l+1,l}^{\beta,sd} - J_{l+1,l}^{\alpha,sd} + J_{l,l-1}^{\alpha ds} = 0 \tag{B.10}$$

One may carry out a similar calculation for the phase variables $\theta_{l+1}^s$and θ_{l+1}^d for the (l+1)-th S layer. By setting the conditions $\delta S_{eff}/\delta\theta_{l+1}^s = 0$ and $\delta S_{eff}/\delta\theta_{l+1}^d = 0$, one can obtain the Euler-Lagrange equation for $\theta_{l+1}^s$and θ_{l+1}^d as

$$\frac{\partial}{\partial t}\frac{\partial L}{\partial \dot{\theta}_{l+1}^{s}}-\frac{\partial}{\partial t}\frac{\partial L}{\partial \theta'^{s}_{l+1}}-\frac{\partial L}{\partial \theta_{l+1}^{s}}=0, \tag{B.11}$$

$$\frac{d_s}{4\pi\lambda_s^2}\frac{\partial}{\partial x}\left(\frac{\Phi_0}{2\pi}\frac{\partial\theta_{l+1}^{s}}{\partial x}-A_{l+1}^{x}\right)-\frac{d_s}{4\pi m_s^2}\frac{\partial}{\partial t}\left(\frac{\Phi_0}{2\pi}\frac{\partial\theta_{l+1}^{s}}{\partial t}+\varphi_{l+1}\right)-J_{in}\sin\chi_{l+1}$$

$$+J_{l+2,l+1}^{\beta,ss}-J_{l+1,l}^{\beta,ss}-J_{l+2,l+1}^{\alpha,ss}+J_{l+1,l}^{\alpha,ss}+J_{l+2,l+1}^{\beta,ds}-\ J_{l+1,l}^{\beta,sd}-J_{l+2,l+1}^{\alpha,ds}+J_{l+1,l}^{\alpha,ds}=0\,, \tag{B.12}$$

and

$$\frac{d_s}{4\pi\lambda_d^2}\frac{\partial}{\partial x}\left(\frac{\Phi_0}{2\pi}\frac{\partial\theta_{l+1}^{d}}{\partial x}-A_{l+1}^{x}\right)-\frac{d_s}{4\pi m_d^2}\frac{\partial}{\partial t}\left(\frac{\Phi_0}{2\pi}\frac{\partial\theta_{l+1}^{d}}{\partial t}+\varphi_{l+1}\right)-\ J_{in}\sin\chi_{l+1}$$

$$+J_{l+2,l+1}^{\beta,dd}-J_{l+1,l}^{\beta,dd}-J_{l+2,l+1}^{\alpha,dd}+J_{l+1,l}^{\alpha,dd}+J_{l+2,l+1}^{\beta,sd}-\ J_{l+1,l}^{\beta,ds}-J_{l+2,l+1}^{\alpha,ds}+J_{l+1,l}^{\alpha,sd}=0, \tag{B.13}$$

respectively. One may now combine the Euler-Lagrange equation for the phase variables θ_l^s, $\theta_l^d, \theta_{l+1}^s$and $\theta_{l+1}^d$to obtain the equation of motion for the coupled LJJs. One may calculated

$$\frac{4\pi\lambda_s^2}{d_s d_I}\left(-\frac{\delta S_{eff}}{\delta\theta_l^s}+\frac{\delta S_{eff}}{\delta\theta_{l+1}^d}\right)+\left(-\frac{\delta S_{eff}}{\delta\theta_l^d}+\frac{\delta S_{eff}}{\delta\theta_{l+1}^d}\right)\frac{4\pi\lambda_d^2}{d_s d_I}=0, \tag{B.14}$$

by substituting the result from above and obtain the equation of motion as

$$-\frac{\lambda_s^2}{d_I\mu_s^2}\left\{\frac{\partial}{\partial t}\left[\frac{\Phi_0}{2\pi}\frac{\partial(\theta_{l+1}^{s}-\theta_l^{s})}{\partial t}-i(\varphi_{l+1}-\varphi_l)\right]+\frac{\partial}{\partial x}\left[\frac{\Phi_0}{2\pi}\frac{\partial(\theta_{l+1}^{s}-\theta_l^{s})}{\partial x}-i(\varphi_{l+1}-\varphi_l)\right]\right\}$$

$$+\frac{1}{d_I}\left\{\frac{\partial}{\partial x}\left[\frac{\Phi_0}{2\pi}\frac{\partial(\theta_{l+1}^{s}-\theta_l^{s})}{\partial x}-(A_{l+1}^{x}-A_l^{x})\right]+\frac{\partial}{\partial x}\left[\frac{\Phi_0}{2\pi}\frac{\partial\left(\theta_{l+1}^{d}-\theta_l^{d}\right)}{\partial x}-(A_{l+1}^{x}-A_l^{x})\right]\right\}$$

$$-J_{in}\frac{4\pi\lambda_s^2}{d_s d_I}(\sin\chi_{l+1}-\sin\chi_l)-J_{in}\frac{4\pi\lambda_d^2}{d_s d_I}(\sin\chi_{l+1}-\sin\chi_l)$$

$$+\frac{4\pi\lambda_s^2}{d_s d_I}\left[\left(J_{l+2,l+1}^{\beta,ss}+J_{l,l-1}^{\beta,ss}-2J_{l+1,l}^{\beta,ss}\right)-\left(J_{l+2,l+1}^{\alpha,ss}+J_{l,l-1}^{\alpha,ss}-2J_{l+1,l}^{\alpha,ss}\right)\right.$$

$$\left.+\left(J_{l+2,l+1}^{\beta,ds}+J_{l,l-1}^{\beta,sd}-\ \ J_{l+1,l}^{\beta,ds}-J_{l+1,l}^{\beta,sd}\right)-\left(J_{l+2,l+1}^{\alpha,ds}+J_{l,l-1}^{\alpha,sd}-J_{l+1,l}^{\alpha,ds}-J_{l+1,l}^{\alpha,sd}\right)\right]$$

$$+\frac{4\pi\lambda_s^2}{d_s d_I}\left[\left(J_{l+2,l+1}^{\beta,dd}+J_{l,l-1}^{\beta,dd}-2J_{l+1,l}^{\beta,dd}\right)-\left(J_{l+2,l+1}^{\alpha,dd}+J_{l,l-1}^{\alpha,dd}-2J_{l+1,l}^{\alpha,dd}\right)\right.$$

$$\left.+\left(J_{l+2,l+1}^{\beta,sd}+J_{l,l-1}^{\beta,ds}-J_{l+1,l}^{\beta,sd}-J_{l+1,l}^{\beta,ds}\right)-\left(J_{l+2,l+1}^{\alpha,sd}+J_{l,l-1}^{\alpha,ds}-J_{l+1,l}^{\alpha,sd}-J_{l+1,l}^{\alpha,ds}\right)\right]=0\,. \tag{B.15}$$

The equation of motion of (B.15) can be simplified by using the following relations:

$$\frac{\Phi_0}{2\pi}\sum_i \frac{1}{\mu_i^2}\frac{\partial \tilde{\phi}^{ii}_{l+1,l}}{\partial t} = -4\pi \sum_i\left(\rho^i_{l+1}-\rho^i_l\right) - \left[(\varphi_{l+1}-\varphi_l)+\frac{\partial A^z_{l+1,l}}{\partial t}\right]\sum_i \frac{1}{\mu_i^2}, \tag{B.16}$$

$$J^{x,s}_{l+1} + J^{x,d}_{l+1} - J^{x,s}_{l} = \frac{1}{4\pi\lambda_d^2}\left(\frac{\Phi_0}{2\pi}\frac{\partial \tilde{\phi}^{dd}_{l+1,l}}{\partial x} - d_I B^y_{l+1,l}\right) + \frac{1}{4\pi\lambda_s^2}\left(\frac{\Phi_0}{2\pi} - d_I B^y_{l+1,l}\right). \tag{B.17}$$

The magnetic and electric field in the insulator layer between l–th and (l+1)-th S layer are given by

$$B^y_{l+1,l} = -\left(\frac{\partial A^z_{l+1,l}}{\partial x} - \frac{A^x_{l+1}-A^x_l}{d_I}\right), \tag{B.18}$$

$$E^z_{l+1,l} = -\frac{(\varphi_{l+1}-\varphi_l)}{d_I} - \frac{1}{d_I}\frac{\partial A^z_{l+1,l}}{\partial x}.$$

By using the above result, one may rewrite Eq. (B.15) as

$$-\frac{\Phi_0}{2\pi d_I}\sum_i \frac{\lambda_i^2}{\mu_i^2}\frac{\partial \tilde{\phi}^{ii}_{l+1,l}}{\partial t^2} - \frac{\Phi_0}{2\pi d_I}\sum_i \frac{\partial \tilde{\phi}^{ii}_{l+1,l}}{\partial t^2}\frac{2\epsilon - \frac{\lambda_s^2}{\mu_s^2}-\frac{\lambda_d^2}{\mu_d^2}}{\frac{1}{\mu_s^2}+\frac{1}{\mu_d^2}}\left[\frac{\Phi_0}{2\pi d_I}\sum_i \frac{1}{\mu_i^2}\frac{\partial \tilde{\phi}^{ii}_{l+1,l}}{\partial x^2} + \frac{4\pi}{d_I}\sum_i \frac{\partial\left(\rho^i_{l+1}-\rho^i_l\right)}{\partial t}\right]$$

$$+ J_{in}\frac{4\pi(\lambda_s^2-\lambda_d^2)}{d_s d_I}(\sin\chi_{l+1}-\sin\chi_l) + \frac{8\pi}{c}J_8 - \frac{4\pi\lambda_s^2}{d_s d_I}\left(J_5+J_9+J_6+J_7\right)$$

$$-\frac{\epsilon\,\Phi_0}{2\pi}\Lambda\left[\frac{\partial^2(\chi_{l+1}-\chi_l)}{\partial t^2} - 2\frac{\partial^2(\chi_l-\chi_{l+1})}{\partial t^2} + \frac{\partial^2(\chi_{l-1}-\chi_l)}{\partial t^2}\right] + \frac{\epsilon\,\Phi_0\Lambda d_I}{2\pi}\frac{\partial^2(\chi_l-\chi_{l+1})}{\partial t^2} - \frac{\Phi_0}{2\pi d_I}\frac{\partial^2(\chi_l-\chi_{l+1})}{\partial t^2}$$

$$+ J_{in}\frac{4\pi\lambda_d^2}{d_s d_I}(\sin\chi_{l+1}-\sin\chi_l) + J_{in}\frac{4\pi(\lambda_d^2-\lambda_s^2)}{d_s d_I}(\sin\chi_{l+1}-\sin\chi_l) = 0, \tag{B.19}$$

by noting that the Maxwell' equation $\nabla\times\vec{B} - \epsilon(\partial E/\partial t) = 4\pi J$ may be written as

$$\frac{\partial B^y_{l+1,l}}{\partial x} - \epsilon\frac{\partial E^z_{l+1,l}}{\partial t} = 4\pi\sum_{i,j}\left(J^{\beta,ij}_{l+1,l} + J^{\alpha,ij}_{l+1,l}\right). \tag{B.20}$$

One may now use the fact that the phase difference between the d-bands (i.e., $\tilde{\phi}^{dd}_{l+1,l}$) of the two adjacent S layers may be written in terms of that between the two s-bands (i.e., $\tilde{\phi}^{ss}_{l+1,l}$) as

$$\tilde{\phi}^{dd}_{l+1,l} = \theta^d_{l+l} - \theta^d_l - 2eA^z_{l+1,l} = \tilde{\phi}^{ss}_{l+1,l} - \chi_{l+1} + \chi_l$$

where $\chi_l = \theta_l^d - \theta_l^s$ is the relative phase difference between the two condensates of the same S layer. This substitution allows one to obtain the sine-Gordon equation for the phase difference $\tilde{\phi}_{l+1,l}^{ss}$ which can be written as

$$\frac{\epsilon\Phi_0\overline{\Lambda}}{2\pi d_s d_I^2}\frac{\partial^2}{\partial t^2}\left[\tilde{\phi}_{l+2,l+1}^{ss} + \tilde{\phi}_{l,l-1}^{ss} - \left(2 + \frac{2d_s d_I}{\overline{\Lambda}}\right)\tilde{\phi}_{l+1,l}^{ss}\right] - \frac{\Phi_0}{2\pi d_I}\frac{\partial^2\tilde{\phi}_{l+1,l}^{ss}}{\partial x^2} - 8\pi J_8$$

$$+\frac{\epsilon\,\Phi_0}{2\pi d_I}\frac{\overline{\Lambda}}{\mu_d^2 d_s d_I}\frac{\partial^2}{\partial t^2}\left[\chi_{l+1} - \chi_{l+2} + \chi_{l-1} - \chi_l - \left(2 + \frac{2d_I d_s}{\overline{\Lambda}}\right)(\chi_l - \chi_{l+1})\right]$$

$$+\frac{4\pi\lambda_s^2}{d_s d_I}(J_5 + J_7) + \frac{4\pi\lambda_d^2}{d_s d_I}(J_6 + J_9) - \frac{\Phi_0\Lambda}{2\pi d_I}\frac{\partial^2(\chi_l - \chi_{l+1})}{\partial t^2}$$

$$+\frac{\Phi_0}{2\pi d_I}\frac{\partial^2(\chi_l - \chi_{l+1})}{\partial x^2} - J_{in}\frac{4\pi(\lambda_d^2 - \lambda_s^2)}{d_s d_I}(\sin\chi_{l+1} - \sin\chi_l) \cong 0, \tag{B.21}$$

where $\overline{\Lambda} = [(\lambda_s^2/\mu_s^2) + (\lambda_d^2/\mu_d^2)]/(\mu_s^{-2} + \mu_d^{-2})$ and $\Lambda = (\lambda_s^2\mu_s^{-2} - \lambda_d^2\mu_d^{-2})/(\mu_s^{-2} + \mu_d^{-2})$. Here, the Josephson current density $J_{l+1,l}^{\beta,ij}$ and the quasi-particle current density $J_{l+1,l}^{\alpha,ij}$ to define the following current density terms in the phase equation of motion:

$$J_5 = \left(J_{l+2,l+1}^{\beta,ss} + J_{l,l-1}^{\beta,ss} - 2J_{l+1,l}^{\beta,ss}\right) - \left(J_{l+2,l+1}^{\alpha,ss} + J_{l,l-1}^{\alpha,ss} - 2J_{l+1,l}^{\alpha,ss}\right). \tag{B.22}$$

$$J_6 = J_{l+2,l+1}^{\beta,dd} + J_{l,l-1}^{\beta,dd} - 2J_{l+1,l}^{\beta,dd} - \left(J_{l+2,l+1}^{\alpha,dd} + J_{l,l-1}^{\alpha,dd} - 2J_{l+1,l}^{\alpha,dd}\right), \tag{B.23}$$

$$J_7 = \left(J_{l+2,l+1}^{\beta,sd} + J_{l,l-1}^{\beta,ds} - J_{l+1,l}^{\beta,sd} - J_{l+1,l}^{\beta,ds}\right) - \left(J_{l+2,l+1}^{\alpha,sd} + J_{l,l-1}^{\alpha,ds} - J_{l+1,l}^{\alpha,sd} - J_{l+1,l}^{\alpha,ds}\right), \tag{B.24}$$

$$J_8 = J_{l+1,l}^{\beta,ss} + J_{l+1,l}^{\beta,dd} + J_{l+1,l}^{\beta,sd} + J_{l+1,l}^{\beta,ds} + J_{l+1,l}^{\alpha,ss} + J_{l+1,l}^{\alpha,dd} + J_{l+1,l}^{\alpha,sd} + J_{l+1,l}^{\alpha,ds}, \tag{B.25}$$

and

$$J_9 = J_{l+2,l+1}^{\beta,ds} + J_{l,l-1}^{\beta,sd} - J_{l+1,l}^{\beta,ds} - J_{l+1,l}^{\beta,sd} - \left(J_{l+2,l+1}^{\alpha,ds} + J_{l,l-1}^{\alpha,sd} - J_{l+1,l}^{\alpha,ds} - J_{l+1,l}^{\alpha,sd}\right). \tag{B.26}$$

Note that the equation of motion of Eq. (B.21) may be used to account for the phase dynamics in the two-coupled LJJs by considering only l=1 and l=2 superconducting layers.

REFERENCES

[1] A. L. Fetter and J. D. Walecka, *Quantum theory of Many Particle* (McGraw Hill, New York, 1971) p225.

[2] S. G. Chung, Physica E**12**, 931 (2002).

[3] J. Bardeen, L. N. Cooper, J. R. Schrieffer, Phys. Rev. **108**, 1175 (1957).

[4] T. Dahm, *Frontiers in Superconducting Materials* (Springer, Berlin, 2005).

[5] A. J. Leggett, Prog. Theore. Phys. **36**, 901 (1966).

[6] Y. Ota, M. Machida, T. Koyama, and H. Aoki, e-print arXiv: 1008:3212 (to be published)

[7] G. Blumberg, A. Mialitsin, B. S. Dennis, M. V. Klein, N. D. Zhigadlo, and J.Karpinski, Phys. Rev. Lett. **99**, 227002 (2007).

[8] L. N. Bulaevakii, M. Jamora and D. Baeriswyl, H. Beck, and J. R. Clem, Rev. B**50**, 12831 (1994).

[9] W. Lee, S. C. Zhang, and C. Wu, Phys. Rev. Lett. **102**, 217002 (2009).

[10] T. Loufwander, V. S. Shumeiko, and G. Wendin, Phys. Rev. B**62**, 14653 (2000).

[11] J. Garaud, J. Carlstroum, and E. Babaev, Phys. Rev. Lett. **99**, 227002 (2007).

[12] X. Hu and Z. Wang, e-print arXiv: 1103.0123 (to be published)

[13] C. Platt, R. Thomale, C. Honerkamp, S. C. Zhang, and W. Hanke, e-print arXive: 11006.5964 (to be published).

[14] H. Susanto and J. A. Espinola-Rocha, Phys. Lett. A**373**, 1387 (2009).

[15] T. K. Ng, and N. Nagaosa, EPL **87**, 17003 (2009).

[16] U. Kienzle, T. Gaber, KBuckenmaier, K. Ilin, M. Siegel, D. Koelle, R. Kleiner, and E. Goldobin, Phys. Rev. B**80**, 014504 (2009).

[17] E. Babaev, Phys. Rev. Lett. **89**, 067001 (2002).

[18] Y. Ota, M. Machida, T. Koyama, and H. Matsumoto, Phys. Rev. Lett. **102**, 237003 (2009).

[19] Y. Ota, M. Machida, and T. Koyama, Phys. Rev. B**83**, 060503 (R) (2011).

[20] H. Bluhm, N. C. Koshnick, M. E. Huber, and K. A. Molar, Phys. Rev. Lett. **97**, 237002 (2006).

[21] Y. Tanaka, Phys. Rev. Lett. **88**, 017002 (2002).

[22] S. V. Kuplevaskhsky, A. N., Omelyanchouk, and Y. S. Yerin, J. Low. Temp. Phys. **37**, 667 (2011).

[23] Y. Tanaka, A. Iyo, K. Tokiwa, T. Watanabe, A. Crisan, A. Sundaresan, and N. Tereda, Physica C**470**, 1010 (2010).

[24] A. Gurevich and V. M. Vinokur, Phys. Rev. Lett. **97**, 137003 (2006).

[25] D. W. McLaughlin and A. C. Scott, Phys Rev. A**18**, 1652 (1978).

[26] A. Sanchez, A. R. Bishop, and F. D. Adame, Phys. Rev. E**49**, 4603 (1994).

[27] C. Vanneste, A. Gilabert, P. Sibillot, and D. B. Ostrowsky, J. Low Temp. Phys. **45**, 517 (1981).

[28] G. S. Mkrtchyan and V. V. Schmidt, Solid State, Commun. **30**, 791 (1979).

[29] B. A. Malomed and M. I. Tbribelsky, Phys. Rev. B**41**, 11271 (1990).

[30] H. Suhl, B. T. Matthias, and L. R. Walker, Phys. Rev. Lett. **3**, 552 (1959).

[31] Y. Tanaka, A. Iyo, K. Tokiwa, T. Watanable, A. Crisan, A. Sundaresan, and N. Tereda, Physica C**470**, 966 (2010).

[32] Y. Tanaka, P. M. Shirage, and A. Iyo, Physica C**470**, 2023 (2010).

[33] S.-Z. Lin, e-print arXiv: 1204.0538 (to be published).

[34] M. Machida, T. Koyama, A. Tanaka, and M. Tachiki, Physica C**331**, 85 (2000).

[35] S. G. Sharaporv, V. P. Gusynin, and H. Beck, EPJ B**30**, 45 (2002).

[36] S. Sakai, P. Bodin, and N. F. Pedersen, J. Appl. Phys. **73**, (1993) 2411.

[37] S. Sakai, A. V. Ustinov, H. Kohlstedt, A. Peetraglia, and N. F. Pedersen, Phys. Rev. B**50**, 12905 (1994).

[38] S. Sakai and H. Yamamori, Physica C**362**, 1 (2001).

[39] Y. Tanaka, Phys. Soc. Jpn. **70**, 2844 (2001).

[40] U. Eckern, G. Schon, and V. Ambegaokar, Phys. Rev. B**30**, 6419 (1984).

[41] Y. S. Kivshar, Boris A. Malomed, Phys. Rev. B**37**, 9325 (1988).

[42] D. F. Agterberg, Eugene Demler, B. Janko, Phys. Rev. B**66**, 214507 (2002).

[43] E. Goldobin and A. V. Ustinov, Phys. Rev. B**59**, 11532 (1999).

[44] T. Koyama, Y. Ota, and M. Machida, Physica C**470**, 1481 (2010).

[45] M. B. Fogel, S. E. Trullinger, A. R. Bishop, and J. A. Krumhansl, Phys. Rev. Lett. **24**, 1411(1976).

[46] M. B. Fogel, S. E. Trullinger, A. R. Bishop, and J. A. Krumhansl, Phys. Rev. B**15**, 1578 (1977).

[47] V. Ambegaokar, U. Eckern, and G. Schon, Phys. Rev. Lett. **48**, 1745(1982).

[48] U. Eckern, G. Schon,and V. Ambegaokar, Phys. Rev. B**30**, 6419(1984).

[49] M. R. Eskildsen, M. Kugler, S. Tanaka, J. Jun, S. M. Kazakov, J. Karpinski, and O. Fischer, Phys. Rev. Lett. **89**, 187003 (2002).

[50] H. J. Choi, D. Roundy, H. Sun, M. L. Cohen, and S. G. Louie, Phys. Rev. B**66**, 020513(2002).

[51] A. Y. Liu, I. I. Mazin, and J. Kortus, Phys. Rev. B**86**, 5771 (2001).

[52] J. E. Moij, T. P. Orlando, L. Levito, L. Tian, C. H. Van der Wal, and S. Lloyd, Science **28**, 1036 (1999).

[53] X. X. Xi, Rep. Prog. Phys. **71**, 116501 (2008).

[54] G. Karapetrov, M. Iavarone, W. K. Kwok, G. W. Crabtree, and D. G. Hinks, Phys. Rev. Lett. **86**, 4374 (2001).

[55] F. Giubileo, D. Roditchev, W. Sacks, R. Lamy, D. X. Thankh, J. Klein, S. Miraglia, D. Fruchart, J. Marcus, and Ph. Monod, *ibid*. **87**, 177008 (2001).

[56] T. Yokoya, T. Kiss, A. Chainani, S. Shin, M. Nohara, and H. Takagi, Science **294**, 2518 (2001).

[57] J. H. Kim and J. Pokhrel, Physica C**384**, 425 (2003).

[58] Y. Kong, O. V. Dolgov, O. Jepsen, and O. K. Andersen, Phys. Rev. B**64**, 020501 (1990).

[59] K. P. Bohnem, R. Heid, and B. Renker, Rev. Lett. **86**, 5771 (2001).

[60] M. Tinkham, *Introduction to Superconductivity* (McGraw Hill, New York, 1996) p127.

[61] Y. Kamihara, T. Watanaba, M. Hirano, and H. Hosono, J. Am. Chem. Soc. **130**, 3296 (2001).

[62] J. H. Tapp, Z. Tang, B. Lv, K. Sasmal, B. Lorentz, P C W Chu, and A. M Guloy, Phys. Rev. B**78**, 060505 (2008).

[63] M. Rotter, M. Tegel, and M. D. Johrendt, Phys. Rev. Lett. **101**, 107006 (2008).

[64] S. L. Yu, J. Kang, and J. X. Li, Phys. Rev. B**79**, 064517 (2009).

[65] K. Kuroki, S. Onari, R. Arita, H. Usui, Y. Tanaka, H. Kontani, and B. Aoki, Phys. Rev. B**79**, 064517 (2009).

[66] I. I. Mazin, D. J. Singh, M. D. Johannes, and M. H. Du, Phys. Rev. Lett. **101**, 057003 (2008).

[67] C. Buzea and Yamashita, Supcn. Sc. and Techn. **14**, 115 (2001).

[68] J. H. Kim, B. R. Ghimire, and H. Y. Tsai, Phys. Rev. B**85**, 134511 (2012).